การสังเคราะห์พอลิแอนิลีนและพอลิแอนิลีนที่เติมด้วยอนุภาคเงินโดยใช้พัลส์อินดักทีฟลีคัปเพิลพลาสมา

นางสาวศศิกานต์ สุวรรณประทีป

วิทยานิพนธ์นี้เป็นส่วนหนึ่งของการศึกษาตามหลักสูตรปริญญาวิทยาศาสตรดุษฎีบัณฑิต
สาขาวิชาวัสดุศาสตร์ ภาควิชาวัสดุศาสตร์
คณะวิทยาศาสตร์ จุฬาลงกรณ์มหาวิทยาลัย
ปีการศึกษา 2555

SYNTHESES OF POLYANILINE AND POLYANILINE FILLED WITH SILVER PARTICLES USING PULSED INDUCTIVELY COUPLED PLASMA

Miss Sasikan Suwanprateep

A Dissertation Submitted in Partial Fulfillment of the Requirements
for the Degree of Doctor of Philosophy Program in Materials Science
Department of Materials Science
Faculty of Science
Chulalongkorn University
Academic Year 2012

Thesis Title	SYNTHESES OF POLYANILINE AND POLYANILINE FILLED WITH SILVER PARTICLES USING PULSED INDUCTIVELY COUPLED PLASMA
By	Miss Sasikan Suwanprateep
Field of Study	Materials Science
Thesis Advisor	Associate Professor Vimolvan Pimpan, Ph.D.
Thesis Co-advisor	Assistant Professor Rattachat Mongkolnavin, Ph.D.

Accepted by the Faculty of Science, Chulalongkorn University in Partial Fulfillment of the Requirements for the Doctoral Degree

.....Dean of the Faculty of Science
(Professor Supot Hannongbua, Dr. rer. nat.)

THESIS COMMITTEE

.....Chairman
(Assistant Professor Sirithan Jiemsirilers, Ph.D.)

.....Thesis Advisor
(Associate Professor Vimolvan Pimpan, Ph.D.)

.....Thesis Co-advisor
(Assistant Professor Rattachat Mongkolnavin, Ph.D.)

.....Examiner
(Associate Professor Onusa Saravari)

.....Examiner
(Assistant Professor Duanghathai Pentrakoon, Ph.D.)

.....External Examiner
(Associate Professor Paiparn Santisuk)

ศศิกานต์ สุวรรณประทีป : การสังเคราะห์พอลิแอนิลีนและพอลิแอนิลีนที่เติมด้วยอนุภาคเงินโดยใช้พัลส์อินดักทีฟลีคัปเพิลพลาสมา. (SYNTHESES OF POLYANILINE AND POLYANILINE FILLED WITH SILVER PARTICLES USING PULSED INDUCTIVELY COUPLED PLASMA) อ.ที่ปรึกษาวิทยานิพนธ์หลัก : รศ.ดร.วิมลวรรณ พิมพ์พันธุ์, อ.ที่ปรึกษาวิทยานิพนธ์ร่วม : ผศ.ดร.รัฐชาติ มงคลนาวิน, 155 หน้า.

พอลิแอนิลีนสามารถสังเคราะห์โดยใช้พลาสมาแบบพัลส์ที่กำเนิดจากเครื่องทีตาพินช์และเครื่องพีไอซีพีที่ความดันและกระแสไฟฟ้าเดียวกัน คือ 2 ปาสคาล และ125 กิโลแอมแปร์ ตามลำดับ ในขณะที่เครื่องแรกทำงานที่ศักย์ไฟฟ้า 20 กิโลโวลต์ เครื่องหลังทำงานที่ศักย์ไฟฟ้าเป็น 9.5 กิโลโวลต์ โดยปรับเปลี่ยนจำนวนครั้งในการยิงพลาสมาตั้งแต่ 5, 10, 15, 20, 25 ถึง 30 ครั้ง และใช้ชนิดของแก๊สที่แตกต่างกันคือ อาร์กอน ออกซิเจน และไนโตรเจน ซึ่งพารามิเตอร์เหล่านี้ส่งผลอย่างเห็นได้ชัดต่อโครงสร้างทางเคมีของพอลิแอนิลีนที่ได้ ดังเห็นจากฟูเรียร์ทรานสฟอร์มอินฟราเรดสเปกทรา พอลิแอนิลีนที่ถูกโดปด้วยกรดซัลฟูริกมีสมบัติการนำไฟฟ้าและสมบัติทางความร้อนดีกว่าของพอลิแอนิลีนที่ถูกโดปด้วยกรดไฮโดรคลอริก โดยภาวะที่เหมาะสมในการสังเคราะห์ คือ ที่จำนวนครั้งในการยิง 20 ครั้งสำหรับอาร์กอน ซึ่งให้พอลิแอนิลีนที่มีค่าการนำไฟฟ้าสูงสุดที่ 10^{-7} ซีเมนต์ต่อลูกบาศก์เซนติเมตร นอกจากนี้ยังพบว่า การใช้เครื่องพีไอซีพีให้พอลิแอนิลีนที่มีสมบัติดีกว่าการใช้เครื่องทีตาพินช์ ดังนั้นจึงใช้เครื่องพีไอซีพีในการเตรียมพอลิแอนิลีนที่เติมอนุภาคเงิน

การสังเคราะห์พอลิแอนิลีนที่เติมอนุภาคเงินสามารถทำได้ในขั้นตอนเดียว โดยใช้สารละลายผสมของสารละลายแอนิลีนในกรดไนตริกกับสารละลายซิลเวอร์ไนเทรตในการทำพลาสมาพอลิเมอไรเซชัน โดยปรับเปลี่ยนจำนวนครั้งในการยิงพลาสมา ชนิดของแก๊ส และความเข้มข้นของสารละลายซิลเวอร์ไนเทรต ซึ่งพารามิเตอร์เหล่านี้ส่งผลอย่างเห็นได้ชัดต่อโครงสร้างทางเคมีของพอลิแอนิลีนที่ได้ ดังเห็นจากฟูเรียร์ทรานสฟอร์มอินฟราเรดสเปกทรา การนำไฟฟ้าของพอลิแอนิลีนเหล่านี้มีค่าประมาณ 10^{-4} ซีเมนต์ต่อลูกบาศก์เซนติเมตร ซึ่งดีกว่าของพอลิแอนิลีนที่ไม่เติมอนุภาคเงิน นอกจากนี้ยังมีเสถียรภาพทางความร้อนที่ดีกว่าด้วย ภาพจากกล้องจุลทรรศน์อิเล็กตรอนแบบส่องกราด แสดงให้เห็นอนุภาคเงินทรงกลมที่มีขนาดเส้นผ่านศูนย์กลางประมาณ 50-80 นาโนเมตรและเส้นใยพอลิแอนิลีนที่มีขนาดเส้นผ่านศูนย์กลางประมาณ 50-100 นาโนเมตร

ภาควิชา	วัสดุศาสตร์	ลายมือชื่อนิสิต	
สาขาวิชา	วัสดุศาสตร์	ลายมือชื่อ อ.ที่ปรึกษาวิทยานิพนธ์หลัก	
ปีการศึกษา	2555	ลายมือชื่อ อ.ที่ปรึกษาวิทยานิพนธ์ร่วม	

5173860923 : MAJOR MATERIALS SCIENCE
KEYWORDS : POLYANILNE/ SILVER PARTICLES/ CONDUCTIVITY/ PLASMA POLYMERIZATION/ THETA-PINCH DEVICE/ PICP DEVICE

SASIKAN SUWANPRATEEP : SYNTHESES OF POLYANILINE AND POLYANILINE FILLED WITH SILVER PARTICLES USING PULSED INDUCTIVELY COUPLED PLASMA. ADVISOR : ASSOC. PROF. VIMOLVAN PIMPAN, Ph.D., CO-ADVISOR : ASST. PROF. RATTACHAT MONGKOLNAVIN, Ph.D., 155 pp.

Polyanilines were synthesized using pulsed plasma generated from a theta-pinch device and a pulsed inductively coupled plasma (PICP) device at same pressure of 2 Pa and discharging current of 125 kA. While a voltage of 20 kV was applied to the former, a voltage of 9.5 kV was used in the latter. The numbers of the plasma shots were varied from 5, 10, 15, 20, 25, to 30 shots and different types of gases including argon, oxygen and nitrogen were used. These parameters significantly affected the chemical structures of the obtained polyanilines as revealed by FTIR spectra. Polyanilines doped with sulfuric acid had better electrical and thermal properties than those doped with hydrochloric acid. The suitable condition that yielded polyaniline with highest conductivity of 10^{-7} S.cm^{-1} was at 20 shots of argon. In addition, it was found that using PICP device yielded polyanilines with better properties than using theta-pinch device. Therefore, PICP device was used for preparing polyanilines filled with silver particles.

Polyanilines filled with silver particles can be synthesized in one step by using the mixture of aniline in nitric acid solution and silver nitrate solution in plasma polymerization. The numbers of the plasma shots, the gas types and the concentration of silver nitrate solution were varied. These parameters significantly affected the chemical structures of the obtained polyanilines as revealed by FTIR spectra. Electrical conductivity of these polyanilines was about 10^{-4} S.cm^{-1} higher than that of unfilled polyanilines. They also had better thermal stability. FE-SEM images showed the spherical silver particles with diameters about 50-80 nm and the nanofibrils of polyaniline with diameters about 50-100 nm.

Department : Materials Science Student's Signature .....
Field of Study : Materials Science Advisor's Signature .....
Academic Year : 2012 Co-advisor's Signature .....

ACKNOWLEDGEMENTS

Appreciation is expressed to those who have made the contributions to this dissertation. First of all, I gratefully acknowledge my advisor, Associate Professor Dr. Vimolvan Pimpan and co-advisor, Assistant Professor Dr. Rattachat Mongkolnavin for giving me the opportunity to be in the interesting avenue of research, their attention to the development of this work, invaluable knowledge, meaningful guidance, tolerance, and their encouragement all along the way.

I wish to extend my sincere thanks to Assistant Professor Dr. Sirithan Jiemsirilers, Associate Professor Paiparn Santisuk, Associate Professor Onusa Saravari, and Assistant Professor Dr. Duanghathai Pentrakoon for their kindly participation as dissertation committee, making comments, and their helpful ideas and suggestions.

I gratefully acknowledge Dr. Dusit Ngamrungroj, Mr. Eakluck Chandrema and staffs at Plasma Technology and Nuclear Fusion Research Unit, Chulalongkorn University, for their help in the operation of the plasma devices, suggestions and assistance on my experiment.

I would like to thank for the contributions, wonderful friendship, liveliness, and supports from my friend, Dr. Datchanee Kraisiri, and all members at the Department of Materials Science, Faculty of Science, Chulalongkorn University.

This work would not be carried out successfully without the financial supports provide by the Program Strategic Scholarships for Frontier Research Network for the Join Ph.D. Program Thai Doctoral degree from the Office of the Higher Education Commission, Rajamangala University of Technology Suvarnabhumi, Chulalongkorn University Centenary Academic Development Project and Center of Excellence on Petrochemical and Materials Technology. Moreover, sincere thank is extended to Thai Microelectronics Center, Thailand for providing the silicon substrate.

Finally, and the most of all, I would like to express my deep gratitude to my family for their unconditional love, continual encouragement, patience and understanding.

CONTENTS

Page

Page

Page

Page

LIST OF TABLES

Table **Page**

Table **Page**

Table **Page**

LIST OF FIGURES

Figure **Page**

Figure **Page**

Figure **Page**

Figure **Page**

Figure **Page**

Figure **Page**

LIST OF SCHEMES

Scheme **Page**

CHAPTER I

INTRODUCTION

Polyaniline is one of the conducting polymers which show unique electrical, optical and thermal properties. It is significantly cheaper than other conducting polymers [1]. Polyaniline is generally synthesized by chemical [2-4], electrochemical [5-6] and other [7-8] methods. However, some of these methods require long and sophisticated synthetic routes. Conventional method based on the oxidation of aniline with an oxidant yields polyaniline in the powder form which is difficult for film formation due to its poor solubility [9]. On the other hand, in electrochemical method, polyaniline film can only be deposited on a conducting substrate. Therefore, plasma polymerization has been introduced as a method for preparing a polyaniline thin film on an insulator due to its fewer fabrication and simpler process than conventional methods [10].

Plasma is an ionized gas containing both charged and neutral species, including free electrons, ions, radicals, atom and molecules. Normal gases such as argon, oxygen or nitrogen and the monomers in gas phase such as ethylene can be used to generate the corresponding plasma. Plasma polymerization uses the active gaseous species to initiate the polymerization. The deposition of a polymeric film onto an insulator such as a glass substrate occurs during the process. However, it is necessary to employ additional acid-doping step to the obtained polyaniline in order to get the conducting property. Continuous plasma has been proposed as a new way to synthesize polyaniline under dry condition. However, it induces intense molecular fragmentation through bond breaking leading to highly cross-linked and amorphous film [11]. Therefore, instead of using continuous plasma, pulsed plasma has been employed since its process is fast and environmentally friendly and it is easier to control the plasma exposure [12-17].

In addition, metal particles such as silver, gold or platinum can be added into polyaniline matrix in order to improve its properties such as optical, electrical and thermal properties [18]. Metal-added polymers are applied in many applications such chemical and biological sensors, batteries and electronic devices [19-20]. Silver is a

metal of choice due to its low price and its ease in preparation. It was reported that polyaniline filled with silver particles was prepared from the oxidation of aniline by silver nitrate. This method resulted in polyaniline with improved properties such as electrical and thermal conductivity [21-22]. It was found that the reduction of the silver salt in aqueous aniline yielded the silver nanoparticles which in turn catalyzed the oxidation of aniline into polyaniline [23].

Therefore, in this research, one-step process for synthesizing a conductive polyaniline is studied. Aniline dissolved in acid solution is polymerized into polyaniline by pulsed plasma to ensure the polymerization occurs in conjunction with acid-doping. Different types of gases and various numbers of the plasma shots are employed. Two pulsed plasma generators operating based on the principle of pulsed inductively coupled plasma (PICP) are used in this research. They are a theta-pinch device and a PICP device which is a device modified from a theta-pinch device with lower voltages at equivalent energy of plasma [24]. After determining the suitable device, it is then used to synthesize polyanilines filled with various amounts of silver nanoparticles from aniline dissolved in acid solution and silver nitrate solution. It is expected that the plasma polymerization of aniline and the reduction of silver nitrate into silver nanoparticles should occur simultaneously. The characteristics and the properties of all synthesized polyanilines and polyanilines filled with silver nanoparticles are investigated. The objectives of this research can be summarized as follows:

1. To synthesize polyanilines by plasma polymerization of aniline with acid doping in one step using pulsed plasma generated from a theta-pinch device and a PICP device and to determine the optimum condition for the synthesis.

2. To synthesize polyanilines filled with silver particles by plasma polymerization of aniline with the reduction of silver nitrate in one step using pulsed plasma generated from a suitable device determined from the previous section of the research and to determine the optimum condition for the synthesis.

3. To study the characteristics and properties of the obtained polyanilines and polyanilines filled with silver particles.

CHAPTER II

THEORY AND LITERATURE REVIEW

2.1 Polyaniline

Polyaniline is one of the widely known conductive polymers. This group of polymers was discovered by Alan G. MacDiarmid and others [25] in 1976. Before their discovery, all polymers were considered as the insulating materials. But their discovery which later earned them the Nobel Prize in Chemistry in 2000 found the simplest conductive polymers such as polyacetylene. After exposing to vapor iodine at room temperature, its doped form exhibited an increase in the conductivity. This discovery of polyacetylene has established a new field of the conducting polymers.

2.1.1 Principles of Conducting Polymers

„Intrinsically conducting polymers" or also called „Synthetic metals" are organic polymers which possesss the electrical and optical properties of a metal while retaining its mechanical properties and processability. These properties are intrinsic to the doped form of the polymer. Inherently conducting polymers have alternating double and single bonds, as so called the conjugated double bonds that provide the electronic conductivity after doping with suitable dopants. Therefore, the research involving with the synthesis of materials, structural characteristics, solubility and processability, structure-properties relationship, conducting mechanism and their applications have been widely studied and significant progresses have been achieved [26-28].

Typical polymers including polyacethylene (PA), polyaniline (PANI), polypyrrole (PPy), polythiophene (PTh), polyfuran (PF), poly(phenylenevinylene) (PPV) and poly(p-phenylene) (PPP) have been reported as the conducting polymers [29-30]. Their molecular structures are given in Table 2.1. The common features of these conducting polymers consist of σ bonds and π bonds. The covalent bonds

between the carbon atoms are described by immobiled σ bonds. In addition, the polymer backbone in conducting polymers consists of π-conjugated chain, where are the π-electrons of the carbon atoms and the overlap of their wave function. The wave overlap is called conjugation, because it leads to a sequence of alternating double and single bonds, resulting in the unpaired electrons delocalized along the polymeric chain. As a result, unusual electronic properties such as low energy optical transitions, low ionization potentials and high electron affinities occurs in the polymer leading to special electrical properties of the conducting polymer [31]. However, the limits in the applications of a conducting polymer are the results of its insolubility and poor mechanical properties due to the presence of the π-conjugated in the polymer chain.

Table 2.1 Molecular structures of common conductive polymers

Name	Structure
Polyacethylene	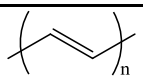
Polyaniline	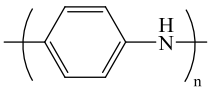
Polypyrrole	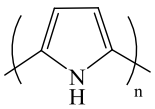
Polythiophene	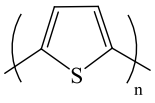
Polyfuran	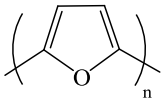
Poly(phenylenevinylene)	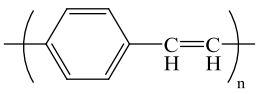
Poly(p-phenylene)	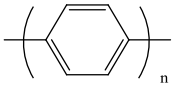

As previously mentioned, the doped form of a conducting polymer shows an increase in its conductivity. Doping is the process used to converts an insulating polymer to a conducting polymer. On the other hand, the conducting polymer can be consequently reveresed to insulate state by de-doping. Therefore, the conductivity of the conducting polymers depends on the doping degree and can be altered to cover the conductivity range of insulator, semiconductor and metal as shown in Figure 2.1 [32].

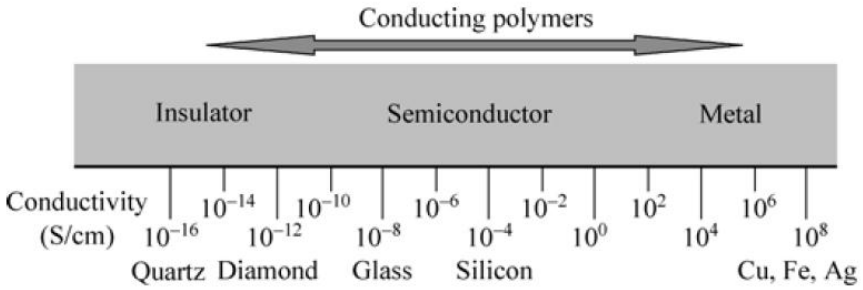

Figure 2.1 Conductivity range of the materials

Doping of a conducting polymer is done via an oxidation (p-type) or a reduction (n-type) of the polymer backbone. The oxidation and reduction reactions can be induced by the chemical species such as iodine or attached the polymer to the electrodes. The processes are called chemical and electrochemical dopings, respectively. For example, the reactions of the oxidation and reduction of polyacetylene are written as follows:

Oxidation with halogen : $[CH]_n + 3x/2I_2 \rightarrow [CH]_n^{x+} + xI_3^-$ (2.1)

Reduction with alkali metal : $[CH]_n + xNa \rightarrow [CH]_n^{x-} + xNa^+$ (2.2)

The conductivity can be controlled by the structure of the polymer (i.e. π-conjugated length) and the nature of the dopant. Other doping methods such as 'photo doping' and 'charge-injection doping' are also applied. [33]. Another doping method called 'proton doping' is an efficient doping method for polyaniline [34]. In this

method, the number of electrons associated with the polymer chain does not change during the doping process which is different from redox doping. Doping reaction of polyaniline having the structure of emeraldine base by a protonic acid is shown in Scheme 2.1.

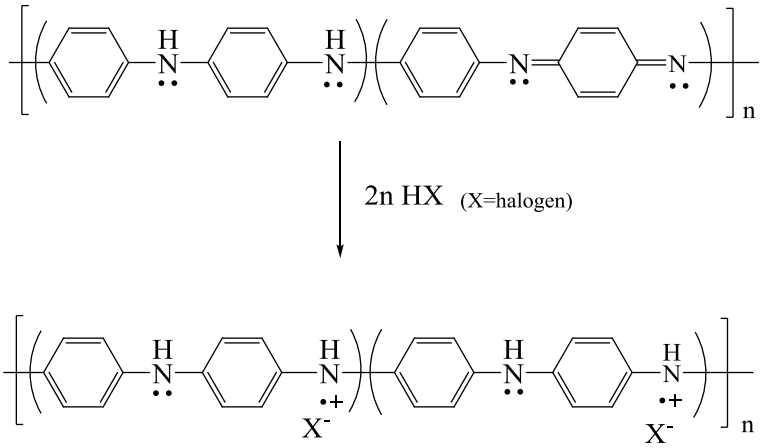

Scheme 2.1 Doping reaction of polyaniline with emeraldine base structure by a protonic acid

To explain the conductivity of a material, the band theory is generally applied. The electronic structures of an insulator, a semiconductor and a conductor are shown in Figure 2.2. Quantum mechanics specify that the electrons of an atom can only have specific or quantized energy levels. However, in the lattice of a crystal, the electronic energy of individual atoms is altered. Therefore, the energy levels are form bands when the atoms are closely spaced. While the highest occupied band is called the valence band, the lowest unoccupied band is called the conduction band. The difference in the energy between the valence and conduction band levels is called the band gap. In classical semiconductors, thermal excitation of electrons across from the valence band to the conduction band due to narrow band gap leading to conductivity. While the insulators are insufficient to excite electrons across wider band gap resulting in a decrease in the conductivity, high conductivity is founded in the conductors since they have no band gap.

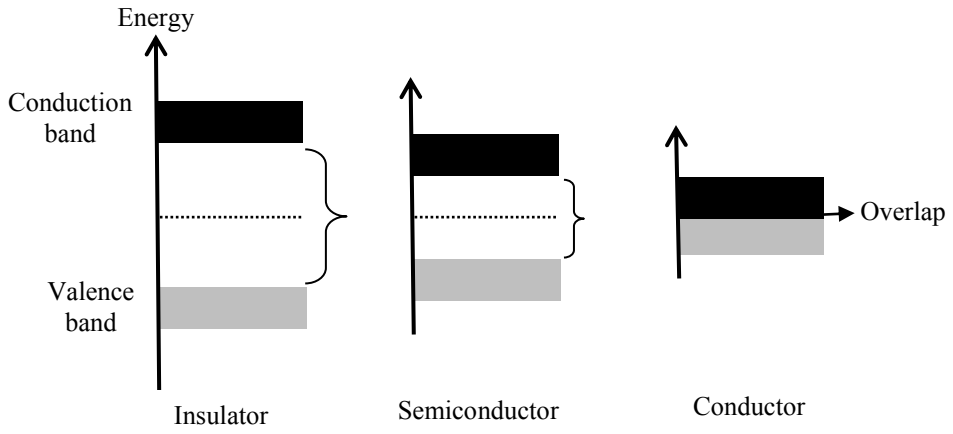

Figure 2.2 Energy bands of an insulator, a semiconductor and a conductor

However, for the conductivity polymers, the band theory cannot be applied. The conjugated π-systems of a conducting polymer can mobile charge carriers through doping resulting in the electrical conductivity which can be explained in terms of soliton, polaron and bipolaron. Conducting polymers such as polythiophene, polypyrrole, polyaniline, polyparaphenylene and their derivatives have nondegenerate ground states. These polymers are transformed into the conductors by doping with either an electron donor or an electron acceptor. For example, an electron is removed from the π-conjugated system of polypyrrole making a radical cation called polaron, which is delocalized over a polymer backbone. This creates a new localized electronic state in the gap with lower energy state being occupied by a single unpaired electron. In further oxidation, the free radical of the polaron is removed resulting in two possibilities. The electron can come from either a different segment of the polymer chain thus creating another independent polaron or from a polaron level (removal of an unpaired electron) to create a dication separating the domain of quinone bands from the sequence of aromatic-type bonds in the polymer chain, called a bipolaron. This is of lower energy than the creation of two distinct polarons. At higher doping levels it becomes possible that two polarons combine to form a bipolaron. With continued doping, the overlap between the bipolaron states forms two continuous bipolaron bands in the gap as shown in Figure 2.3 [26]. For a very heavily doped polymer, it is conceivable that the upper and the lower bipolaron bands merge with

the conduction and valence bands respectively to produce partially filled bands and metal-like conductivity.

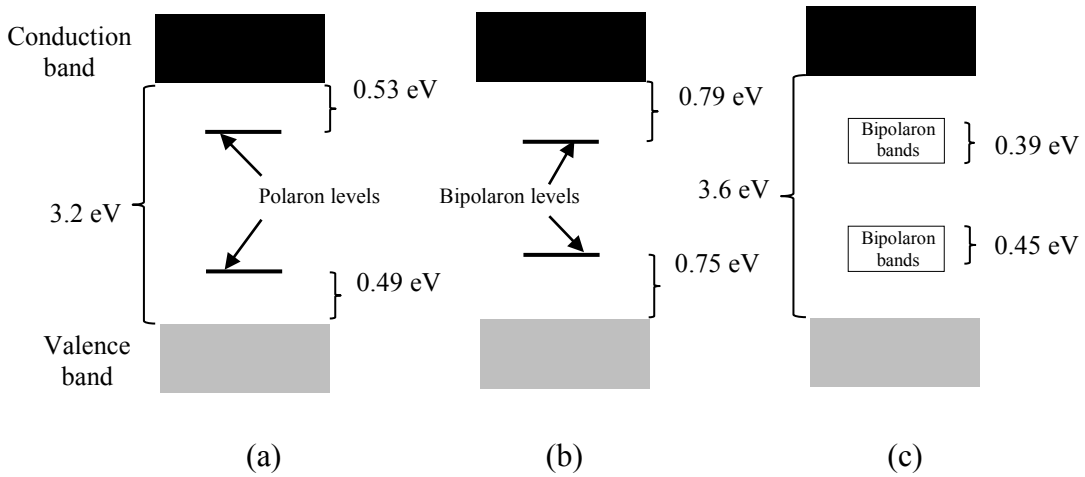

Figure 2.3 Polypyrrole band structure (a) polaron formation (b) bipolaron formation (c) formation of bipolaron bands

2.1.2 Structures of Polyaniline

The general structure of polyaniline containing reduced repeating unit and oxidized repeating unit is shown in Figure 2.4.

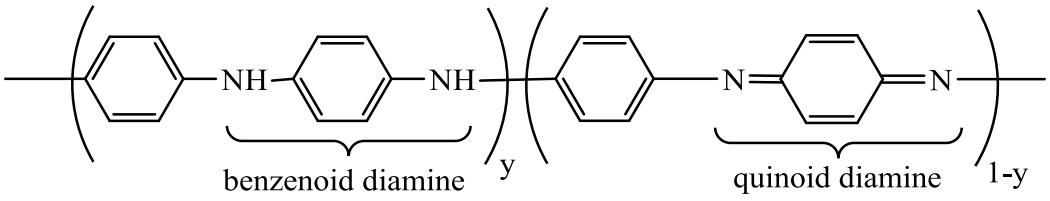

Figure 2.4 General structure of polyaniline

Polyaniline exhibits four idealized oxidation states including leucoemeraldine base, emeraldine base, pernigraniline base and emeraldine salt as shown in Figure 2.5.

The electrical conducting form of polyaniline is emeraldine salt which is a partially oxidized compound. Leucoemeraldine is a fully reduced compound corresponding to a value of y=1 with electrical insulating characteristic. Pernigraniline is a fully oxidized compound corresponding to a value of y=0 without conducting characteristic. Emeraldine base can be converted from an insulator to a conductor when it is protonated with a proton donor corresponding to a value of y=0.5.

Leucoemeraldine base 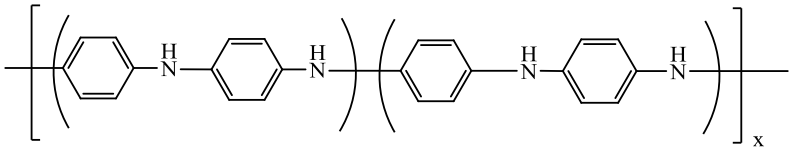

Pernigraniline base 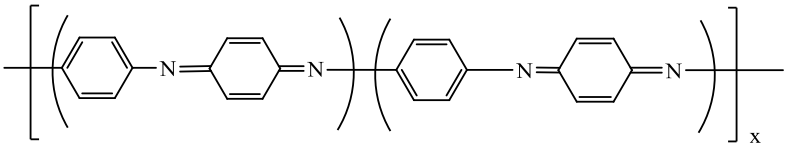

Emeraldine base 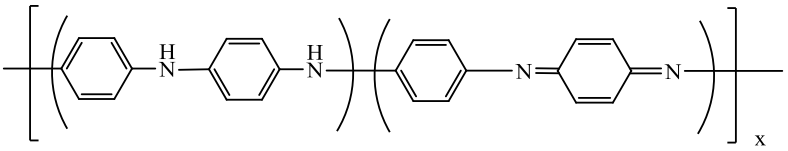

Emeraldine salt 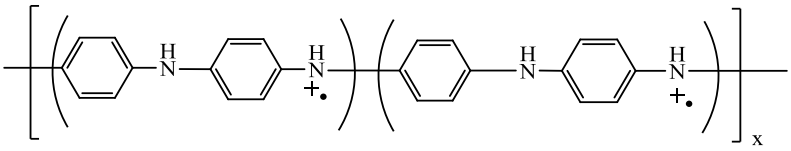

Figure 2.5 Four idealized oxidation states of polyaniline

As previously mentioned, the emeraldine base can be converted into the conducting structure of the emeraldine salt by two following doping methods.

1. Oxidation doping method via chemical reaction with a suitable oxidizing agent followed by electrochemical charge transfer reaction causing a change in the total number of π-electron on the conjugated chain.

2. Protonation doping method via acid-base reaction in an aqueous media with pH less than 2-3. There is no change in the number of π-electron.

Polyaniline is found in many forms such as granules, nanofibers, nanotubes, colloidal particles, nanospheres and microspheres depending on the type of the nucleation [35]. The dimensions of these forms are in the range of 50–250 nm depending on the experimental conditions and seem to be proportional to the molecular weight of polyaniline.

Most common form of polyaniline powder is the granular form usually prepared by precipitation polymerization using strong oxidants at high aniline concentrations and strongly acidic conditions [36]. On the other hand, the most common form found in the conducting polyaniline is nanogranules which may be the result of the random aggregation of the nucleates. This form occurs at a high concentration of the nucleates which are produced during the short induction period.

Nanofibers are classified as one-dimensional form with high aspect ratio. Their diameters are normally in the range of 20–100 nm whereas their lengths are in the range of several micrometers. They are most frequently found in the conducting polymer nanostructures. They are often branched and produce networks, arrays, bundles and more complex hierarchical structures. Polyaniline nanofibers can be prepared by the dilution method as reported by Shedd, B. and others [37].

Another one-dimensional form of polyaniline is nanotubes. They differ from the nanofibers in the cases of the presence of an internal cavity and a template is necessary for the growth of the nanotubes. The diameter of the cavity is usually in the range of 10–150 nm. On the other hand, the wall thickness is typically in the range of 50–200 nm at given experimental conditions. They are occasionally found with the nanorods. In general, various forms of polyaniline can be found together including the hollow nanospheres and the globules. This may be due to an acidity drift during the

oxidation of aniline. Previous experiment done by Huang, Y.F._and coworkers [38] showed that the nanotubes can be prepared by oxidizing aniline (0.2 M) with ammonium peroxydisulfate (0.25 M) in aqueous solution of 0.4 M succinic acid.

The polymerization of aniline in the presence of suitable water-soluble polymers or nanoparticulate stabilizers yields the colloidal particles. They occur in various shapes and sizes usually in the range of 100–500 nm. They are the composites in nature and always comprise a stabilizer. Colloidal polyaniline nanoparticles are prepared by the oxidation of aniline in the presence of a suitable water-soluble polymer. This process is called a dispersion polymerization. In this process, the monomer is miscible with the reaction medium but the obtained polymer is insoluble. In the contrast to precipitation polymerization, the macroscopic separation of the polymer is prevented adding a steric stabilizer, and a colloid is formed [39].

Polyaniline nanotubes are sometimes accompanied by polyaniline nanospheres having average diameters lower than 200 nm [40]. However, these nanospheres have never been the dominating species. The spheres in sub-micrometer range have been prepared by oxidizing aniline hydrochloride in ethylene glycol using an excess oxidant [41]. The difference of the nanospheres and the microspheres are that the latter are larger and composed mainly of oligomers.

2.1.3 Synthesis of Polyaniline

Polyaniline can be synthesized by various methods. The commonly used methods including chemical or electrochemical methods usually involve the oxidation reactions [42]. Both methods were synthesized using common strong acids such as sulfuric acid (H_2SO_4) and hydrochloric acid (HCl) as medium. Some previous studies found that the conductivity of polyaniline synthesized in H_2SO_4 is higher than that synthesized in hydrochloric acid. This may be because hydrogen chloride is a gas that partly diffuses out of the sample or causes the chlorination of aromatic rings or both [43,44]. However, some strong acids such as nitric acid can oxidize polyaniline during the polymerization resulting in a decrease in conductivity [45]. The advantages and disadvantages of these methods are summarized in Table 2.2.

Table 2.2 Comparison of chemical and electrochemical polymerization of polyaniline

	Advantages	Disadvantages
Chemical Method	- Larger-scale production possible - Modification of bulk polyaniline posssible - Sophisticated synthetic routes to modify polyaniline backbone covalently	- Cannot make thin films - Complicated process
Electrochemical Method	- Thin film synthesis possible - Ease of synthesis - Entrapment of molecules in polyaniline - Doping is simultaneous	- Difficult to remove film from electrode surface - Modification of bulk polyaniline is difficult

2.1.3.1 Chemical methods

Chemical synthesis of polyaniline is based on the chemical oxidation of aniline monomer in acidic medium with an oxidant. The common acids used are hydrochloric acid (HCl) and sulfuric acid (H_2SO_4). The oxidation are occurred with the oxidants such as ammonium persulfate ($(NH_4)S_2O_8$), potassium dichromate ($K_2Cr_2O_7$), potassium ferricyanide ($K_3(Fe(CN)_6)$) and hydrogen peroxide (H_2O_2). Chemical methods are categorized into solution, interfacial, seeding, metathesis, self-assembling and sonochemical polymerizations.

Solution polymerization of aniline can be done in the presence of a solvent such as HCl and H_2SO_4 [46]. Generally, the processability of polyaniline is very poor because of its poor solubility in all available solvents. Therefore, polyaniline obtained by solution polymerization has better processability because it is already in the solution form.

Interfacial polymerization is carried out in the interfaces of two immiscible solvents. For example, aniline was dissolved in the organic phase such as hexane, benzene and toluene. While oxidizing agent such as ammonium persulfate is dissolved in aqueous phase such as water and chloroform in the presence of different acids acting as dopants. Then, the two solutions were mixed to generate interface between the two layers. The polyaniline products ranging from a one-dimensional radially aligned nanofiber to a spherical shaped are isolated by centrifugation. The shaped polyaniline depend on reaction parameter and reagents [7,47]. Chen and others [48] prepared polyaniline by interface polymerization method. The different shaped polyaniline including nanorods, spherical and bud-like structure were obtained by varying aniline to salicylic acid (dopant) ratio.

Seeding polymerization is carried out in the presence of the small amount of a foreign material such as some polyaniline powder acting as a seed. The morphology of polyaniline nanofiber depends on the type of seed, type of acid used, the acid concentration and the solvent used. Zhang and others [49] prepared the polyaniline by adding a small amount of various the nanofibers in diameter of 12-50

nm into the reaction solution of aniline and ammonium peroxydisulfate as oxidant. The products of seeded polyaniline was fibrillar with diameter about 20-60 nm.

Sonochemical polymerization is prepared by dropwise addition of an acidic APS solution to acidic aniline solution with aid of ultrasonic irradiation. Jing and others [50] successfully synthesized polyaniline with high polymer yield. Polyaniline nanofibers in diameters of 50 nm and lengths of 200 nm to several micrometers were prepared. In the conventional method, with continuing of the reaction, primary nanofibers grow and agglomerate into irregular shaped polyaniline particles in the mechanical stirred system, while in the case of the ultrasonic irradiation, the growth and agglomeration are effectively prevented. One of the advantages of this method is its scalability in comparison with other methods such as interfacial polymerization.

Self-assembling polymerization is carried out in a vapor phase as shown in Figure 2.6. The polyaniline films are directly grown on the polymeric film substrates. Yang and coworkers [51] prepared polyaniline copolymer from aniline and m-aminobenzene sulfonic acid using APS as oxidant on indium tin oxide as substrate. Kim and coworkers [52] prepared polyaniline films on polymeric substrates such as polystyrene. 10 wt% solution of oxidant was coated on the substrates by dipping or spin coating. Then the dry coated film was exposed to aniline vapor for 5-60 min in reaction chamber at different temperatures.

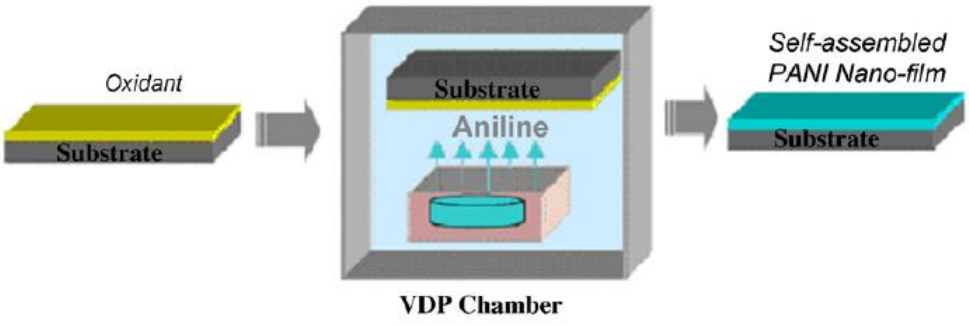

Figure 2.6 Schematic procedure of self-assembling method

2.1.3.2 Electrochemical methods

Three electrochemical methods can be used to synthesize polyaniline. These methods include a constant current (galvanostatic), a constant potential (potentiostatic) and a potential scanning/cycling or sweeping. In all process, a three electrode assembly compose the reactor vessel (a working electrode on which the polymer is deposited), a counter electrode also named auxiliary electrode (platinum grid) and a reference electrode (a saturated calomel electrode). However, polyaniline can be only deposited onto the conducting substrates such as glass covered by indium-doped tin oxide electrode, iron and gold [2]. Langer and coworkers [53] prepared polyaniline by anodic oxidation of aniline hydrochloride in water or a water–methanol (1:1) mixture. Polyaniline microrods of almost uniform shape were obtained with a diameter of 0.7 μm and a length of 2–3 μm.

2.1.4 Improvement of Electrical Conductivity of Polyaniline

The electrical conductivity of polyaniline can be improved by adding silver particles [18]. It has been reported that polyaniline filled with silver particles can be prepared in three ways. The first method is that silver particles are embedded into polyaniline matrix during the conventional polymerization based on the oxidation of aniline with oxidant. However, a decrease in chain length results in low conductivity because of the incompatibility between organic and inorganic portions. In second method, polyaniline is used to reduce the silver salts into metal particles causing the reduction in polyaniline‟s conductivity due to the formation of a non-conductive form. For last method, the oxidation of aniline with silver nitrate can result in polyaniline with improved properties [19].

Gupta, K. and others [18] synthesized polyaniline-silver nanocomposite by chemical oxidative polymerization of aniline using ammonium peroxydisulfate as an initiator in presence of negatively charged silver nanoparticles. Silver nanoparticles were prepared by standard citrate reduction method. TGA and DSC results showed that polyaniline-silver nanocomposite had higher electrical conductivity and was more

thermally stable than those of pure polyaniline. The electrical conductivity of the nanocomposite increased with increasing silver nanoparticles content.

Blinova N. V. and others [21] obtained polyaniline-silver composites from the oxidation of aniline by silver nitrate in aqueous solutions of nitric acid according to Scheme 2.2. The oxidation products consisted of two conducting components, polyaniline and silver nanoparticles. The various structures of polyaniline were observed including the nanofiber having the thickness of 10-20 nm, the nanotubes and the nanorods of various diameters. Silver nanoparticles having diameter of 50 nm were obtained accompanying by macroscopic silver flakes. The reaction was slow and took several weeks to reach 10-15 %yield. The resulting composites contained 50-80 wt% of silver nanoparticles. The conductivity of polyaniline-silver composites were 10-1000 S/cm.

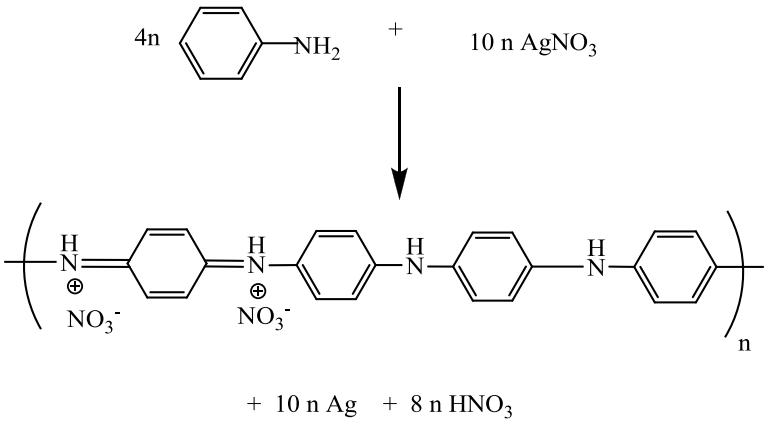

Scheme 2.2 Oxidation of aniline by silver nitrate into polyaniline (emeraldine) nitrate

Bober, P. and others [22] prepared polyaniline-silver composites by the oxidation of aniline with silver nitrate in aqueous solutions of sulfonic acid. The silver nanoparticles having average size of 50 nm were dominating species accompanying by hairy polyaniline nanorods having diameter of 150-250 nm. It was proposed that interfaces between the polymer matrix and dispersed silver nanoparticles played a dominating role in macroscopic level of conductivity.

Khanna P. K. and others [23] synthesized polyaniline-silver nanocomposite via *in situ* photoredox mechanism. The reduction of the silver salt in aqueous aniline yielded the silver nanoparticles which in turn catalyzed the oxidation of aniline into polyaniline.

Tamboli, M.S. and others [20] synthesized polyaniline-silver nanocomposite via *in situ* polymerization method using ammonium persulfate as an oxidant in the presence of dodeclybenzene sulfonic acid and silver nitrate. Thermal stability of the composites was enhanced when compared to pure polymer. In addition, the polyaniline-Ag nanocomposite showed antibacterial activity against model organisms.

Stejskal, J. and others [54] prepared polyaniline-silver composite by reducing silver nitrate to metallic silver with emeraldine form of polyaniline as shown in Scheme 2.3. The partial conversion of emeraldine salt to pernigraniline was associated with the reduced degree of protonation. Only the residual emeraldine units remained protonated and the original acid was replaced with nitric acid, which was a by-product. The conductivity of composite was in the range of $1.7x10^{-6}$ - 22.8 S cm^{-1} depending on the type of the acids used for protonating polyaniline. The composites contained raspberry-like morphology of silver particles with the size of 40-80 nm.

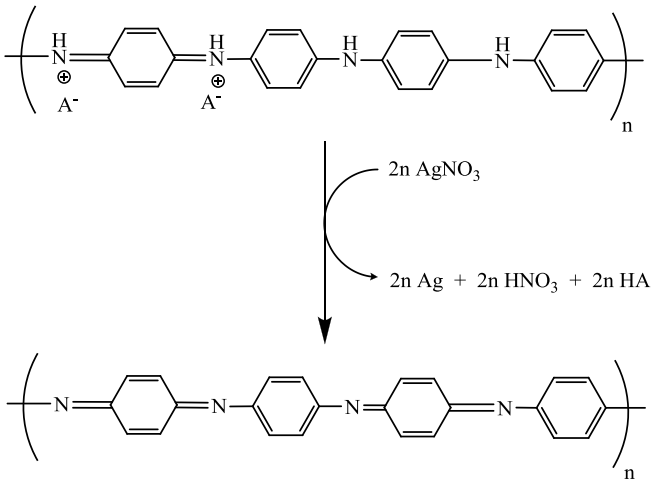

Scheme 2.3 Preparation of polyaniline-silver composite according to the method of Stejskal, J. and others

Moreover, polyaniline/silver nanocomposites were prepared under extreme or non-classical conditions. The mechanisms were based on both hydroxyl and hydrogen radicals of water molecule acting as an oxidizing agent for the polymerization process of aniline monomer and as a reducing agent for silver ions, respectively [55].

The methods previously described for polyaniline synthesis and the improvement of its properties are based on chemical and electrochemical methods. Due to their disadvantages as given in Table 2.2, plasma polymerization has been introduced as a method for preparing a polyaniline thin film on an insulator due to its fewer fabrication and simpler process than conventional methods [10].

2.2 Plasma polymerization

2.2.1 Definition of Plasma

Plasma is often called the fourth state of a matter. As a substance is heated to the temperatures above the binding energies for particular states and it undergoes phase transitions. Plasma is a distinct phase different from the traditional solids, liquids and gases. Gas is heated to the point where a significant fraction of the atoms are dissociated into negatively charged electrons and positively charged ions to form an ionized gas. The fraction of the atoms that are dissociated is called the degree of ionization. Plasma is a partially ionized gas containing free electrons, ions, radicals, photons, atoms and molecules with equal numbers of positive and negative charge carriers [56]. The collisions process among the particles in the plasma may occur as four elementary processes as shown below.

Scattering	$e + A \rightarrow A + e$
Excitation	$e + A \rightarrow A^{\bullet} + e$
Ionization	$e + A \rightarrow A^{+} + 2e$
Recombination	$e + A^{+} \rightarrow A + h\upsilon$

The scattering process results from elastic collision where the electron transfers a small fraction of its kinetic energy to an atom or ion. The excitation

process occurs when electron with sufficient energy lastically colliding with an atom or ion. Most of the excited states have a short life time. The excited electron decays back to its original level and then it emits a photon which is equivalent to the energy difference. If the colliding electron has sufficiently high energy, the atom or ion loses an electron to ionized process. They become one charge state. The last recombination process occurs when electron collides with ion and the electron is captured and occupies the vacancy inside the ion. Excess energy of electron is released in a form of photon.

Plasma states can be classified into two types as hot and cold plasma. Hot plasma or thermal equilibrium plasma are characterized by very high temperatures (>10000 K, close to 1 eV) of electrons and heavy particles both charged and neutral. They are close to maximal degrees of ionized (100%). For example, hot plasma are electrical arcs, plasma jets of rocket engines, nuclear fusion generated by thermonuclear reaction, etc. Cold plasma or non-thermal plasma is also partially-ionized with low degrees of ionization (10^{-4}-10%). The electric field for cold plasma is generated by power supplies such as direct current (DC), alternating current (AC), radio frequency (RF), microwave (MW) power and corona discharge. Plasma generation may also be performed at various pressures including low, high and atmospheric pressures. Cold plasma has been used in a wide variety of applications such as surface etching and polymerization due to low heat resistance of most polymeric materials [57]. However, cold plasma system involves continuous processes; therefore, the exposure of the material surfaces to the plasma is difficult to control [13, 15-17].

2.2.2 Concept of plasma polymerization

Plasma polymerization is one of the important techniques used for fabricating polymer films. Plasma species such as electrons, ions, and radials initiate the polymerization of the monomer into its corresponding polymer. Most plasma-polymerized polymers have different chemical compositions and chemical and physical properties compared to the polymers obtained from conventional polymerizations. This process offers the following advantages over conventional methods [58].

1. The starting feed gases used may not contain the type of functional groups normally associated with conventional polymerization.
2. Such films are often highly coherent and adherent to a variety of substrates, including conventional polymers, glasses, and metals.
3. Polymerization may be achieved without the use of solvents.
4. Polymer films can be easily produced with thicknesses of nanometers scale.
5. Ultrathin, “pin-hole” free films may be prepared through careful control of the polymerization parameters.

It is possible to tailor the films with respect to specific chemical functionality, thickness and other chemical and physical properties.

This uniqueness results from the reaction mechanism of the polymer-forming process. Polymer formation in plasma polymerization contains plasma activation of monomers to radicals, recombination of the formed radicals, and reactivation of the recombined molecules. Plasma-polymerized polymers do not consist of the chains with regular repeating monomer units, but instead complicated units containing cross-linked, fragmented, and rearranged units from the monomers. Figure 2.7 shows a postulated molecular model for plasma polymerized ethylene containing unsaturated groups, aromatic groups, and side branched [59]. In most cases, plasma-polymerized polymers have higher elastic modulus and do not exhibit a distinct glass transition temperature [60].

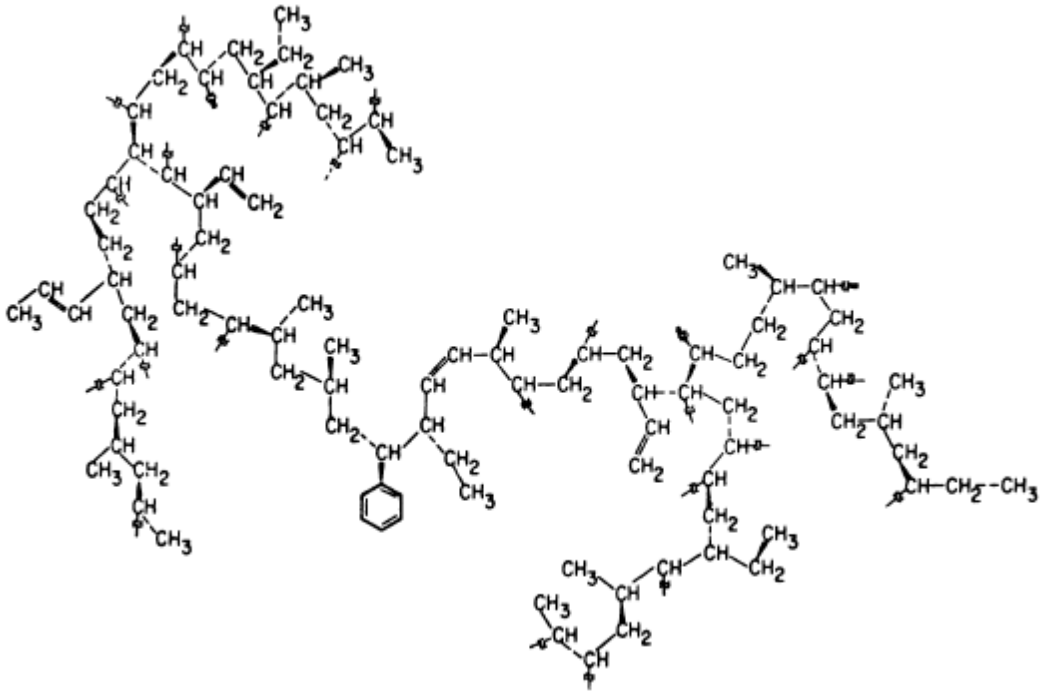

Figure 2.7 Model structure of plasma-polymerized ethylene film [59]

Many mechanisms for plasma polymerization have been proposed [61-62]. The overall polymer formation is the consequence of many complex reactions. Yusuda and others [63], proposed mechanism for plasma polymerization that take place at atmospheric pressure as shown in Figure 2.8. At low pressure, the excitation mechanism leading to the activated monomer ($M_i^{\bullet}$ or $M_k^{\bullet}$) is mostly due to collisions between the monomer ($M_i^{\bullet}$) with an electron inducing the breaking of a chemical bond leading to two radicals:

$$M_i + e^- \rightarrow M_j^{\bullet} + M_k^{\bullet} + e^-$$

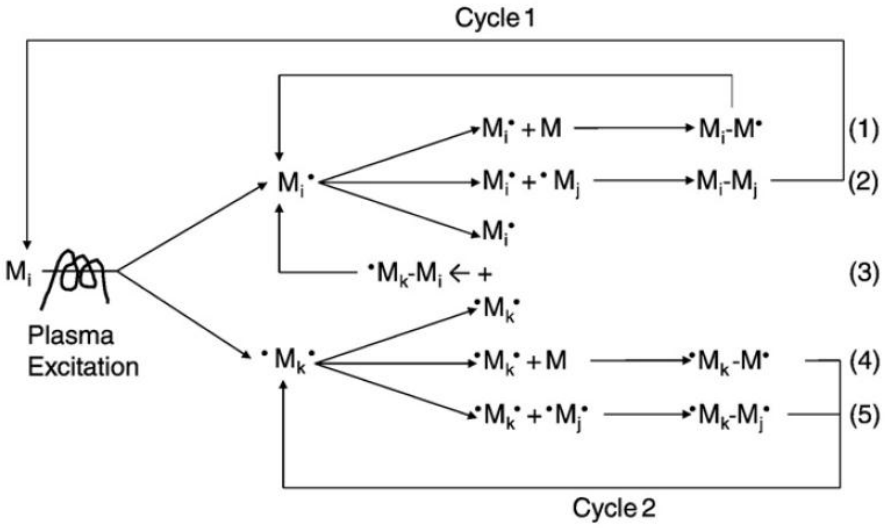

Figure 2.8 Mechanism for plasma polymerization at atmospheric pressure.

2.2.3 Plasma polymerization of aniline

Lahshmi G.B.V.S. and others [64] prepared polyaniline thin film by RF-plasma polymerization onto silicon and glass substrates. Monomer vapors were continuedly fed in vacuum chamber to polymerize by radical mechanism under plasma conditions. However, the formation of highly cross-linked and amorphous film were formed by breaking of the benzene ring and main chain leading to lower values of conductivity and solubility in solvents and high mechanical strength. Cruz, G.J. and others [65] synthesized polyaniline and I_2-doped polyaniline flims deposited on glass and metal surfaces. The characteristic peaks of polyaniline exhibited the presence of some benzene rings. The physical properties and solubility of the films suggested that the crosslinking occurred due to the continuous impact of the electrons. The electrical conductivities at 40% of relative humidity were 10^{-10} and 10^{-12} for polyaniline and 10^{-4} to 10^{-11} S/cm for I_2-doped polyaniline. Wang, J. and others [10] showed that the structure of plasma-polymerized polyaniline were different from polyanilines synthesized by chemical and electrochemical methods.

On the other hand, Merian T. and others [12] revealed low scission of aromatic ring leading to linear structures rather than cross-linked polymers when pulsed plasma was used. In addition, the oxidative doping was more efficient than the

acidic doping leading to more poralons. Airoudj A. and others [11] prepared optical sensor based on pulsed plasma-polymerized aniline for ammonia detection. Polyaniline has a low absorption coefficient which is suitable as optical sensor. However, the *ex situ* (out of the plasma reactor) doping method was used. Two types of dopants are hydrochloric acid and iodine. This method consists of introducing polyaniline deposited on substrate into an aqueous solution of hydrochloric acid or into a chamber saturated with iodine vapors.

In addition, Shepsis, L.V. and others [66] presented a model for predicting the deposition rates of plasma-polymerized aniline films using pulsed inductively-coupled plasma reactor with RF generator. The model indicates a two-step deposition mechanism: electron impact dissociation of monomer and diffusion of radicals to the substrate. Generally, radical polymerization of aniline is proposed with three major steps:

Step 1 Initiation	(Gas phase) :	$M \rightarrow M^*$
Step 2 Propagation	(Gas phase) :	$M^* + M \rightarrow M\text{-}M^*$
	(Solid phase):	$M_s^* + M \rightarrow M_s\text{-}M_s^*$
	(Solid phase):	$M_s + M^* \rightarrow M_s\text{-}M_s^*$
Step 3 Termination	(Gas phase):	$M^* + M^* \rightarrow M\text{-}M$
	(Solid phase):	$M_s^* + {}^*M \rightarrow M_s\text{-}M_s$

where M is a monomer unit, s is surface, and * represents a radical site. Plasma parameters such as initial electron temperature, electron density and dissociation cross-section are varied to confirm the data.

In this research, pulsed plasma generated from a theta-pinch device and pulsed inductively coupled plasma (PICP) device are selected for the polymerization of aniline in acidic solution since the plasma exposure is easier to control compared to conventional continuous plasma. Moreover, its process is fast and environmentally friendly. It is expected that plasma polymerization of aniline should occur in conjunction with acid doping process as shown in Scheme 2.4

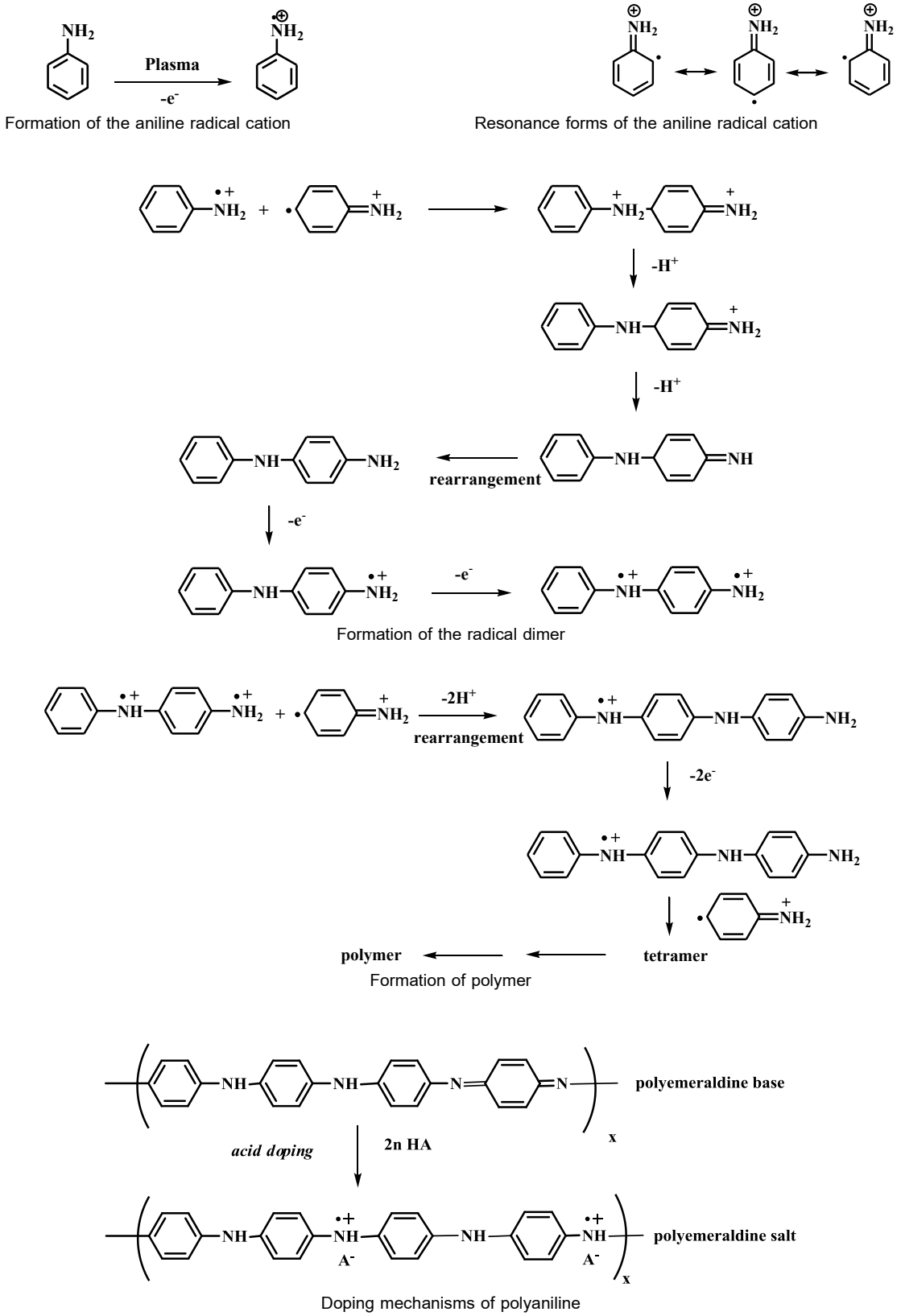

Scheme 2.4 Proposed polymerization mechanism of polyaniline doped with acid solution

2.3 Pulsed inductively coupled plasma

2.3.1 Principle of pulsed inductively coupled plasma

The principle of pulsed inductively coupled plasma (PICP) is that an increase in the magnetic field induces an electrical field opposing to the direction of the discharge current which produces plasma current that rapidly compresses toward the tube axis. The dynamic process of PICP is given in Figure 2.9. Figure 2.9(1) shows the cross-section of single turn coil and quartz tube filled with a gas. The discharge current is discharged inducing a uniform axial magnetic field as shown in Figure 2.9(2). The next step, when the axial magnetic field is changing in time, it induces an electrical field that opposes the changing current. The maximum electric field usually occurs near the wall of quartz tube and ionizes the gas; consequently, a plasma current sheath is initiated, which flows opposite to the direction of the discharge current in the coil as shown in Figure 2.9(3). The last step, the force rapidly compresses the plasma current sheath toward the tube axis, and the gas is simultaneously ionized by the confliction of the sheath as shown in Figure 2.9(4). At last, the plasma density and temperature are simultaneously enhanced [24].

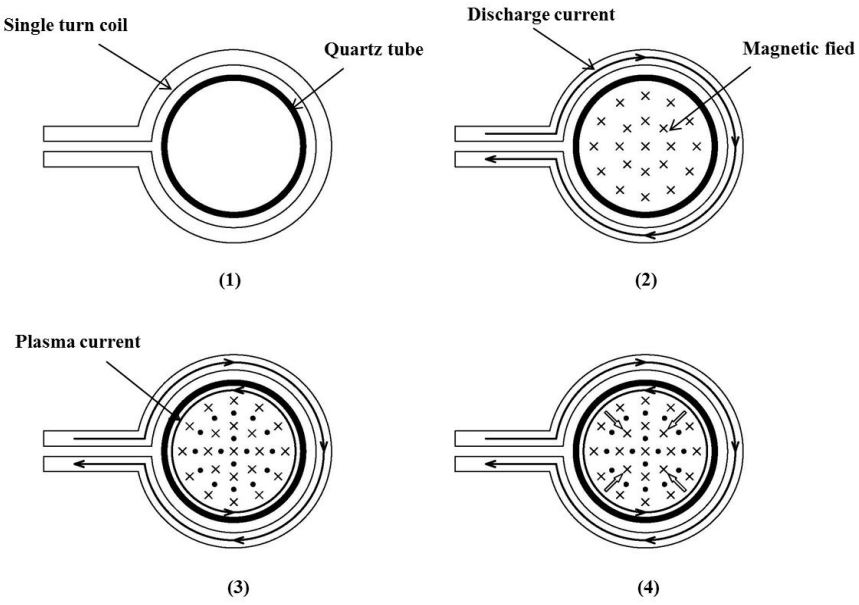

Figure 2.9 Dynamic process of PICP discharge [24]

2.3.2 Plasma generators

2.3.2.1 Theta-pinch device

Theta-pinch device is a pulsed plasma generator. It is relatively simple in its structure compared with other devices and originated from the research in the field of controlled thermonuclear fusion. It can produce a fully ionized gas having density in excess of about 10^{16} particles/cm^3 and temperature in excess of some 10^6 K (1 eV= 11,600 K). This device has been used in many applications, such as the deposition of thin films, including amorphous carbon film, α-Si film, diamond like carbon film, etc. Moreover, it has been used to process the superconducting films for lithography, which reveals its potential advantages over other methods [67].

Figure 2.10 shows the components of a theta-pinch device [67]. AC current at 50 Hz and 220 V is applied to high voltage charger for charging. Plasma generating process begins when the capacitor bank is charged to a voltage of a few ten KVs by the charger. The switching of the spark gap controlled by a triggering unit is closed, resulting in discharging to a single turn coil. A typical theta-pinch coil consists of a single-turn coil that wraps cylindrically around the quartz tube filled with a gas. This gas is released from the gas inlet after the quartz tube is pumped to vacuum condition. The gas in the quartz tube is ionized to plasma [68] based on the process as previous described in section 2.3.1.

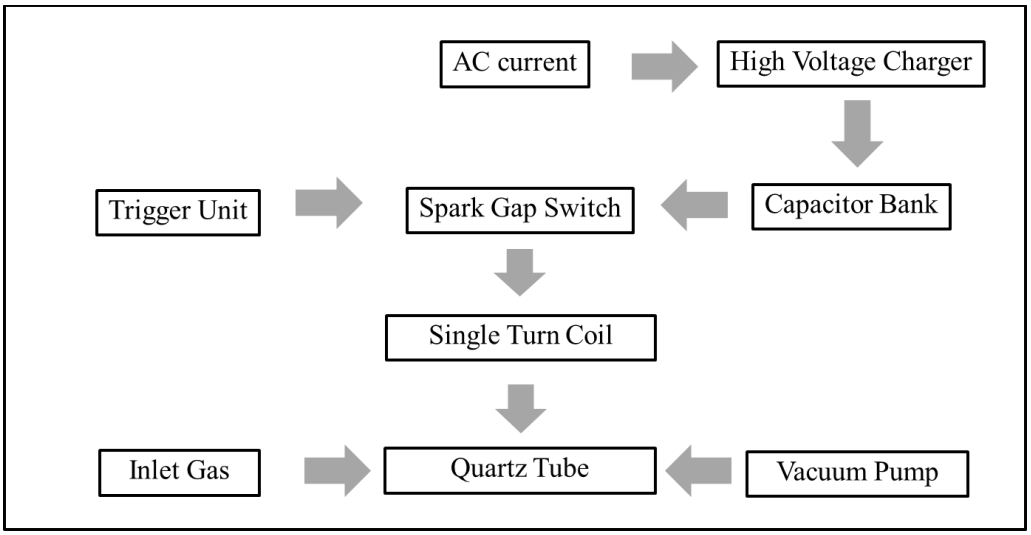

Figure 2.10 The components of a theta-pinch device

There have been several reports on surface modification of polymeric materials such as textiles and polymers with this device.

Chuenchon, S. [69] applied a theta-pinch device to modify the surface of man-made fibers, including polypropylene, polyester, and rayon fibers. The properties and morphology of treated fibers were investigated. Oxygen and nitrogen plasmas generated at different number of plasma shots caused and increased the roughness of the fiber surface. Because of this, tensile properties, linear densities and diameters of plasma-treated fibers were affected by the both type of gases and the number of plasma shots. However, the flammability of both treated and untreated fibers were comparable.

Khaymapanya, P. [70] modified surface of polyester, nylon, silk and cotton fabrics using 20 and 40 shots of plasma oxygen and nitrogen plasmas generated from a theta-pinch device. The morphology revealed etching effect on the surface and the wetting time measurement indicated the formation of hydrophilic groups on the fabric surface. It was found that oxygen and nitrogen plasma treatments did not affected dyeing properties and colorfastness to washing of highly hydrophilic silk and cotton fabrics. However, the gas type and the number of plasma shots significantly affected these two properties of PET and nylon 6 fabrics. In order to improve these properties, optimum conditions for surface modification of PET and nylon 6 fabrics were achieved when 20 and 40 shots of nitrogen plasma were applied, respectively.

Ngamaroonchote, A. [71] prepared adhesion free laminated poly(ethylene terephthalate) or PET films by surface modification of PET film using high temperature pulsed plasma generated from theta-pinch device before compression with metallized PET film at 220^{o}C. The number of plasma shot varied as 5, 10, 15 and 20 shots and three types of gas including nitrogen, oxygen and argon were used to determine the optimum condition for the treatment. When the films were stored for 7 and 14 days, the contact angle increased. The morphology revealed that after plasma treatment, average roughness of the film surface slightly decreased. It was also found that tensile strength of nitrogen plasma-treated PET films was

comparable to that of the untreated film, while those of oxygen and argon plasma-treated PET films slightly decreased. Tensile properties and adhesion strength of plasma-treated laminated films were higher than those of laminated film prepared from the untreated one. Optimum condition for the treatment was to use oxygen plasma at 5 shots in order to achieve the laminated film having overall mechanical properties better than using other conditions.

2.3.2.2 PICP device

The components of a PICP device [24] are similar to theta-pinch device as shown in Figure 2.11. The difference is that a capacity of PICP device capacitor bank is 60 μF which is higher than 12 μF of a theta-pinch device capacitor bank. The capacitor bank is charged to a voltage of 9.5 kV by high voltage charger.

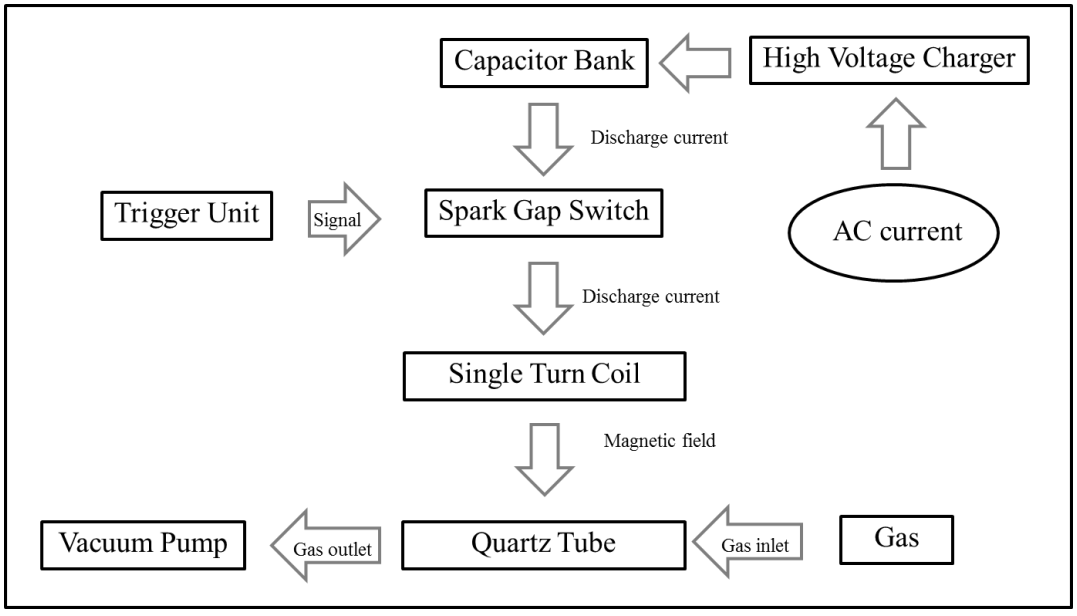

Figure 2.11 The components of a PICP device

Chaisombat, S. [24] constructed a PICP device which modified from Theta-pinch device. The plasma dynamics and plasma properties of this device were studied. It was found that the energy stored of 1.4, 2.4 and 4.32 kJ in the capacitor bank produced the discharge current of 256, 336 and 430 kA, respectively. When 2.4

kJ of the energy was stored in capacitor bank at pressure 2 Pa, the electron temperature of Ar, O_2 and N_2 plasma were 1.61, 14.7 and 11.6 eV, respectively. In addition, the simulation models showed the electron temperature decreased with the operating pressure increased. The frequency of discharge current also affected the velocity of the plasma.

CHAPTER III

EXPERIMENT

3.1 The experimental scope

This research was divided into 2 parts. The first part was to synthesize conductive polyanilines using pulsed plasma generated from a theta-pinch device and a pulsed inductively coupled plasma (PICP) device. For each experiment, aniline monomer was dissolved in an acid solution before plasma-polymerizing in both devices. The type of gas, the type of acid and the number of the plasma shots were varied. Suitable conditions and device for synthesizing a conductive polyaniline were determined after comparing the results obtained from several analyses and characterizations. The experimental procedure of this part is summarized as a flow chart in Figure 3.1(a).

The second part was to improve the properties of polyaniline by adding silver particles. The suitable device and the numbers of the plasma shots determine from the first part were selected for the synthesis of silver-added polyanilines. The type of gas and the concentration of silver nitrate were varied. Suitable conditions for the synthesis were determined after comparing the results obtained from several analyses and characterizations. The experimental procedure of this part is summarized as a flow chart in Figure 3.1(b).

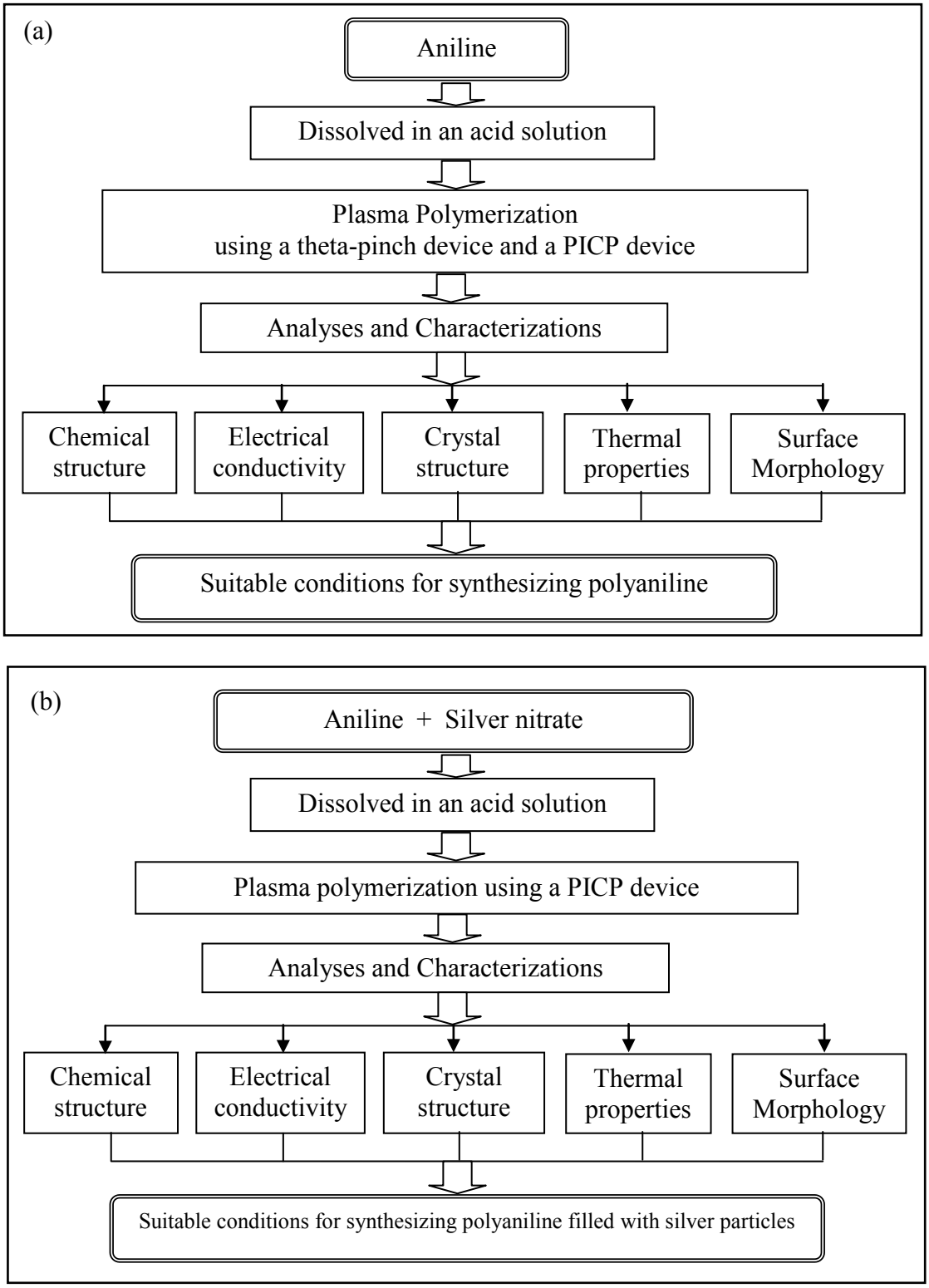

Figure 3.1 The scope of the experiment for (a) synthesis of polyaniline (b) synthesis of polyaniline filled with silver particles

3.2 Materials

Materials used in this research were summarized in Table 3.1.

Table 3.1 Information of the materials

Materials	**Grade**	**Company**
Aniline monomer	99.5% reagent grade	Sigma-Aldrich
Silver nitrate	99.0% reagent grade	Sigma-Aldrich
Sulfuric acid (H_2SO_4)	98.0% analytical grade	RCI LabScan Co., Ltd.
Hydrochloric acid (HCl)	fuming 37.0%	Merck Co., Ltd.
Nitric acid	65.0% analytical grade	RCI LabScan Co., Ltd.
Acetonitrile	99.7% analytical grade	RCI LabScan Co., Ltd.
Toluene	99.5% analytical grade	RCI LabScan Co., Ltd.
Hydrogen peroxide	30 wt% ACS reagent	Sigma-Aldrich
N-methyl-2-pyrrolidone	99.5% analytical grade	RCI LabScan Co., Ltd.
Water	Deionized water	Siam Beta Group Co., Ltd. (Thailand)
Argon gas	99.9% purity	Thai Industrial Gases Public Co., Ltd.
Oxygen gas	99.9% purity	Thai Industrial Gases Public Co., Ltd.
Nitrogen gas	99.9% purity	Thai Industrial Gases Public Co., Ltd.
Glass substrate	CAT.No. 7101. Thickness: 1-1.2 mm Dimension: 25.4 x 25.4 mm	Sail brand (Chaina)
Silicon substrate (SiO_2)	-	Supported by Thai Microelectronics Center, Thailand

3.3 Instruments

The instruments used in this research were summarized in Table 3.2.

Table 3.2 Information of the instruments

Instrument/Device	**Model/Company**
Theta-pinch device	Supported by Asian African Association for Plasma Training (AAAPT)
Pulsed inductively coupled plasma (PICP) device	Constructed by Plasma Technology and Nuclear Fusion Research Unit, Chulalongkorn University
Spin coater	SPINCOATER® Model P6700 series, Specialty Coating System, Inc. USA.
Fourier transformed infrared spectrophotometer (FTIR)	Thermo Scientific Nicolet 6700
Ultraviolet visible spectrophotometer (UV-VIS)	Analytic jena SPECORD S 1000
Field emission scanning electron microscope (FE-SEM)	Jeol JSM-7001F
X-ray diffractometer (XRD)	Bruker AXS D8
Thermogravimetric analyzer (TGA)	Mettler Toledo TGA/SDTA 851
Electrical Conductor	Two-probe method

3.4 Syntheses of polyanilines

3.4.1 Synthesis of polyaniline reference

Polyaniline used as a reference in this research was synthesized via a chemical method. Interfacial polymerization was performed in a 20 mL beaker. A 3.2 mmol of aniline was dissolved in 10 mL of toluene. This solution was slowly added to an acidic aqueous solution prepared from 10 mL of 1 M sulfuric acid and 0.8 mmol of hydrogen peroxide (H_2O_2). The polymerization was conducted without stirring at room temperature for 8 hours. The product was filtered, washed several times with water and dried.

3.4.2 Preparation of aniline solution for plasma polymerization

0.1 M of aniline in 1.0 M of a selected acid solution was prepared using deionized water and kept below 0^{o}C before use. The acids used were H_2SO_4 and HCl.

3.4.3 Coating of aniline on the substrates for plasma polymerization

Acid solutions of aniline were coated on glass and silicon substrates by a spin coater as shown in Figure 3.2. The spin coater was operated in three steps as shown in Figure 3.3 in the presence of the nitrogen gas at room temperature. Generally, the value of the final step was reported as the rate of spin coating. In this research, the spin coating rate was 2000 rpm.

Figure 3.2 SPINCOATER® Model P6700 series spin coater

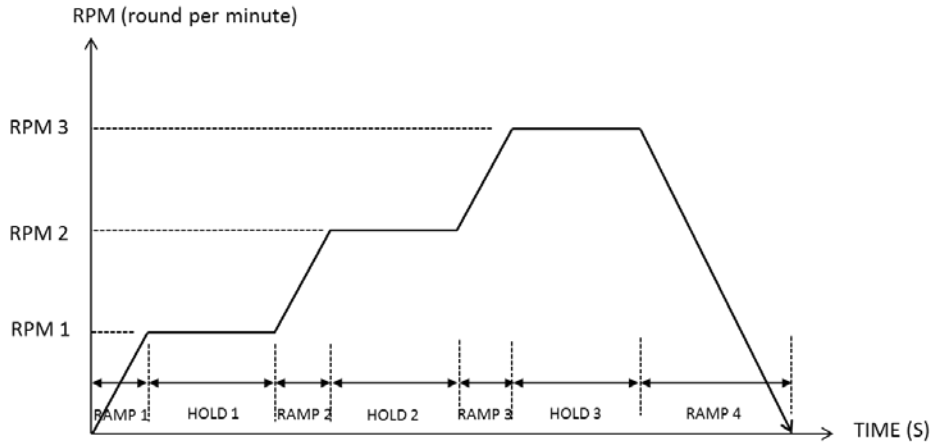

Step 1	RPM 1 RAMP 1 HOLD TIME 1	1200 rpm 0010 sec 0005 sec
Step 2	RPM 2 RAMP 2 HOLD TIME 2	1500 rpm 0010 sec 0005 sec
Step 3	RPM 3 RAMP 3 HOLD TIME 3	2000 rpm 0010 sec 0005 sec
	RAMP 4	0025 sec

Figure 3.3 Operation steps of spin coater

3.4.4 Plasma polymerization of aniline

Two pulsed plasma generators were used in this research. They were a theta-pinch device and a pulsed inductively coupled plasma (PICP) device.

3.4.4.1 Theta-pinch device

Polyanilines were synthesized using a theta-pinch device supported by Asian African Association for Plasma Training (AAAPT) as shown in Figure 3.4. Coated substrate was put on a top of the sample holder which was placed in the middle of the reaction chamber of this device as shown in Figure 3.5. Before starting the process, air and old gases had to be pumped out by the vacuum pump, thus almost a vacuum level was created in the reaction chamber. Afterward, a selected gas was introduced into this chamber. The process was done at a voltage of 20 kV, a pressure of 2 Pa and a discharge current of 125 kA. The number of the plasma shots and the type of gas were varied according to Table 3.3.

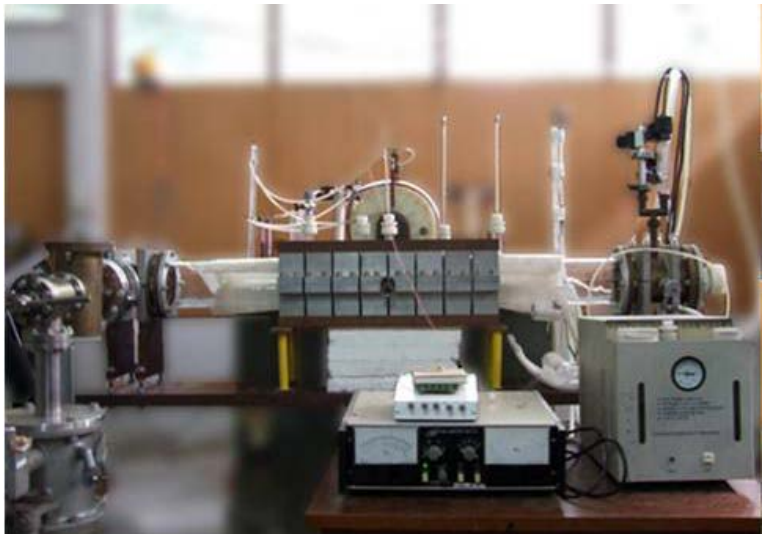

Figure 3.4 AAAPT theta-pinch device

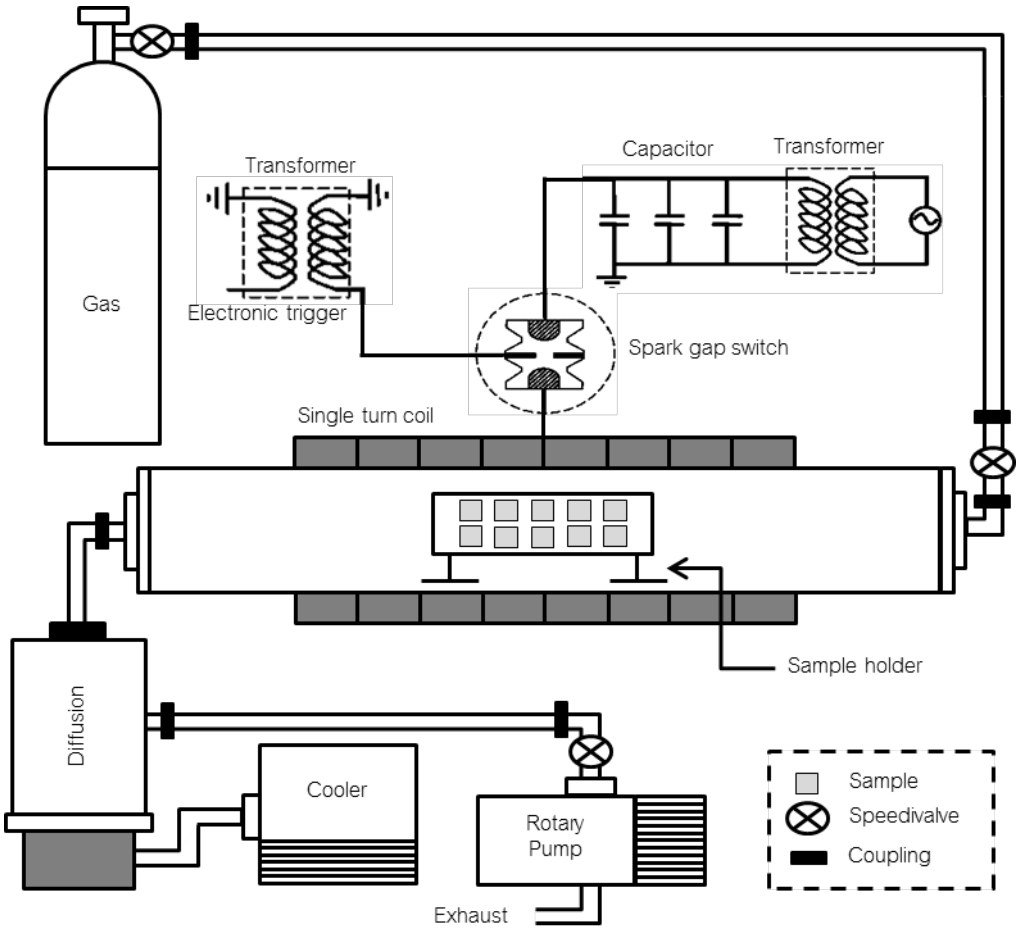

Figure 3.5 Schematic diagram and the position of the substrates in the chamber of AAAPT theta-pinch device

Table 3.3 The conditions used in the syntheses of polyanilines using AAAPT theta-pinch device

Type of gas	**Number of plasma shots**					
Argon	5	10	15	20	25	30
Oxygen	5	10	15	20	25	30
Nitrogen	5	10	15	20	25	30

3.4.4.2 Pulsed inductively coupled plasma (PICP) device

Polyanilines were synthesized using a pulsed inductively coupled plasma device as shown in Figure 3.6. Coated substrate was put on a top of sample holder which was placed in the middle of the reaction chamber of this device as shown in Figure 3.7. Before starting the process, air and old gases had to be pumped out by the vacuum pump, thus almost a vacuum level was created in the reaction chamber. Afterward, a selected gas was introduced into the chamber. The process was done at a voltage of 9.5 kV, a pressure of 2 Pa and a discharge current of 125 kA. The number of plasma shots and the type of gas were varied according to Table 3.4.

Figure 3.6 Pulsed inductively coupled plasma device

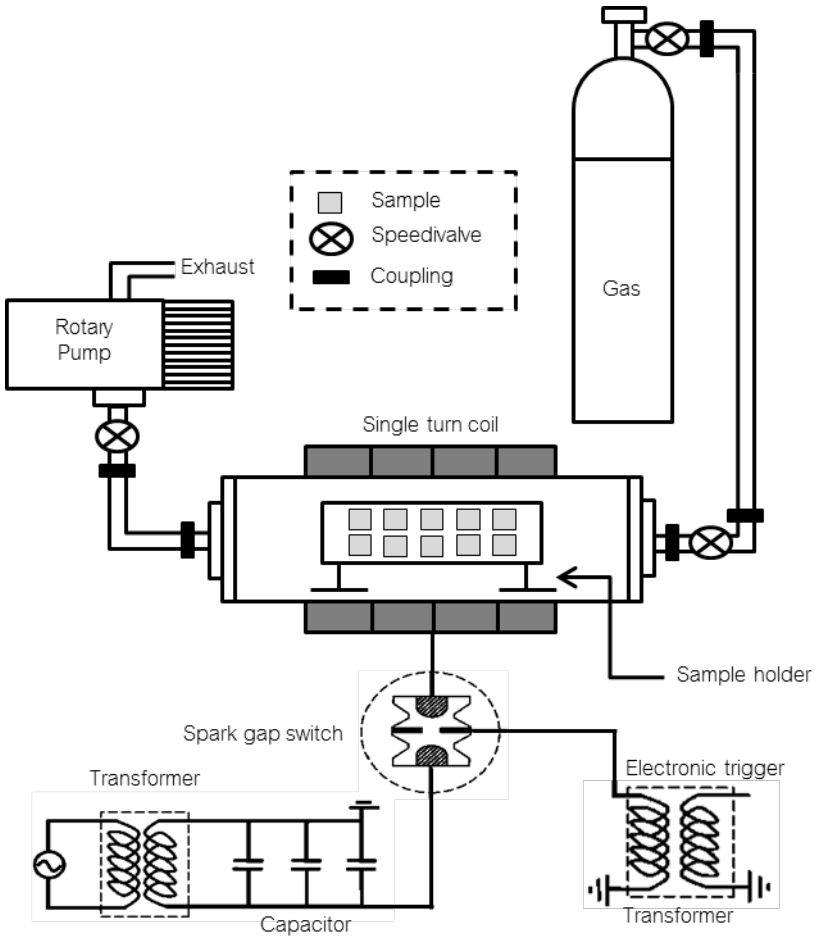

Figure 3.7 Schematic diagram and the position of the substrates in the chamber of PICP device

Table 3.4 The conditions used in the syntheses of polyanilines using PICP device

Type of gas	**Number of plasma shots**					
Argon	5	10	15	20	25	30
Oxygen	5	10	15	20	25	30
Nitrogen	5	10	15	20	25	30

After the process completed, polyanilines were removed from the chamber and dried in vacuum oven at 80^{o}C for 4 hours. All samples were rinsed with ethanol before analyses and characterizations.

3.5 Syntheses of polyanilines filled with silver particles

3.5.1 Preparation of aniline in silver nitrate solution

Silver nitrate solutions (0.5, 1.0, 1.5 and 2.0 M) in deionized water were mixed with 0.5 M of aniline in 1.0 M of HNO_3 solution. These solutions were coated on glass substrate using the spin coater with a spinning rate of 2000 rpm as was described in 3.4.2.

3.5.2 Plasma polymerization of aniline in silver nitrate solution

The polymerization was done using the process and PICP device according to 3.4.3.2. The number of plasma shots and the type of gas were varied according to Table 3.5. After the process completed, polyanilines were removed from the chamber and dried in vacumm oven at 80^{o}C for 4 hours. All samples were rinsed with water and acetonitrile before analyses and characterizations.

Table 3.5 The conditions used in the syntheses of polyanilines filled with silver particles

Silver nitrate (mol/l)	Number of plasma shots		
	Argon	Oxygen	Nitrogen
0.5	20	20	15
1.0	20	20	15
1.5	20	20	15
2.0	20	20	15

3.6 Analyses and Characterizations

3.6.1 Chemical structure

3.6.1.1 Fourier transformed infrared spectroscopy (FTIR)

The chemical structures of polyanilines and polyanilines filled with silver particles were analyzed using Thermo Scientific Nicolet 6700 FTIR spectrophotometer as shown in Figure 3.8. Infrared spectra were recorded in the wavenumber range of 4000 - 400 cm^{-1} with 64 consecutive scans and 4 cm^{-1} resolution. Samples were dispersed in potassium bromide and compressed into pellets.

Figure 3.8 Thermo Scientific Nicolet 6700 FTIR spectrophotometer

3.6.1.2 Ultraviolet-visible spectroscopy (UV-VIS)

The characteristic absorption bands of polyanilines and polyanilines filled with silver particles were determined using Analytic jena SPECORD S 100 UV-VIS spectrophotometer as shown in Figure 3.9. Each sample was dissolved in *N*-methyl-2-pyrrolidone and scanned in the wavelength range of 200-900 nm.

Figure 3.9 Analytic jena SPECORD S 100 Ultraviolet-visible spectrophotometer

3.6.2 Morphology

Field Emission scanning electron microscope (FESEM) (Jeol JSM-7001F) as shown in Figure 3.10 was used to characterize the sample morphology and the thickness of the film. All samples were coated with thin evaporated layer of gold in order to improve the conductivity and prevent the electron charging on the surface before FESEM analysis. A FESEM is microscope that works with electrons instead of light. These electrons are liberated by a Schottky type field emission source with highest resolution of 1.2 nm at 30 kV. A positive acceleration voltage of up to 0.5-30 kV on the first anode controls the amount of electron emission. FESEM photographs were taken at different angles of view with maximum magnification of 1,000,000X. Therefore, the structures observed from this technique may be as small as nanometer size.

Figure 3.10 Field emission scanning electron microscope (Jeol JSM-7001F)

3.6.3 Crystal structure

The crystal structures of polyanilines and polyanilines filled silver particles were determined by X-ray diffraction spectroscopy (XRD) using Bruker AXS model D8 diffractometer as shown in Figure 3.11 with Cu Kα radiation (40kV, 40 mA) and a wavenumber of 1.540 nm. The scan rate was 2.4^{o}/min ranging from 5^{o} to 80^{o}(2θ).

Figure 3.11 Bruker AXS model D8 X-ray diffractometer

3.6.4 Thermal properties

Thermal properties of polyanilines and polyanilines filled silver particles were investigated by Thermogravimetric analysis (TGA) using Mettler Toledo TGA/SDTA 851 as shown in Figure 3.12. About 3-10 mg of each sample were used and the instrument was operated using a heating rate of 20 ^{o}C per minute in N_2 atmosphere over a temperature range of 50-1000^{o}C.

Figure 3.12 Mettler Toledo TGA/SDTA 851 Thermogravimetric analyzer

3.6.5 Electrical conductivity

The electrical conductivity is a measure ability of a material to conduct electricity or the reciprocal of resistivity. The resistivity is determined from a material's resistance (R), which is measured using a two-probe technique as shown in Figure 3.13. The current (I) was measured as a function of the applied voltage (V) from -10 to 10 V using function generator (Hewlett PACKARD 33120A) to generate a sweep sawtooth voltage source. Both the current and voltage were detected by oscilloscope (Tektronix TDS 3034). The resistance was calculated from I-V curve. Each value reported represents an average of at least 3 readings.

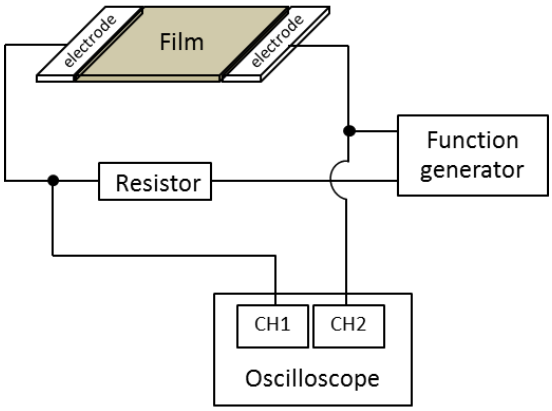

Figure 3.13 Electrical conductor using two-probe method

CHAPTER IV

RESULTS AND DISCUSSION

4.1 Characteristics and properties of polyanilines synthesized using AAAPT theta-pinch device

4.1.1 Chemical structure

In order to compare the chemical structures of plasma-synthesized polyanilines, a polyaniline synthesized using a chemical method as described in section 3.4.1 was used a reference. Its FTIR spectrum is shown in Figure 4.1. The absorption peaks at 1568 and 1484 cm^{-1} are assigned to quinoid and benzenoid rings of polyaniline, which are the characteristic peaks of polyaniline. The absorption peaks at 1306 and 1144 cm^{-1} corresponding to C-N stretching of benzenoid structure and -$N=H^{+}$- vibration, respectively confirm the presence of the emeraldine salt as shown below.

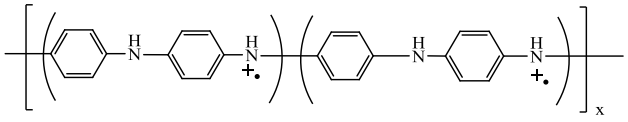

However, the absorption wavenumbers can be different depending on the methods or conditions used for the synthesis. For example, previous studies [72] reported that the spectrum of polyaniline obtained from the oxidation of aniline by hydrogen peroxide is different from the spectrum of that obtained from the oxidation by persulfate. The following phenoxazine structure is found in the former as represented by the peak at 1242 cm^{-1} of C-O-C bond. In addition, the peak at 870 cm^{-1} disappears due to 1,4-disubstitution in benzene ring. This suggests that the spectrum of this polyaniline reference may differ from the spectra of polyanilines synthesized by plasma polymerization.

Phenoxazine structure:

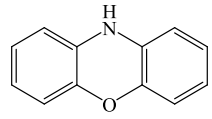

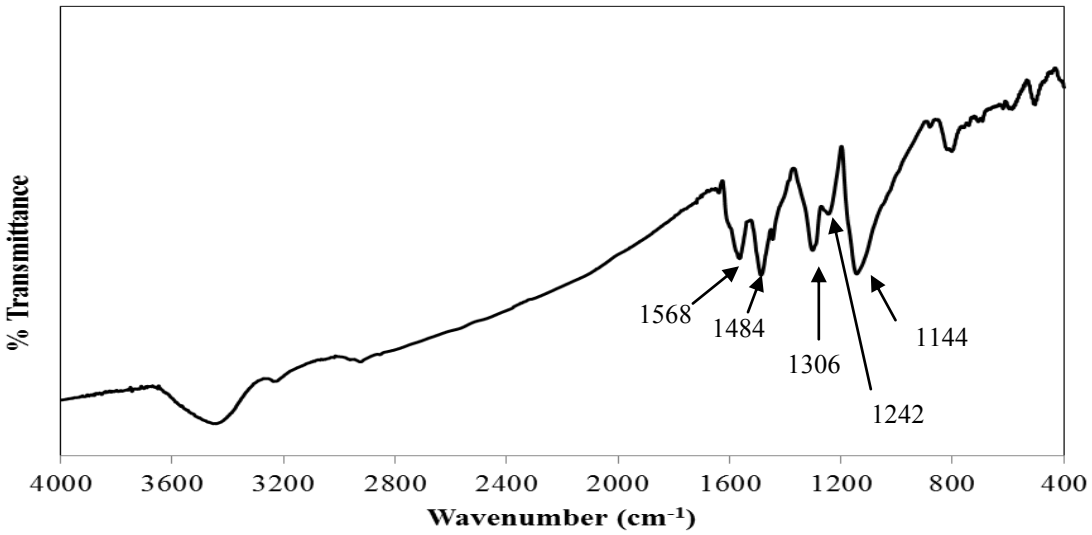

Figure 4.1 FTIR spectrum of polyaniline reference

Figure 4.2 shows FTIR spectra of polyanilines obtained from the polymerization of aniline in H_2SO_4 solution using various shots of argon plasma generated from AAAPT theta-pinch device. All polyanilines exhibit the peak at 3420 cm^{-1} which is assigned to N-H stretching of amine group. In addition, the peaks at 1630 and 1403 cm^{-1} are observed due to C-C stretching of quinoid and benzenoid rings, respectively [11,64,73]. These peaks are the characteristic peaks of polyaniline. The peaks at 1177 and 870 cm^{-1} are due to C-H aromatic and 1,4-disubstitution in benzene ring, respectively. The $–NH^+=$ vibration peak is found at 1155 cm^{-1}. In addition, the peaks at about 1690 cm^{-1} assigned to C-N stretching vibration of imine (-C=N-) [9] occur only in the spectra of polyanilines synthesized at 5, 10 and 15 shots. On the other hand, the peaks at 1200 cm^{-1} assigned to C-O stretching and the peak at 3208 cm^{-1} assigned to O-H stretching occur only in the spectra of polyanilines synthesized at 20, 25 and 30 shots. It was reported that the polymer surface can be etched by argon plasma resulting in the reactive species such as C^+, CH^+, O^-, on the etched surface. These reactive species can react with oxygen in the atmosphere after the polymer exposed to the air [74]. It is obviously seen that the highest intensities of

these peaks are found when 20 shots of argon plasma was applied. This may be because too much plasma etching at higher numbers of the plasma shots can remove the reactive species already formed on the polymer surface.

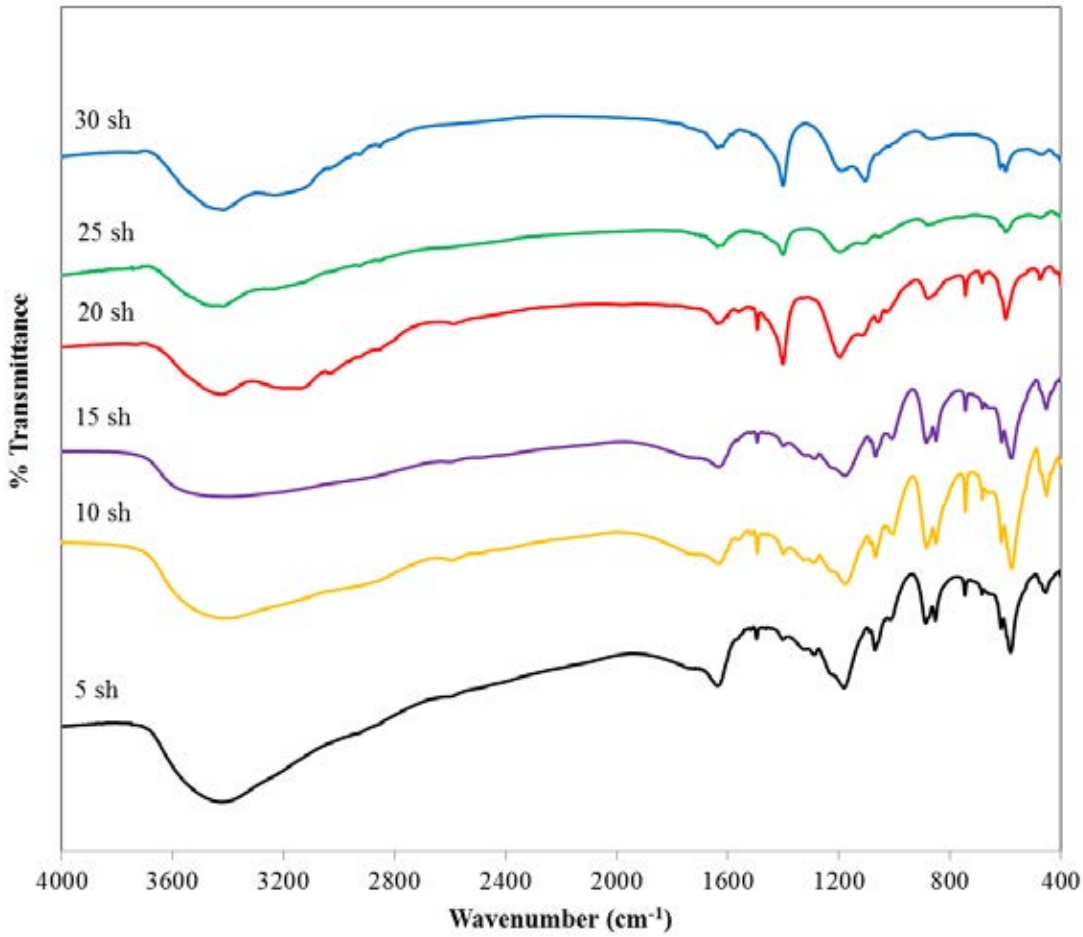

Figure 4.2 FTIR spectra of polyanilines synthesized in H_2SO_4 solution using various shots of argon plasma generated from AAAPT theta-pinch device

FTIR spectra of all polyanilines synthesized with oxygen plasma as shown in Figure 4.3 exhibit the characteristic peaks of polyaniline at about 1630 cm^{-1} and 1403 cm^{-1} which can be assigned to C=C stretching of quinoid ring and C=C stretching of benzenoid group. In addition, the peaks corresponding to C-H aromatic and C-H aromatic in plane bending at 1185 cm^{-1} and 867 cm^{-1} are observed. FTIR spectra of these polyanilines are comparable to those synthesized by conventional synthesis with slight shifts and broader peaks [75]. However, it is clearly seen that the number of the

plasma shots significantly affects the chemical structure of the obtained polyaniline. For example, as the numbers of plasma shots increase, the intensities of the peak at 1403 cm^{-1} increase while those of the peak at 867 cm^{-1} decrease. The peaks at about 1690 cm^{-1} assigned to C-N stretching vibration of imine (-C=N-) occur in the spectra of polyanilines synthesized at 10, 15 and 20 shots. Furthermore, it is obviously seen that at 20, 25 and 30 shots, the peak at 3172 cm^{-1} assigned to O-H stretching and the peak at 1100 cm^{-1} assigned to O-H deformation occur. This suggests the formation of oxygen-containing functional groups on polyaniline structure. This maybe because oxygen plasma exposure to polyaniline increases with increasing the number of the plasma shots resulting in higher reactions between the reactive species of oxygen plasma and polyaniline molecule.

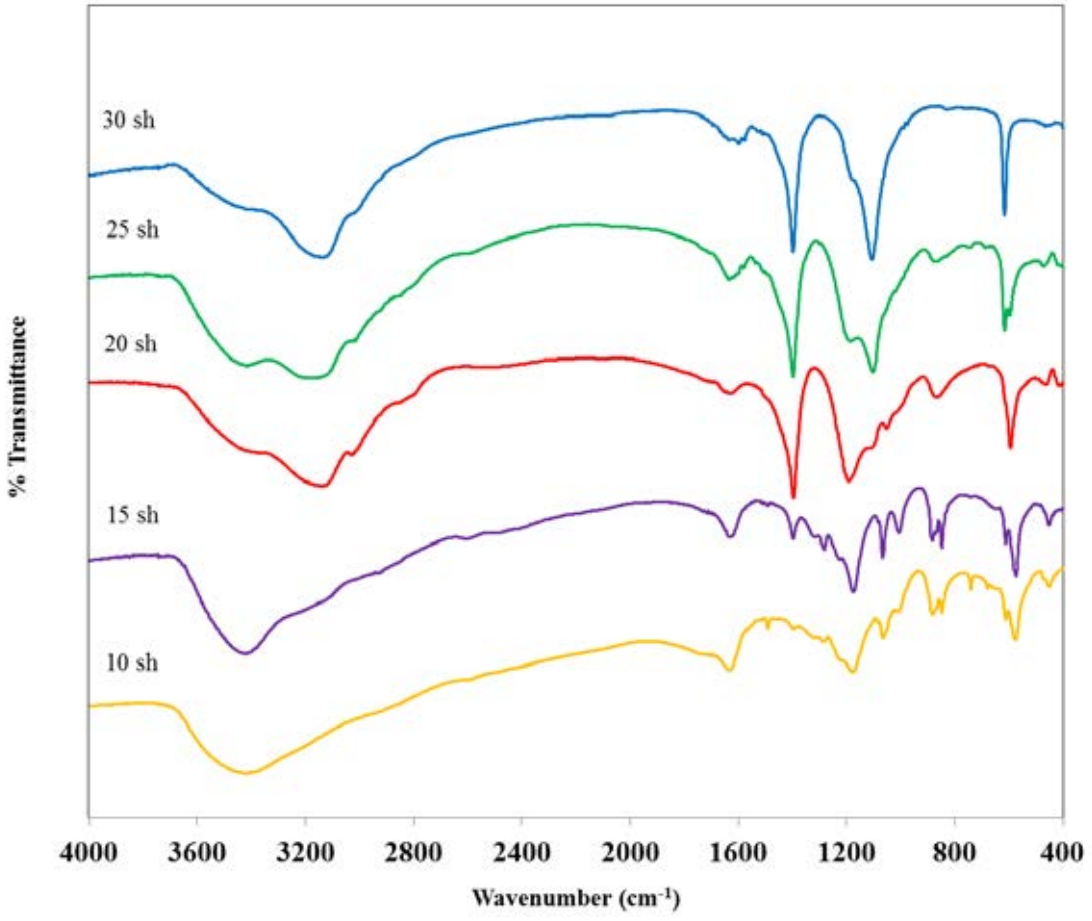

Figure 4.3 FTIR spectra of polyanilines synthesized in H_2SO_4 solution using various shots of oxygen plasma generated from AAAPT theta-pinch device

It can be observed from Figure 4.4 that all polyanilines synthesized with nitrogen plasma exhibit the peak at 1627 cm^{-1} which can be assigned to C-C stretching of quinoid ring and the peak at 1403 cm^{-1} corresponding to C-C stretching of benzenoid ring. Moreover, the peaks at 1185, 3085 and 3384 cm^{-1} attributed to C-H aromatic bending, C-H aromatic stretching and N-H stretching of amine group, respectively are also obtained. Polyanilines synthesized at 5, 10, 15 and 20 shots of plasma show the peaks at 847 cm^{-1} and 579 cm^{-1} corresponding to 1, 4-disubstitution in benzene rings [65]. All spectra also show the peaks corresponding to C-N stretching vibration of imine at about 1690 cm^{-1}. Moreover, those synthesized at 15 and 20 shots of plasma exhibit at 1283 cm^{-1} due to the formation of the sulfonic acid functional group on the benzene ring or on the nitrogen atom of polyaniline [76]. This maybe because plasma exposure at 5 and 10 shots of plasma was not enough for the functionalization whereas plasma exposure at 25 and 30 shots was too high and instead causing the etching of this functional group. On the other hand, polyanilines synthesized at 25 and 30 shots of plasma exhibit the peak at 614 cm^{-1} assigned to 1,3 disubstitution of benzene rings [65].

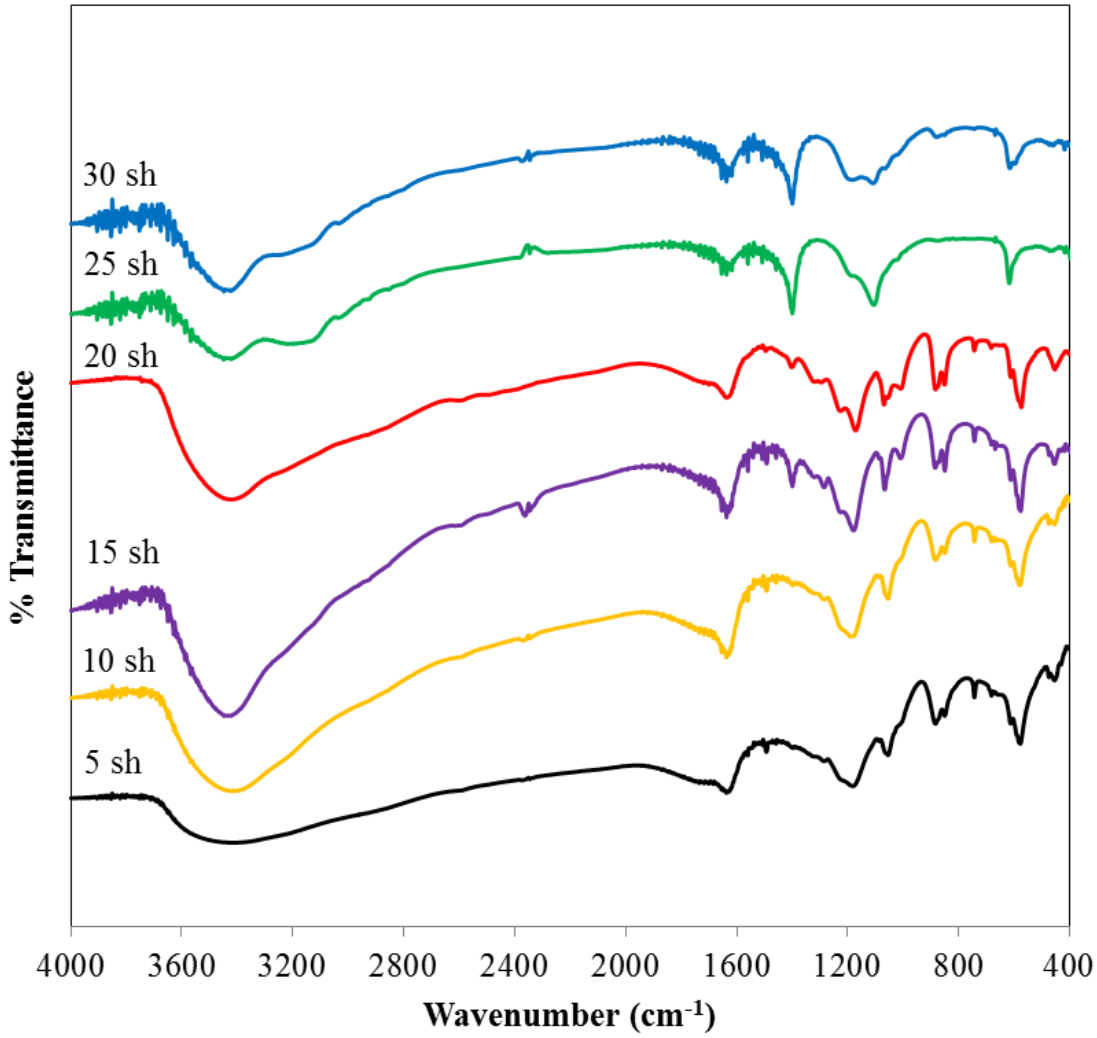

Figure 4.4 FTIR spectra of polyanilines synthesized in H_2SO_4 solution using various shots of nitrogen plasma generated from AAAPT theta-pinch device

4.1.2 Optical characteristics

From Figure 4.5, it can be seen that polyanilines synthesized using 5, 10 and 15 shots of argon plasma show only two absorption peaks at 250 and 290 nm. On the other hand, those synthesized using 20, 25 and 30 shots of argon plasma exhibit the peaks that can be assigned to π-π* transition at 260 nm, the π-polaron transition in benzene rings at 300 nm and the polaron-π* transition at 350 nm. This observation is

in good agreement with previous report [77] that polyaniline doped with H_2SO_4 presents a sharp peak with high intensity at 350 nm in the π-π* transition. This suggests that the conducting form of polyaniline possibly occurred at the plasma shots of 20, 25 and 30 shots when argon plasma was used. However, as the number of the plasma shots increases, a decrease in the absorption intensity occurs. This may be caused by the lower delocalization of the charge carrier of polyaniline leading to lower conductivity [78]. Therefore, this suggests that using 20 shots of argon plasma yielded polyaniline with highest conductivity.

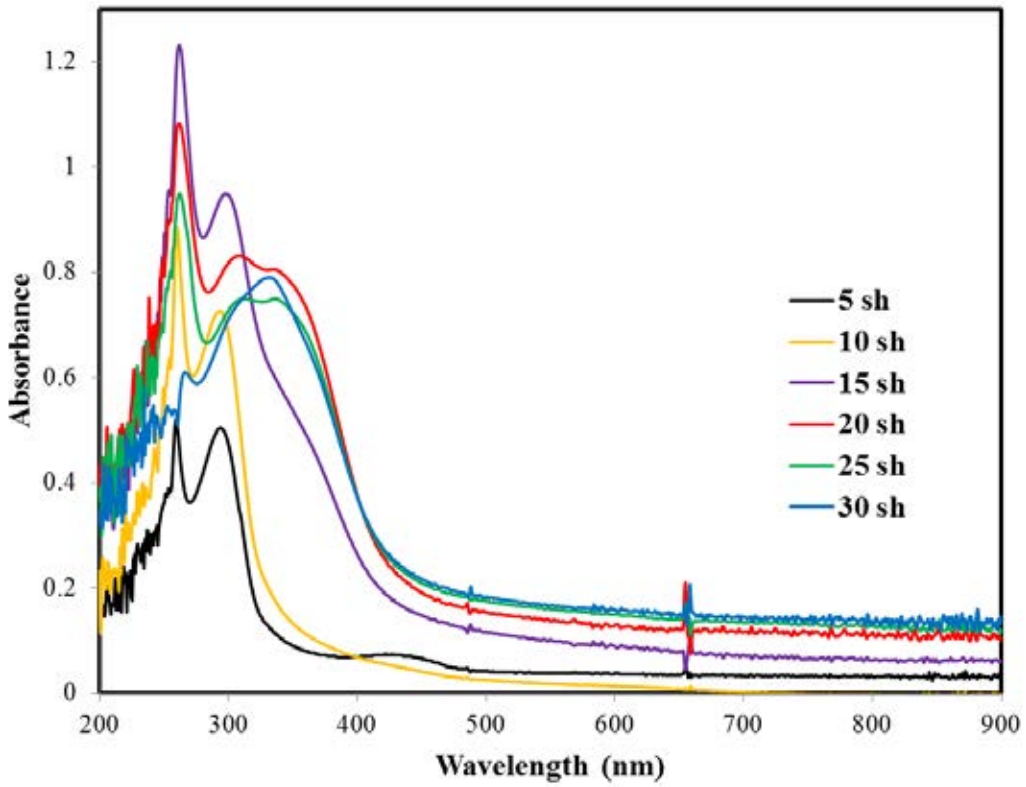

Figure 4.5 UV-VIS spectra of polyanilines synthesized in H_2SO_4 solution using various shots of argon plasma generated from AAAPT theta-pinch device

UV-VIS absorption spectra of all polyanilines synthesized using oxygen plasma are shown in Figure 4.6. They exhibit strong absorption peaks at 260 nm which can be assigned to the π-π* transition of the undoped polyaniline [12].

However, polyaniline synthesized using 20 shots of oxygen plasma shows the small absorption peak at 290 nm.

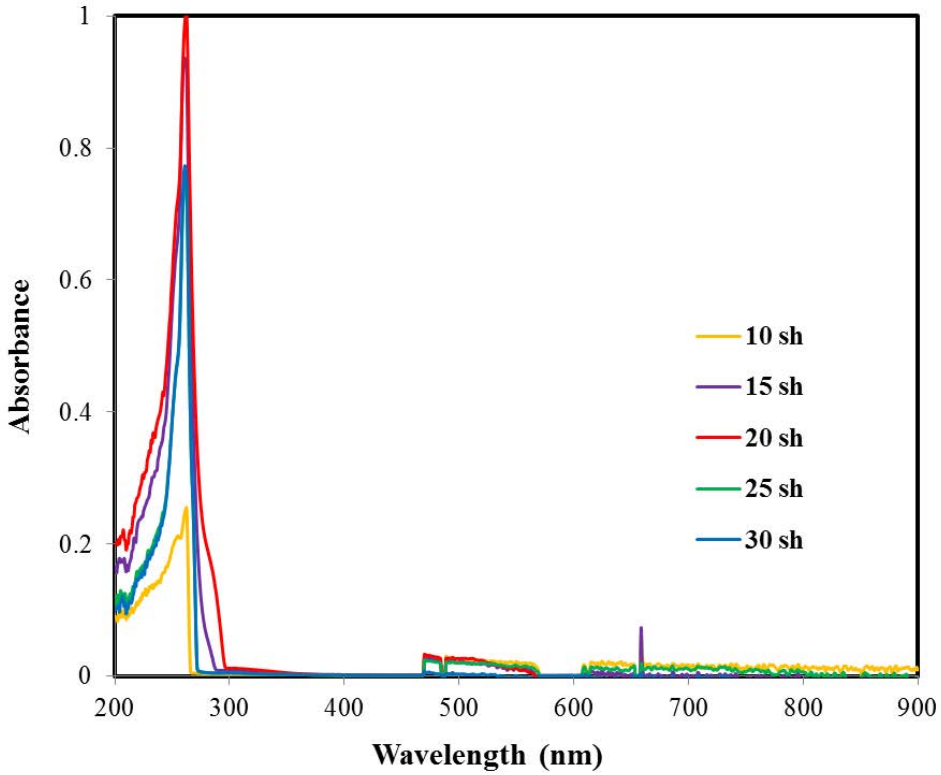

Figure 4.6 UV-VIS spectra of polyanilines synthesized in H_2SO_4 solution using various shots of oxygen plasma generated from AAAPT theta-pinch device

Figure 4.7 shows all polyanilines synthesized using nitrogen plasma exhibit two absorption peaks at 260 and ~288 nm. This provides further evidence of the difference in the structure of plasma-polymerized polyaniline and chemically-polymerized polyaniline. UV-VIS spectrum of the latter usually shows three absorption peaks of conjugated ring at 330 nm for π-π* transition, 430 nm for π-polaron transition and 800 nm for polaron-π* transition [12]. On the contradictory, the former exhibits two dominant absorption peaks shifting to shorter wavelength at around 260 and 290 nm due to shorter chain obtained in plasma polymerization [10]. In this research, polyanilines synthesized at 5 and 10 shots exhibit the absorption peak at 260 nm and 283 nm corresponding to π-π* transition of phenyl ring present in

polyaniline [79]. However, polyanilines synthesized at 15 and 20 shots show the peaks shifting from 283 nm to 285 and 288 nm, respectively. This is possibly caused by the decrease in orbital overlapping between π-electrons of phenyl rings with lone pairs of nitrogen atoms in polyaniline molecules due to their interaction with sulfonic acid groups [1]. Since the amount of sulfonic acid groups was lower in polyanilines synthesized at 25 and 30 shots of plasma, their absorption peaks reappear at 283 nm as shown in Figure 4.6.

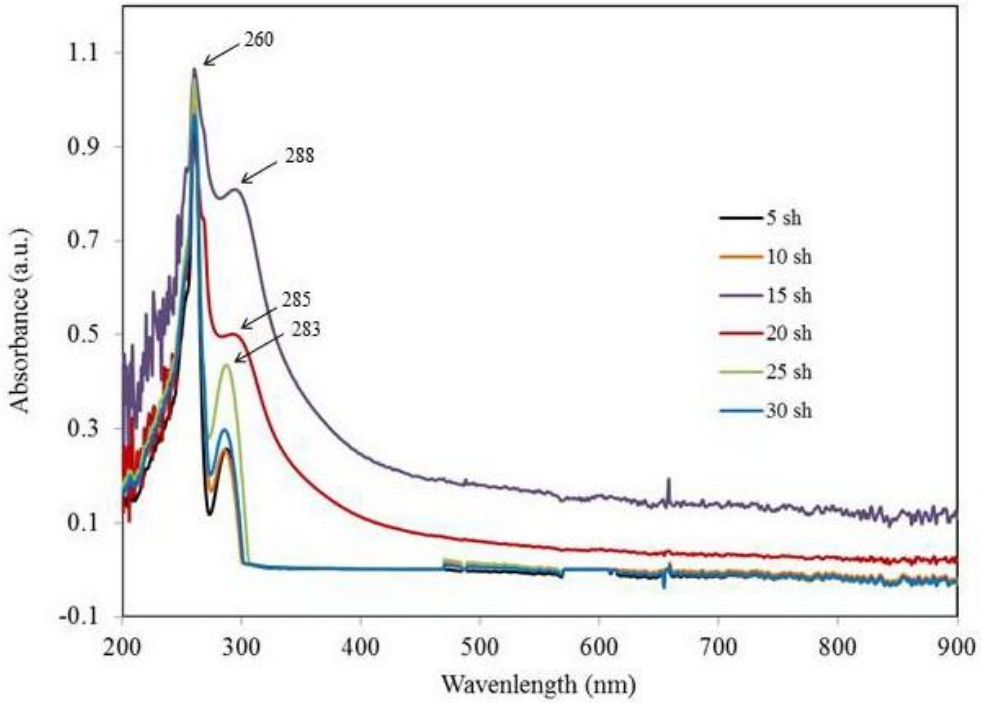

Figure 4.7 UV-VIS spectra of polyanilines synthesized in H_2SO_4 solution using various shots of nitrogen plasma generated from AAAPT theta-pinch device

4.1.3 Electrical conductivity

Electrical conductivities of polyanilines synthesized using argon and oxygen plasma are given in Tables 4.1-4.2, respectively. It is clearly seen that polyanilines synthesized using argon plasma exhibit higher conductivity than those synthesized using oxygen plasma. Normally, the undoped polyaniline exhibits the electrical

conductivity between 10^{-10} and 10^{-12} S/cm [65]. These results are caused by the differences in the chemical structure of the obtained polyanilines previously confirmed by FTIR and UV-VIS spectra. Therefore, due to the number of oxygen species on polymer surface which can lead to an increase in the electrical conductivity [80] and the presence of the polaron-π^* transition, polyaniline synthesized using 20 shots of argon plasma shows the highest conductivity.

Table 4.1 Electrical conductivities of polyanilines synthesized in H_2SO_4 solution using various shots of argon plasma generated from AAAPT theta-pinch device

The number of plasma shots	Conductivity [S/cm]
5	$(2.44 \pm 0.59) \times 10^{-8}$
10	$(5.85 \pm 0.57) \times 10^{-8}$
15	$(7.52 \pm 0.40) \times 10^{-8}$
20	$(8.89 \pm 1.66) \times 10^{-7}$
25	$(5.85 \pm 1.34) \times 10^{-7}$
30	$(1.31 \pm 0.52) \times 10^{-7}$

Table 4.2 Electrical conductivities of polyanilines synthesized in H_2SO_4 solution using various shots of oxygen plasma generated from AAAPT theta-pinch device

The number of plasma shots	Conductivity [S/cm]
10	$(1.18 \pm 0.01) \times 10^{-10}$
15	$(1.35 \pm 0.14) \times 10^{-10}$
20	$(3.35 \pm 5.24) \times 10^{-9}$
25	$(4.85 \pm 1.46) \times 10^{-10}$
30	$(1.74 \pm 0.20) \times 10^{-10}$

However, polyaniline synthesized using nitrogen plasma did not form the dry film. Consequently, the measurement of electrical conductivity, the analyses of crystal structure and thermal properties of these films cannot be done.

4.1.4 Crystal structure

Due to its highest conductivity, polyaniline synthesized using 20 shots of argon plasma was selected for XRD analysis. X-ray diffraction pattern of this polymer in Figure 4.8 reveals a semi-crystalline structure. The crystalline peaks of polyaniline appear at 15^{o} and 34^{o}, which can be assigned to the (001) and (004) reflections, respectively [81]. A broad peak centered at about $2\Theta=25^{o}$ of the doped polyaniline chain is amorphous in structure [82]. For polyaniline synthesized using oxygen plasma at 20 shots also exhibit the similar x-ray diffraction pattern as show in Figure 4.9.

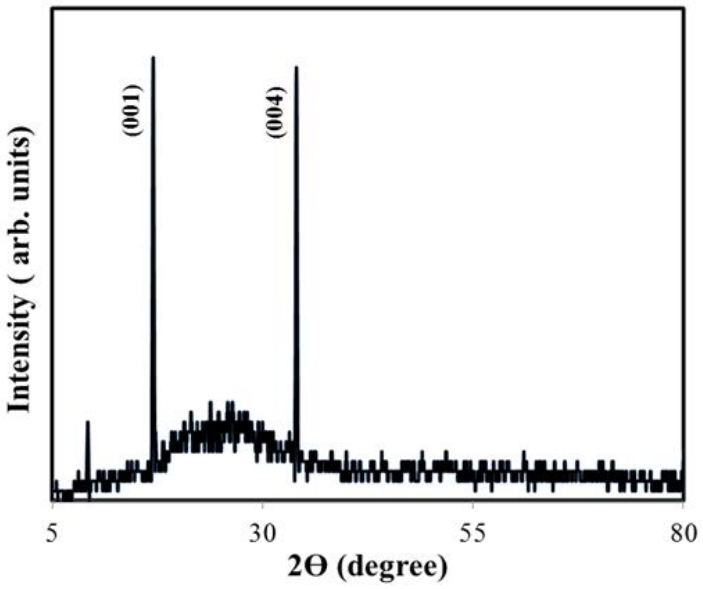

Figure 4.8 XRD spectrum of polyaniline synthesized in H_2SO_4 solution using 20 shots of argon plasma generated from AAAPT theta-pinch device

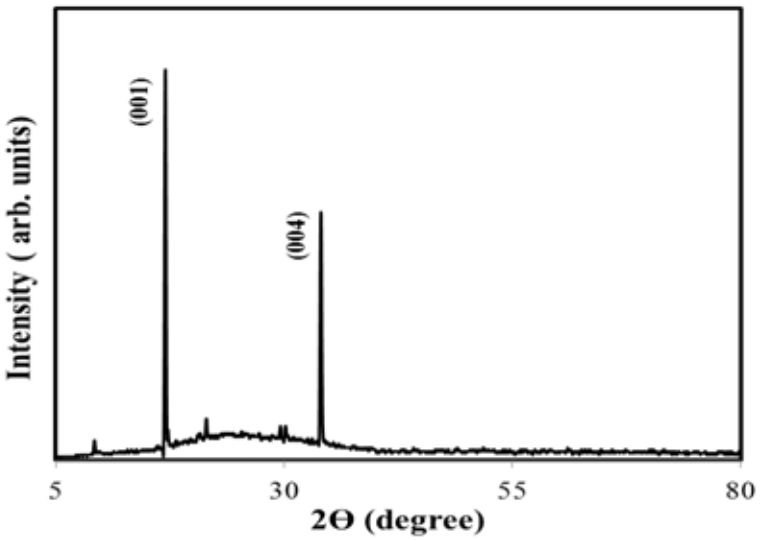

Figure 4.9 XRD spectrum of polyaniline synthesized in H_2SO_4 solution using 20 shots of oxygen plasma generated from AAAPT theta-pinch device

4.1.5 Thermal properties

Figure 4.10 shows TGA curve of polyaniline synthesized using 20 shots of argon plasma exhibiting three major stages of weight losses. The first stage at low temperature results from moisture evaporation. The weight loss at 270^{o}C indicates the degradation of the polymer chain. After that, the weight loss in the third region ranging from 420 to 700 ^{o}C may be attributed to the breakaway of dopant or oligomer. Thermal stability of plasma-polymerized polyaniline can be explained from the presence of the quinoid and benenoid structure in polymer chain [24].

TGA thermogram of polyaniline synthesized using 20 shots of oxygen plasma is given in Figure 4.11. The first decomposition part with the weight loss around 2%-5% is at about 100-180 ^{o}C due to water and solvents molecule. Rapid weight loss of the polymer structure occurs at 262 ^{o}C and the residue products begin to decompose at 780 ^{o}C.

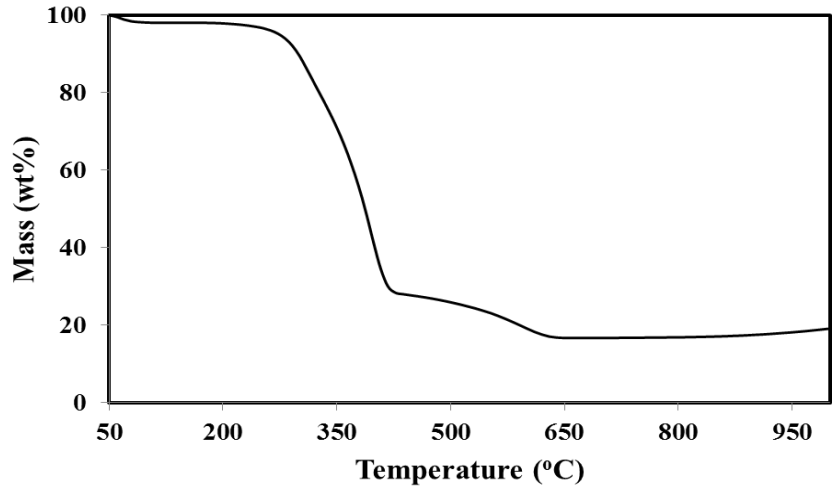

Figure 4.10 TGA thermogram of polyaniline synthesized in H_2SO_4 solution using 20 shots of argon plasma generated from AAAPT theta-pinch device

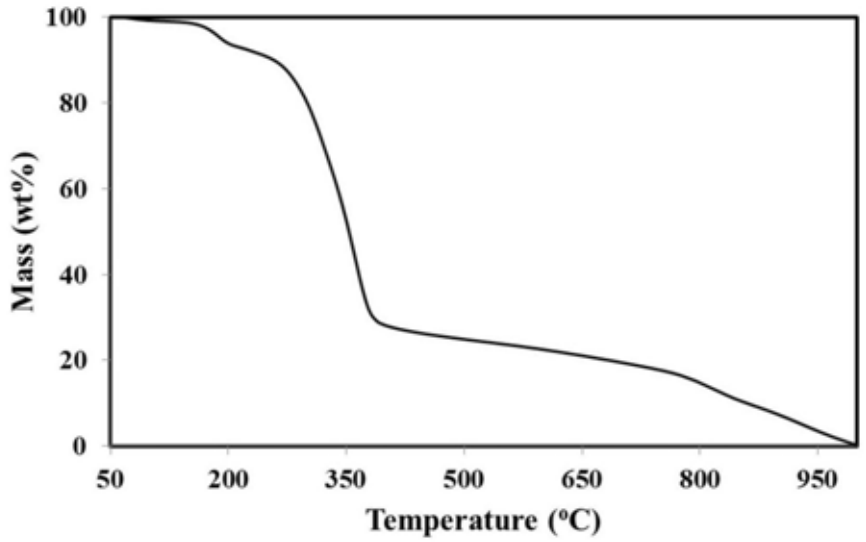

Figure 4.11 TGA thermogram of polyaniline synthesized in H_2SO_4 solution using 20 shots of oxygen plasma generated from AAAPT theta-pinch device

All the results suggest that polyanilines synthesized in H_2SO_4 solution using argon plasma at 20, 25 and 30 shots have the structure of emeraldine salt as confirmed by FTIR and UV-VIS spectra and conductivity measurement. On the other hand, those synthesized with 5, 10 and 15 shots exhibit the emeraldine base structure due to

the appearrance of the peaks attributed to -C=N- and -NH as shown in FTIR spectra and the absorption bands of the undoped structure as observed by UV-VIS spectra. These two structures are shown below:

Emeraldine salt:

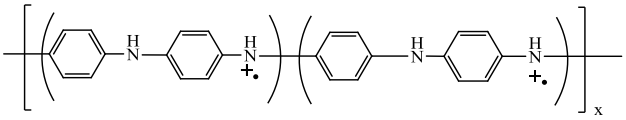

(green color)

Emeraldine base:

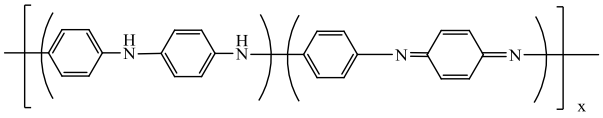

(brown color)

In the cases of oxygen and nitrogen, all the results suggest that all polyanilines have mainly the undoped structure of emeraldine base as confirmed by FTIR and UV-VIS spectra and conductivity measurement.

4.2 Characteristics and properties of polyanilines synthesized using PICP device

4.2.1 Polyanilines synthesized in sulfuric solution

4.2.1.1 Chemical structure

FTIR spectra of polyanilines synthesized in H_2SO_4 solution using various shots of argon plasma generated from PICP device are displayed in Figure 4.12 and their peaks are interpreted and given in Table 4.3. The peaks of C-H aliphatic absorption at around 2900-3000 cm^{-1} are observed in the spectra of polyanilines synthesized using the plasma shots more than 5 shots. This may be caused by a partial fragmentation of the benzene ring due to plasma etching. The characteristic peaks of polyaniline exhibit at about 1612 and 1400 cm^{-1} due to C=C stretching of quiniod ring and C=C stretching of benzeniod group, respectively. This result suggests the presence of the conjugated system and aromatic cyclic structure in the polymer chain. The peaks assigned to C-H aromatic and 1,4-disubstitution in benzene ring at 1166 and 854 cm^{-1} are slightly observed in the spectra of polyanilines

synthesized using 20, 25 and 30 shots. In addition, these polymers also exhibit the peaks assigned to O-H deformation at 3203 cm^{-1}. As previously mentioned, the polymer surface can be etched by argon plasma resulting in the reactive species such as C^+, CH^+, O^-, on the etched surface. These reactive species can react with oxygen in the atmosphere after the polymer exposed to the air. It is obviously seen that the highest intensities of these peaks are found when 20 shots of argon plasma was applied. This may be because too much plasma etching at higher numbers of the plasma shots can remove the reactive species already formed on the polymer surface.

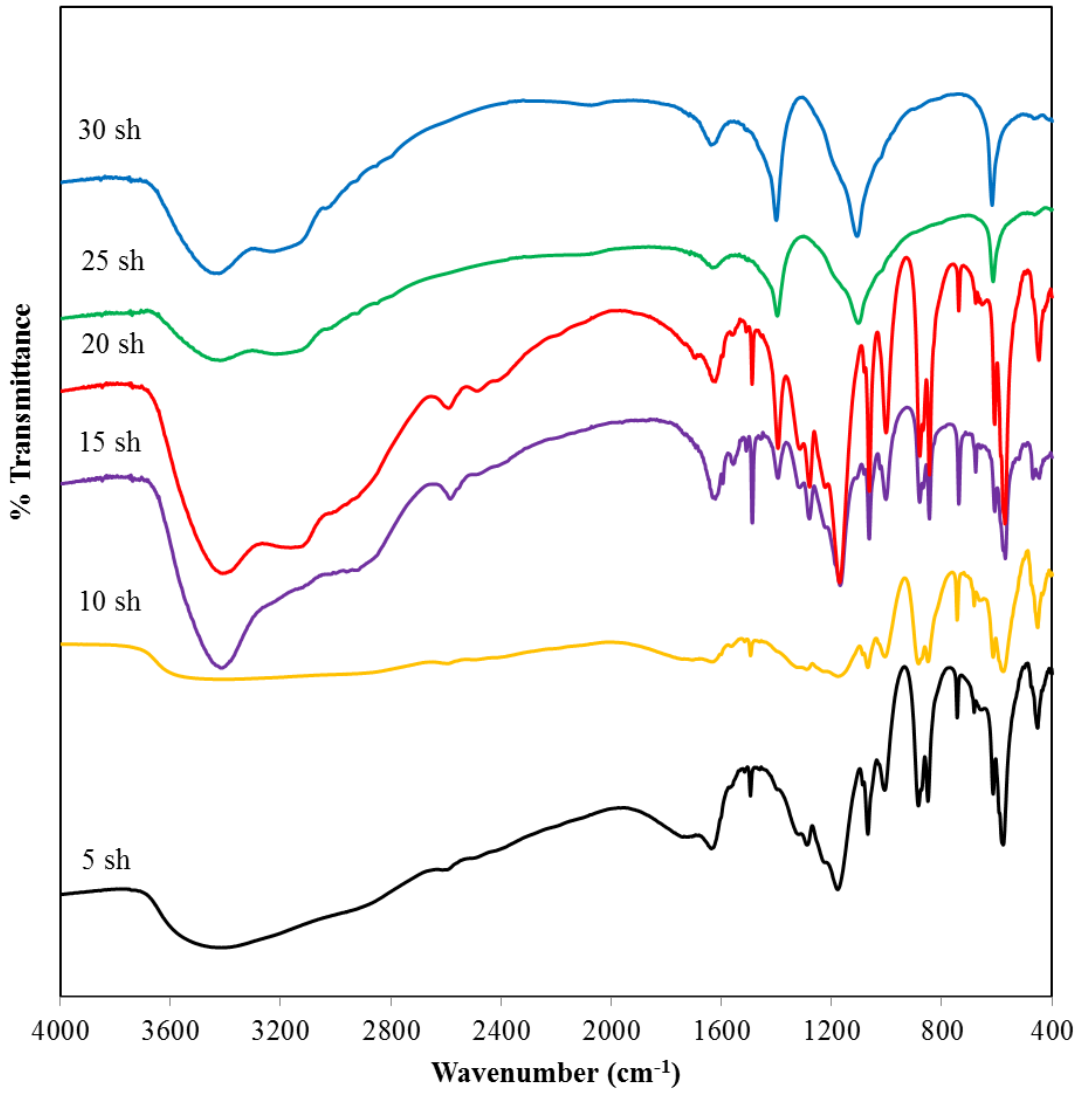

Figure 4.12 FTIR spectra of polyanilines synthesized in H_2SO_4 solution using various shots of argon plasma generated from PICP device

Table 4.3 Interpretation of FTIR spectra of polyanilines synthesized in H_2SO_4 solution using various shots of argon plasma generated from PICP device

Assignments	Wavenumber (cm^{-1})					
	5	**10**	**15**	**20**	**25**	**30**
1. N-H stretching of aromatic amine	3413	3426	3405	3413	3421	3413
2. O-H deformation	-	-	3203	3203	3219	3219
3. C-H stretching of aromatic	3014	3077	3104	3097	3097	3091
4. C-H stretching of aliphatic	2905	2902	2915	2908	2958	2985
5. C=C stretching of quinoid ring	1617	1612	1614	1612	1612	1612
6. C=C stretching of benzenoid group	1378	1378	1400	1400	1400	1400
7. $C\text{-}N^{+\bullet}$ stretching vibration in the polaron structure	-	-	1238	1238	-	-
8. C-H bending of aromatic	1164	1164	1164	1166	-	-
9. SO_4^{2-} group of polyaniline	1064	1064	1064	1064	1079	1087
10. C-H out of plane blending (1,4-disubstitution in benzene ring)	879 572	848 570	854 572	854 572	- -	- -
11. C-H out of plane blending (1,3-disubstitution in benzene ring)	-	-	-	-	607	611

FTIR spectra of polyanilines synthesized in H_2SO_4 solution using various shots of oxygen plasma generated from PICP device are shown in Figure 4.13 and their peaks are interpreted and given in Table 4.4. The similar characteristic peaks as in the spectra of those synthesized using argon plasma are observed. In addition, the peaks corresponding to O-H stretching and O-H deformation at about 3195 cm^{-1} and 1095 cm^{-1}, respectively are present in the spectra of polyanilines synthesized using 25 and 30 shots. This suggests the formation of oxygen-containing functional groups on polyaniline structure due to higher oxygen plasma exposure to polyaniline with increasing the number of the plasma shots.

FTIR spectra of polyanilines synthesized in H_2SO_4 solution using various shots of nitrogen plasma generated from PICP device are shown in Figure 4.14 and their peaks are interpreted and given in Table 4.5. The similar characteristic peaks as in the spectra of those synthesized using argon plasma are observed. In addition, those synthesized at 15 and 20 shots of plasma exhibit the peak at 1283 cm^{-1} due to the formation of the sulfonic acid functional group on the benzene ring or on the nitrogen atom of polyaniline. This maybe because plasma exposure at 5 and 10 shots of plasma was not enough for the functionalization whereas plasma exposure at 25 and 30 shots was too high and instead causing the etching of this functional group. On the other hand, polyanilines synthesized at 25 and 30 shots of plasma exhibit the peak at 614 cm^{-1} assigned to 1,3 disubstitution of benzene rings.

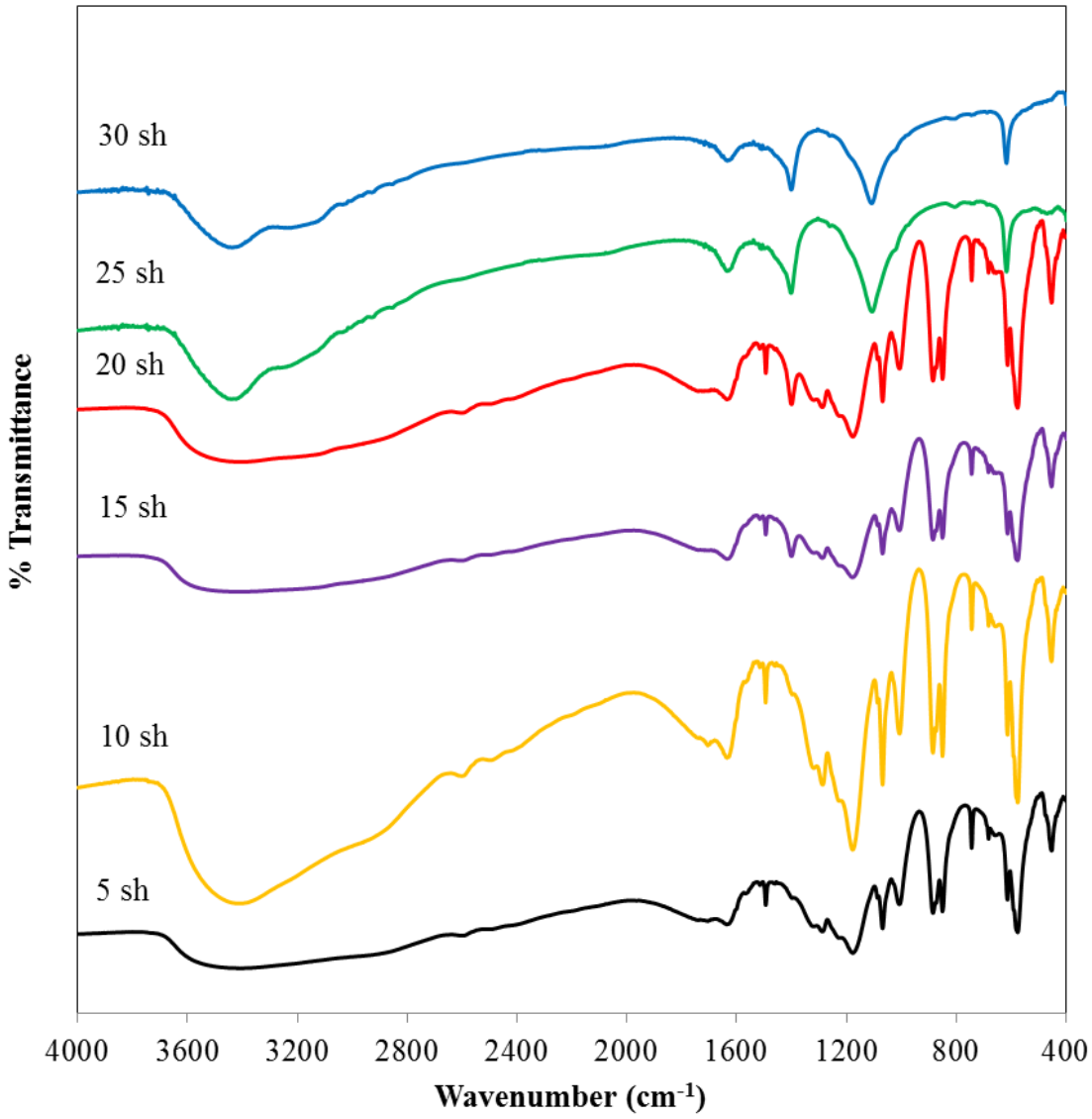

Figure 4.13 FTIR spectra of polyanilines synthesized in H_2SO_4 solution using various shots of oxygen plasma generated from PICP device

Table 4.4 Interpretation of FTIR spectra of polyanilines synthesized in H_2SO_4 solution using various shots of oxygen plasma generated from PICP device

Assignments	Wavenumber (cm^{-1})					
	5	**10**	**15**	**20**	**25**	**30**
1. N-H stretching of aromatic amine	3413	3414	3421	3421	3413	3413
2. O-H stretching	-	-	-	3208	3219	3219
3. C-H stretching of aromatic	3014	3014	3015	3015	3015	3015
4. C-H stretching of aliphatic	2912	2902	2902	2902	-	-
5. C=C stretching of quinoid ring	1614	1617	1617	1617	1600	1600
6. C=C stretching of benzenoid group	1378	1378	1400	1400	1390	1390
7. C-H bending of aromatic	1164	1164	1164	1164	-	-
8. SO_4^{2-} group of polyaniline	1064	1064	1064	1064	1078	1078
9. C-H out of plane blending	846	848	848	848	-	-
(1,4-disubstitution in benzene ring)	572	570	572	572	-	-
10. C-H out of plane blending (1,3-disubstitution in benzene ring)	-	-	-	-	607	607

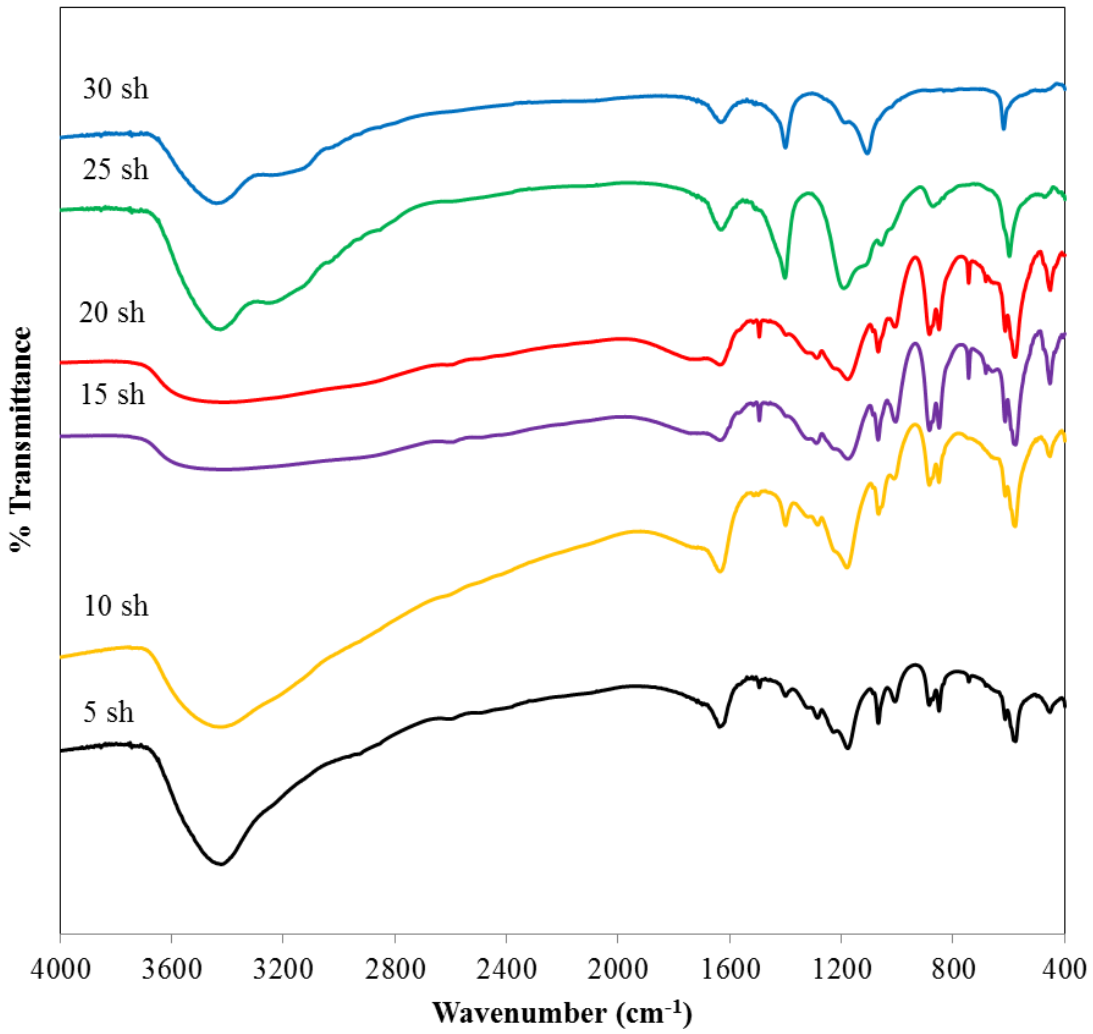

Figure 4.14 FTIR spectra of polyanilines synthesized in H_2SO_4 solution using various shots of nitrogen plasma generated from PICP device

Table 4.5 Interpretation of FTIR spectra of polyanilines synthesized in H_2SO_4 solution using various shots of nitrogen plasma generated from PICP device

Assignments	Wavenumber (cm^{-1})					
	5	**10**	**15**	**20**	**25**	**30**
1. N-H stretching of aromatic amine	3394	3394	3394	3394	3394	3394
2. O-H stretching	-	-	-	-	3228	3214
3. C-H stretching of aromatic	3012	3012	3012	3012	3012	3012
4. C-H stretching of aliphatic	-	-	-	-	-	-
5. C=C stretching of quinoid ring	1617	1617	1617	1617	1617	1617
6. C=C stretching of benzenoid group	1388	1388	1398	1398	1398	1398
7. C-H bending of aromatic	1160	1160	1160	1160	1160	1160
8. SO_4^{2-} group of polyaniline	1064	1064	1064	1064	1064	1064
9. C-H out of plane blending	844	844	844	844	833	-
(1,4-disubstitution in benzene ring)	570	570	570	570	-	-
10. C-H out of plane blending (1,3-disubstitution in benzene ring)	-	-	-	-	600	608

4.2.1.2 Optical characteristics

As shown in Figure 4.15, polyanilines synthesized using 5 and 10 shots of argon plasma exhibit only two UV-VIS absorption peaks at 260 and 290 nm which are attributed to π-π* transition and π-polaron transition, respectively. On the other hand, polyaniline synthesized using 15 and 20 shots of argon plasma show three

absorption peaks at about 260, 290 and 435 nm which can be assigned to π-π* transition, the π-polaron transition in benzene rings and the formation of polarons due to doped polyaniline [83], respectively. For those synthesized using 25 and 30 shots, three absorptions peaks are observed, but the last peak is shifted to 345 nm corresponding to the polarons of polyaniline emeridine base. This may be because at these conditions, plasma exposure was too high leading to the scission of polyaniline conjugated chain whereas plasma exposure at 5 shots was not enough to form long conjugated structure.

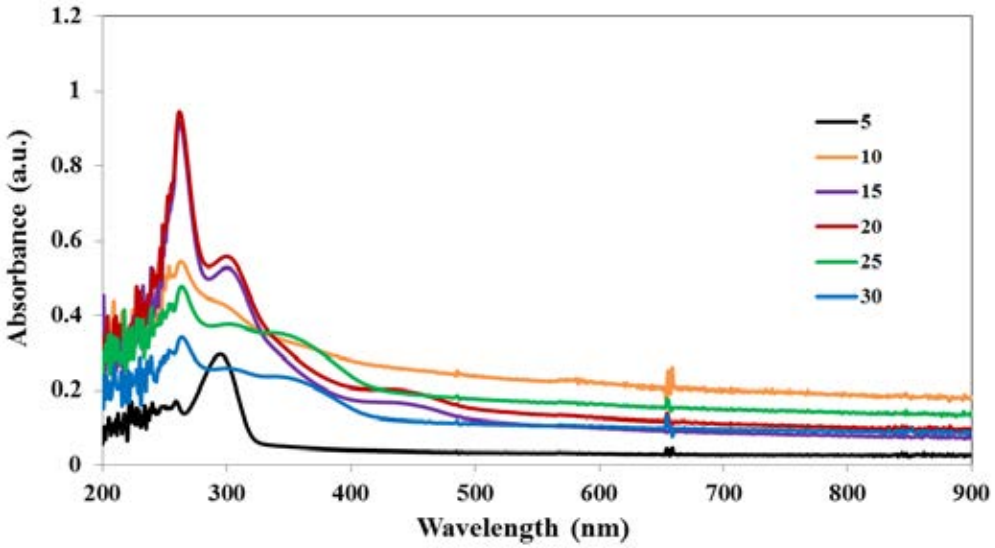

Figure 4.15 UV-Vis spectra of polyanilines synthesized in H_2SO_4 solution using various shots of argon plasma generated from PICP device

UV-VIS spectra of polyanilines synthesized in H_2SO_4 solution using various shots of oxygen and nitrogen plasma are shown in Figures 4.16 and 4.17, respectively. It can be seen that all polymers exhibit two absorption peaks at 260 and 290 nm which can be assigned to π-π* transition and π-polaron transition, respectively. While the former shows the highest intensity when 20 shots was used, the latter shows the highest intensity when 15 shots was used.

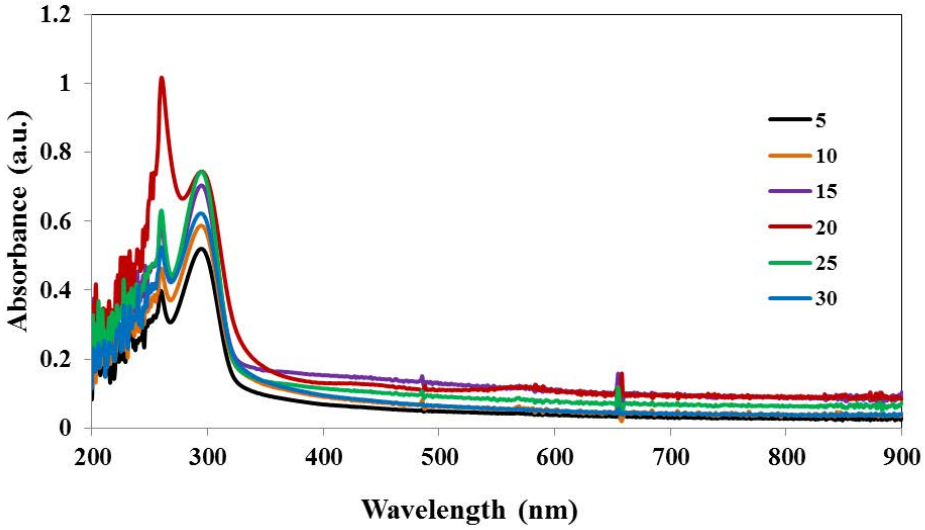

Figure 4.16 UV-Vis spectra of polyanilines synthesized in H_2SO_4 solution using various shots of oxygen plasma generated from PICP device

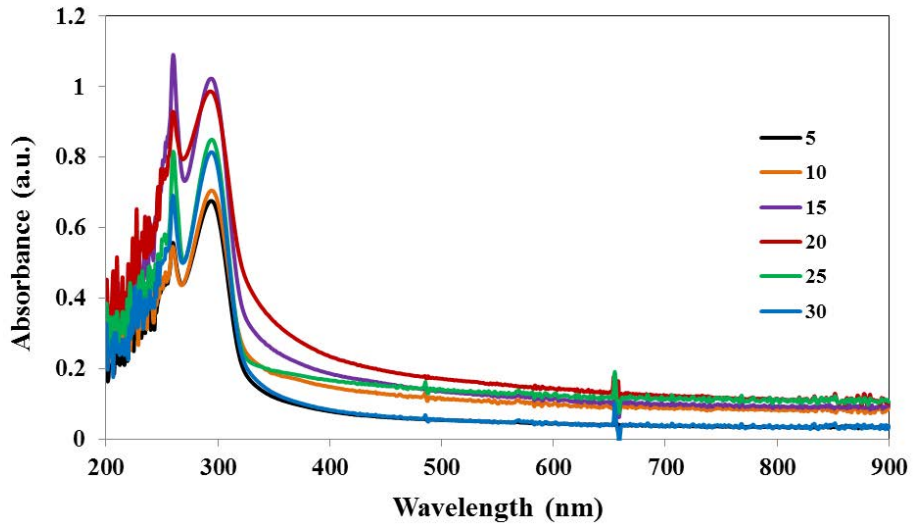

Figure 4.17 UV-Vis spectra of polyanilines synthesized in H_2SO_4 solution using various shots of nitrogen plasma generated from PICP device

4.2.1.3 Solubility

Generally, polyaniline is difficult to dissolve in common solvents but it is easily dissolved in *N*-methyl-2-pyrrolidone as same as aniline monomer as shown in Tables 4.6-4.8. However, its water solubility is completely different from that of aniline as also present these tables. While aniline is water-soluble in both neutral and alkaline conditions, polyaniline is insoluble in neutral water but partially soluble in water having alkaline condition. This suggests the formation of some acidic functional groups on polyaniline chain and the amounts of these functional groups depend on the type of the gas and the number of the plasma shots. When 15 and 20 shots of argon and nitrogen plasma were applied, polyanilines synthesized at these two conditions exhibit higher solubility than the others as shown in Table 4.6. On the other hand, in the case of oxygen plasma, higher solubility of the polymer was obtained when 15, 20 and 25 shots were used.

Table 4.6 Solubility of aniline and polyanilines synthesized in H_2SO_4 solution using various shots of argon plasma generated from PICP device

Solvent	Aniline	Polyanilines synthesized at various numbers of plasma shots					
		5	10	15	20	25	30
water (neutral condition)	+++	-	-	-	-	-	-
water (alkaline condition)	+++	+	+	++	++	+	+
N-Methyl-2-pyrrolidone	+++	+++	+++	+++	+++	+++	+++

(-) insoluble (+, ++) partially soluble (+++) fully soluble

Table 4.7 Solubilities of aniline and polyanilines synthesized in H_2SO_4 solution using various shots of oxygen plasma generated from PICP device

Solvent	Aniline	Polyanilines synthesized at various numbers of plasma shots					
		5	10	15	20	25	30
water (neutral condition)	+++	-	-	-	-	-	-
water (alkaline condition)	+++	-	+	++	++	++	+
N-Methyl-2-pyrrolidone	+++	+++	+++	+++	+++	+++	+++

(-) insoluble (+, ++) partially soluble (+++) fully soluble

Table 4.8 Solubilities of aniline and polyanilines synthesized in H_2SO_4 solution using various shots of nitrogen plasma generated from PICP device

Solvent	Aniline	Polyanilines synthesized at various numbers of plasma shots					
		5	10	15	20	25	30
water (neutral condition)	+++	-	-	-	-	-	-
water (alkaline condition)	+++	+	+	++	++	+	+
N-Methyl-2-pyrrolidone	+++	+++	+++	+++	+++	+++	+++

(-) insoluble (+, ++) partially soluble (+++) fully soluble

4.2.1.4 Electrical conductivity

Electrical conductivity values of polyanilines synthesized using PICP device are summarized in Table 4.9. Their values are higher than those of polyaniline synthesized by chemical and electrical polymerization without doping in the range of 10^{-10}-10^{-12} S.cm^{-1}. It is clearly seen from Figure 4.18 that using argon plasma yielded polyanilines with highest conductivity at every plasma shots due to structural difference as confirmed by FTIR and UV-VIS spectra. Moreover, as corresponding to the highest intensities of UV-VIS absorption peaks, polyanilines which have highest conductivity for each type of plasma are those synthesized with 20 shots of argon plasma, 20 shots of oxygen plasma and 15 shots of nitrogen plasma.

Table 4.9 Electrical conductivities of polyanilines synthesized in H_2SO_4 solution using PICP device

The number of plasma shots	Conductivity (S.cm^{-1})		
	Ar	**O_2**	**N_2**
5	(1.10±0.08)x10^{-7}	(1.64±0.19)x10^{-8}	(8.11±2.29)x10^{-10}
10	(1.40±0.02)x10^{-7}	(2.16±0.18)x10^{-8}	(7.40±2.53)x10^{-9}
15	(1.56±0.06)x10^{-7}	(2.69±0.05)x10^{-8}	(2.23±5.52)x10^{-9}
20	(4.46± 0.17)x10^{-7}	(1.05± 0.26)x10^{-7}	(2.09±0.10)x10^{-8}
25	(2.26± 0.29)x10^{-7}	(5.97± 0.11)x10^{-8}	(1.72± 0.32)x10^{-9}
30	(1.86± 0.17)x10^{-7}	(4.57± 0.93)x10^{-8}	(2.58± 0.31)x10^{-9}

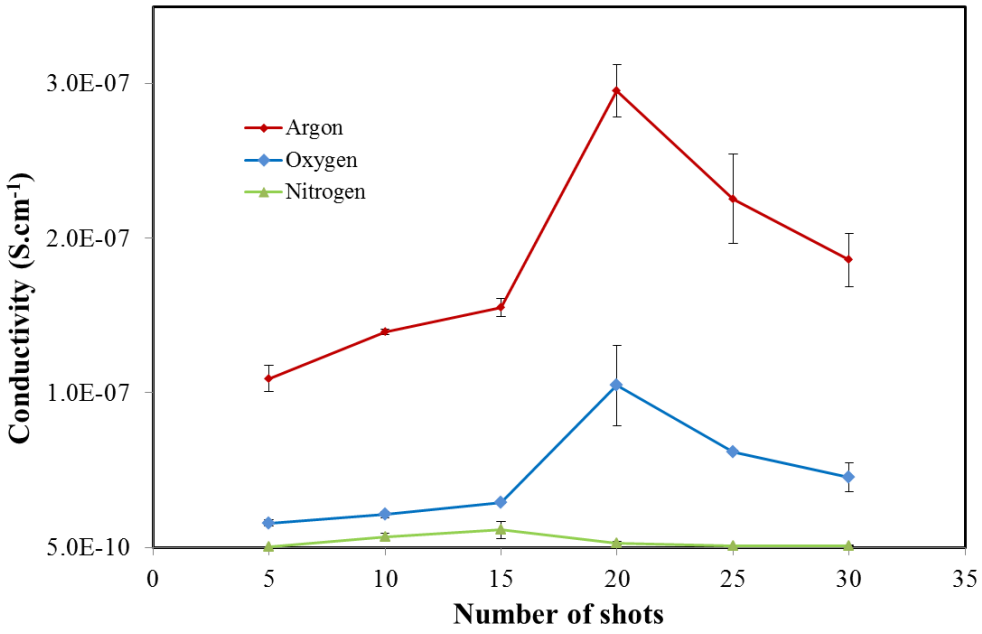

Figure 4.18 The effect of the type of gas on the conductivity of polyanilines synthesized in H_2SO_4 solution using PICP device

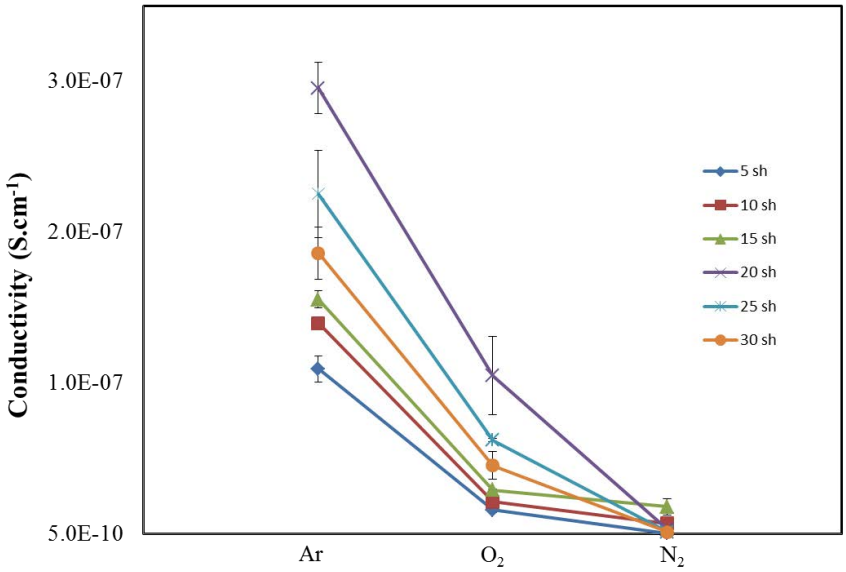

Figure 4.19 The effect of the number of the plasma shots on the conductivity of polyanilines synthesized in H_2SO_4 solution using PICP device

4.2.1.5 Crystal structure

X-ray diffraction patterns of polyanilines synthesized in H_2SO_4 solution using various shots of argon, oxygen and nitrogen plasma are shown in Figures 4.20-4.22, respectively. The amorphous structure of polyanilines synthesized in all gases is confirmed with the presence of the broad peak at $2\Theta = 25.98^o$ at 5 and 10 shots of plasma shots. This peak in polyaniline may occur due to regular repetition of aniline monomer unit which is characteristic peak of polyaniline [18]. While plasma shots increase more over 10 shots, the polyaniline structure become to semi-crystalline structure. The XRD pattern of polyanilines synthesized at 15, 20, 25 and 30 shots show amorphous peak at $2\Theta = 25.98^o$ and major crystalline peak at $2\Theta = 17.12$, 34.16 and 52.28 ^{o} corresponding to which can be assigned to the (011), (004) and (400) reflections, respectively [18,84]. The integrated intensity of the peaks can be used to indicate the crystallinity of polyaniline. The degree of crystallinity is estimated as the percentage ratio of the integrated crystalline intensity based on the integrated amorphous intensity of synthesized polyaniline to its both crystalline and amorphous components as shown in Table 4.10 [76,81]. The synthesized polyaniline at 5 shots of argon is selected for integrated amorphous intensity for calculation of all degree of crystallinity values because this condition shows lower integrated amorphous structure than others. The highest degree of crystallinity peak is found at 20 shots for argon and oxygen gas and 15 shots for nitrogen gas of plasma relatively highest intensity of crystalline structure in polyaniline confirmed by XRD. In addition, the diffraction peak at $2\Theta = 25.98^o$ of these polyanilines are most relatively intense due to an increase in the effective delocalization in polymer chain [85-86]. The intensity of these diffraction peaks decrease with increasing plasma exposure because too high energy can casue the scission of the polymer chain.

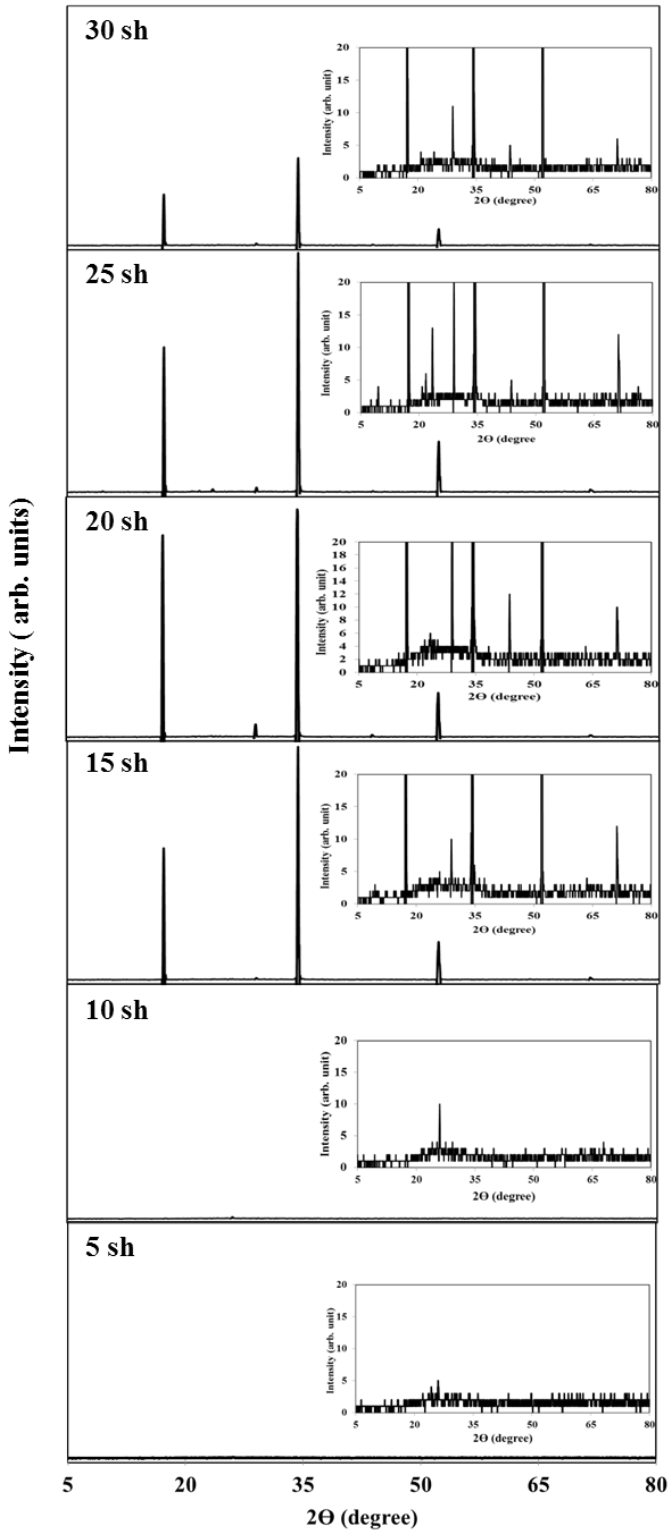

Figure 4.20 XRD patterns of polyanilines synthesized in H_2SO_4 solution using various shots of argon plasma generated from PICP device

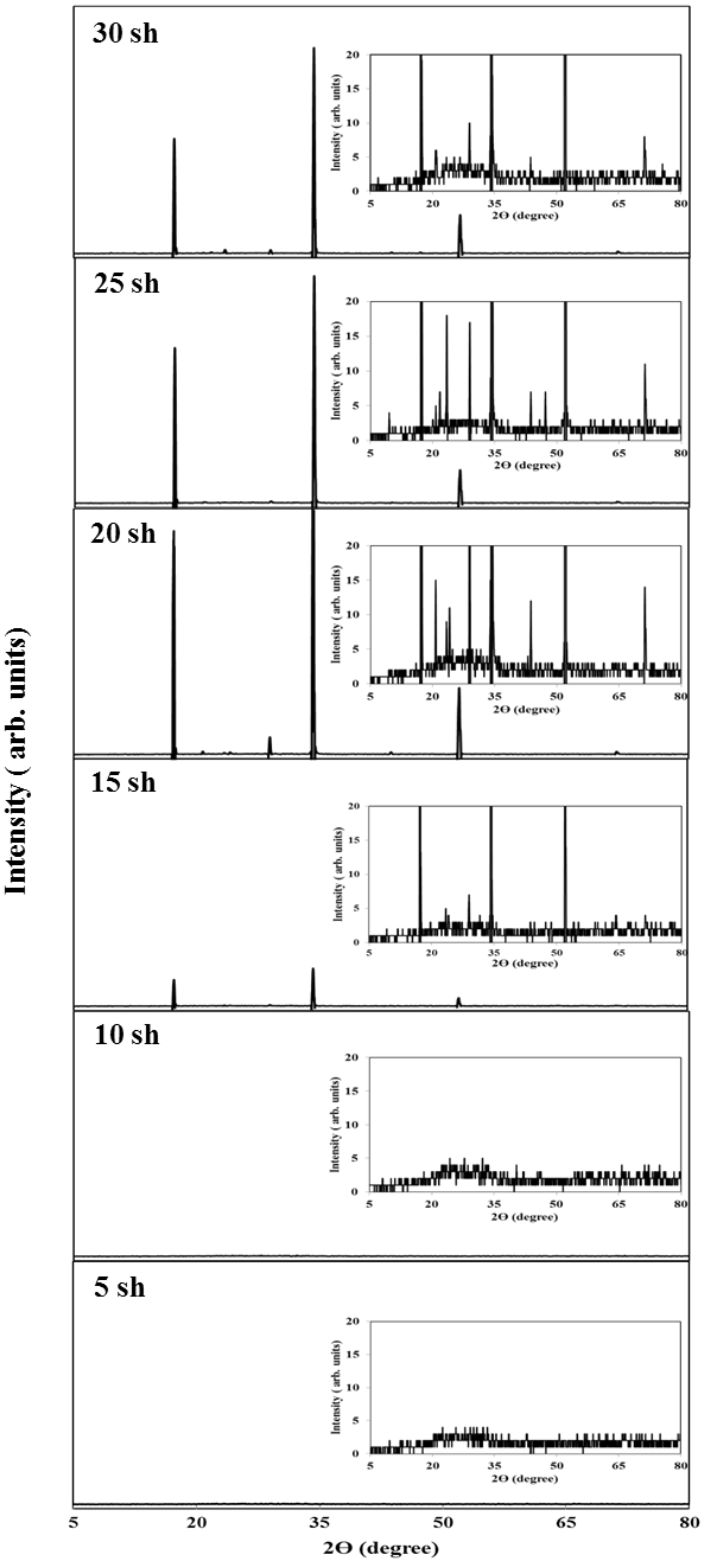

Figure 4.21 XRD patterns of polyanilines synthesized in H_2SO_4 solution using various shots of oxygen plasma generated from PICP device

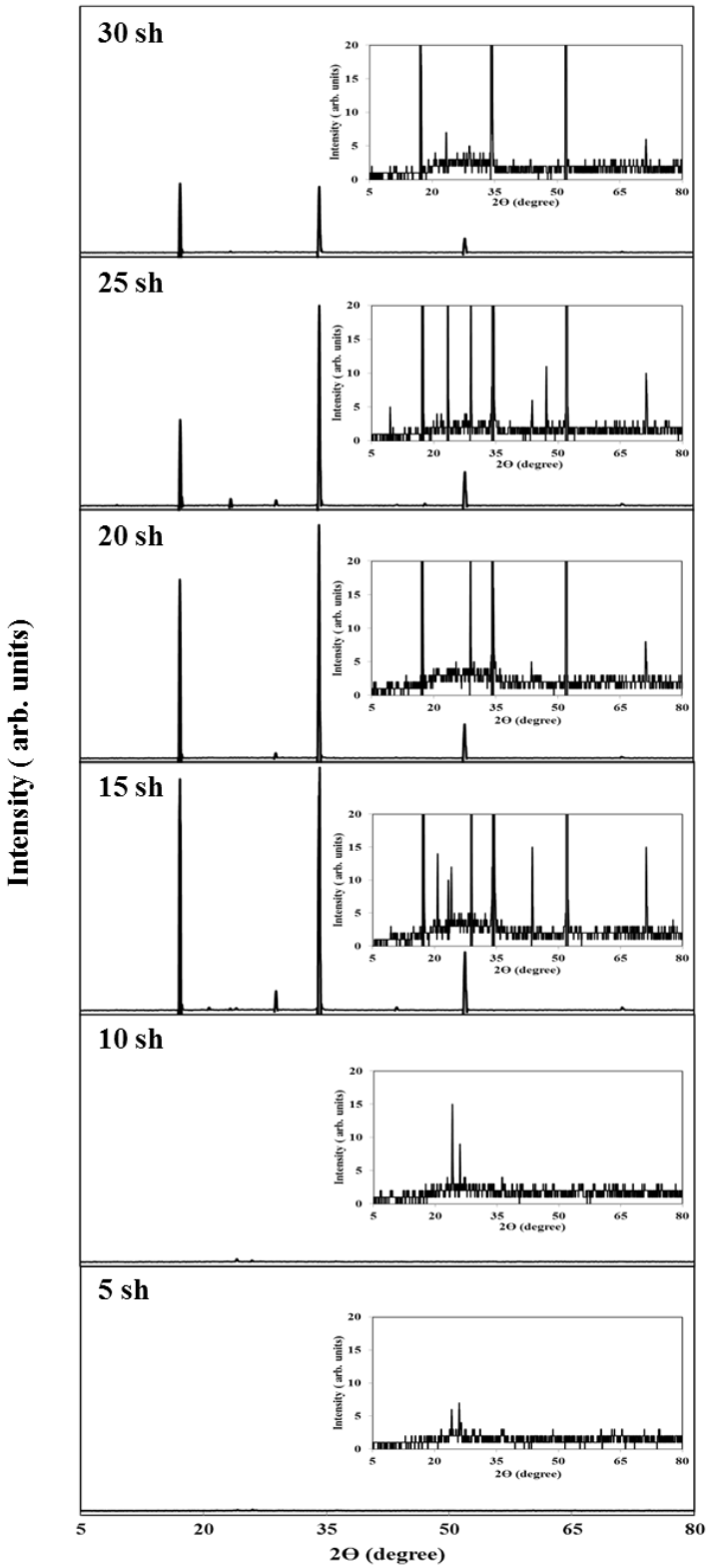

Figure 4.22 XRD patterns of polyanilines synthesized in H_2SO_4 solution using various shots of nitrogen plasma generated from PICP device

Table 4.10 The degree of crystallinity (%) of polyanilines synthesized in H_2SO_4 solution using PICP device

The degree of crystallinity (%)						
Gas Type	**The number of plasma shots**					
	5	**10**	**15**	**20**	**25**	**30**
Argon	-	3.44	76.19	80.23	75.25	54.18
Oxygen	-	-	37.00	82.40	73.42	76.36
Nitrogen	0.59	11.53	82.09	77.52	71.73	55.47

4.2.1.6 Thermal properties

The decomposition temperatures of polyanilines synthesized in H_2SO_4 solution using PICP device are summarized in Table 4.11 and TGA thermograms are shown in Figures 4.23-4.25. The decomposition temperatures of polyanilines synthesized using argon plasma are in the range of 183-187 ^oC. They show a tendency to decrease with increasing the number of the plasma shots. This may be due to the presence of oxygen-containing functional groups on polyaniline structure which increase with increasing the number of the plasma shots as confirmed this functional groups by FTIR. Since these groups are less thermally stable than the other groups, higher amount of these groups results in lower decomposition temperature. After 25 shots of plasma, too much plasma etching can remove these functional groups causing an increase in the decomposition temperature. In case of oxygen plasma, the decomposition temperatures of polyanilines are observed in the range of 182-187 ^oC. The similar trend as in the case of argon plasma is observed due to the same reason. The decomposition temperatures in the range of 182-188 ^oC are observed in the case of nitrogen plasma with lowest decomposition temperature at 15 shots due to the loss of sulfonic acid functional group on polyaniline as seen by FTIR.

Table 4.11 Decomposition temperatures of polyanilines synthesized in H_2SO_4 solution using PICP device

Gas Type	The number of plasma shots	Decomposition Temperature (^oC)
Ar	5	184.51
	10	187.13
	15	185.68
	20	184.73
	25	183.09
	30	185.30
O_2	5	187.70
	10	187.94
	15	187.37
	20	182.57
	25	188.55
	30	187.83
N_2	5	186.15
	10	188.04
	15	182.30
	20	182.45
	25	184.10
	30	186.99

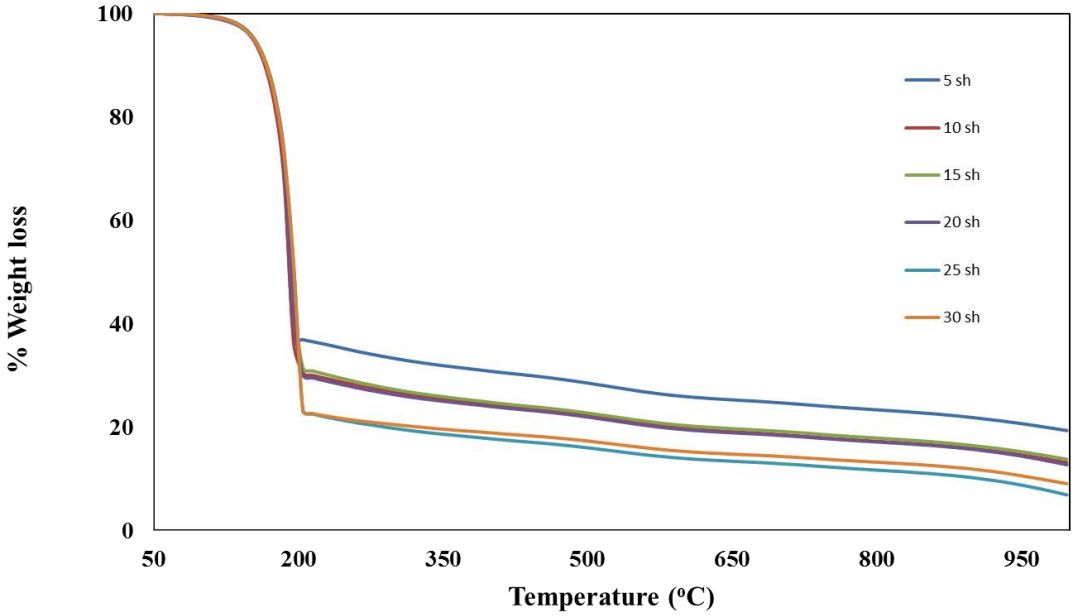

Figure 4.23 TGA Thermograms of polyanilines synthesized in H_2SO_4 solution using various shots of argon plasma generated from PICP device

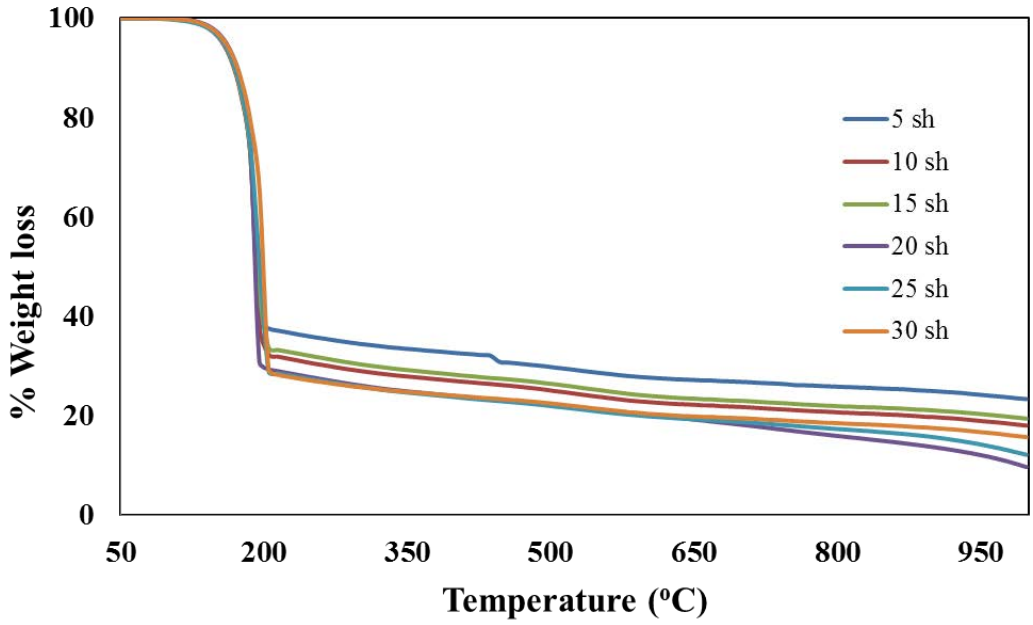

Figure 4.24 TGA Thermograms of polyanilines synthesized in H_2SO_4 solution using various shots of oxygen plasma generated from PICP device

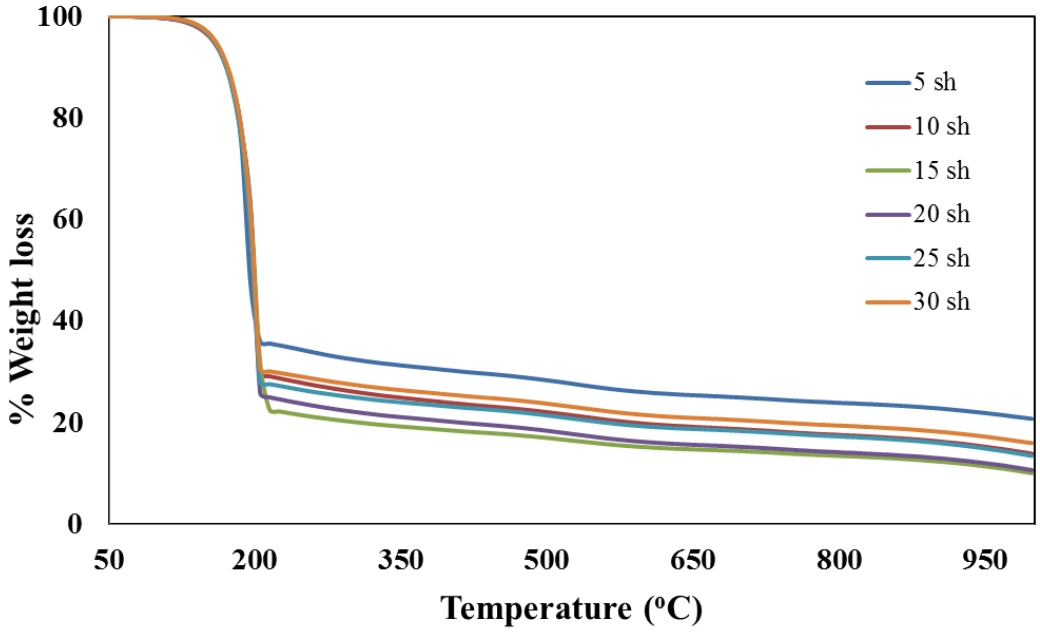

Figure 4.25 TGA Thermograms of polyanilines synthesized in H_2SO_4 solution using various shots of nitrogen plasma generated from PICP device

4.2.1.7 Morphology

Generally, polyaniline can be founded in several structures such as fibril, granular, cluster, etc. [35]. In this research, synthesized polyanilines exhibit fibrils and granulars structure depending on the type of gas and the number of plasma shots as shown in Figures 4.26-4.28. In case of argon, all polyanilines show the fibril structure with diameter of 100±7 nm as seen in Figures 4.26 (a-f). An increase in the number of the plasma shots leads to higher amounts of fibrils. Shorter length of fibril was observed when 25 and 30 shots of plasma were applied due to plasma etching at high plasma exposure. In case of oxygen and nitrogen, granular structure with grain size about 150±11 nm were observed in polyanilines synthesized with 5 and 10 shots of plasma as shown in Figures 4.27 (a-b) and Figures 4.28 (a-b). Fibrils structure with diameter of 100 nm was observed in the others as shown in Figures 4.27 (e-f) and Figures 4.28 (e-f). Additionally, the amount of shorter fibril increases with increasing the number of the plasma shots as previously explained.

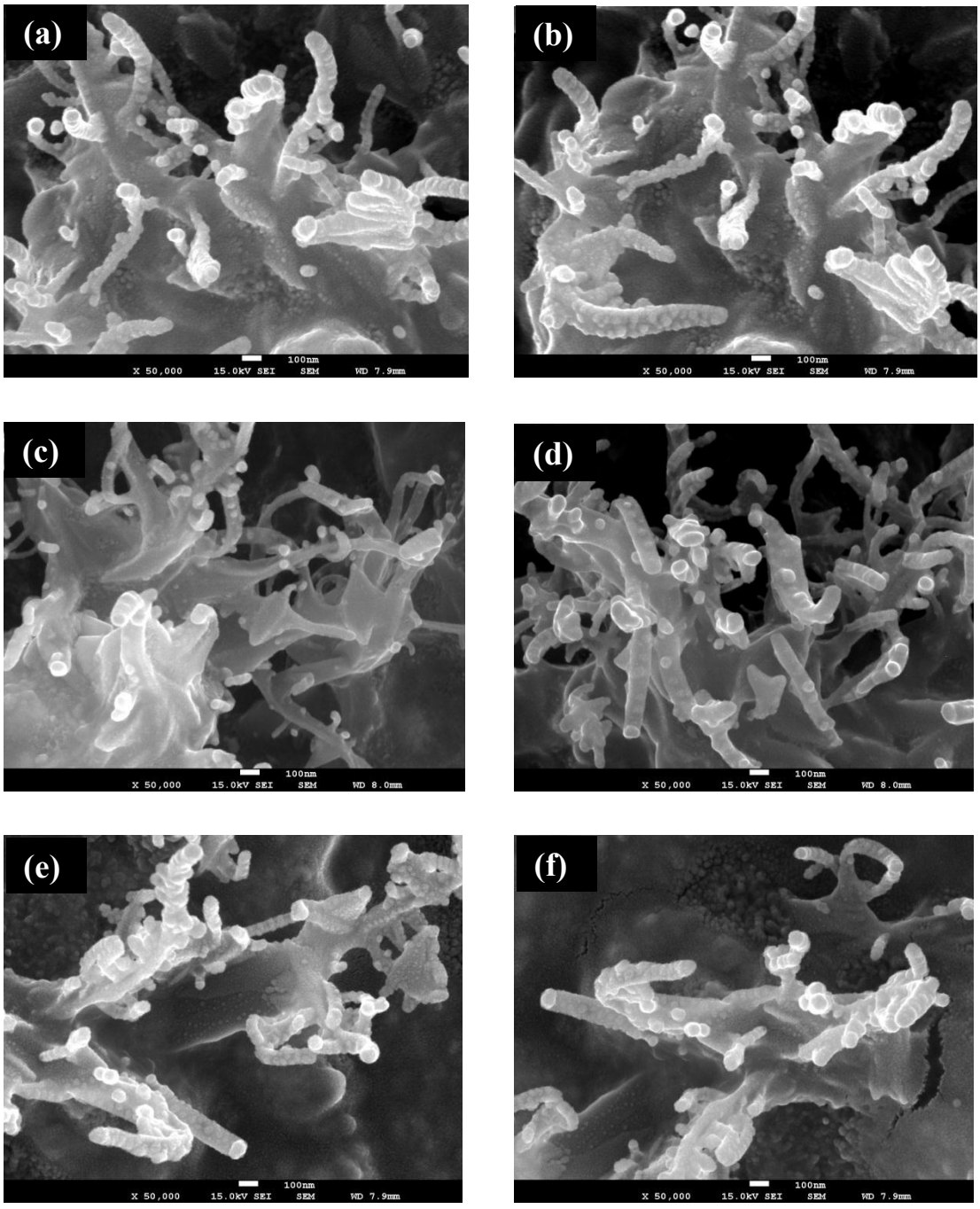

Figure 4.26 FE-SEM images of polyanilines synthesized in H_2SO_4 solution using (a) 5 (b) 10 (c) 15 (d) 20 (e) 25 (f) 30 of argon plasma generated from PICP device

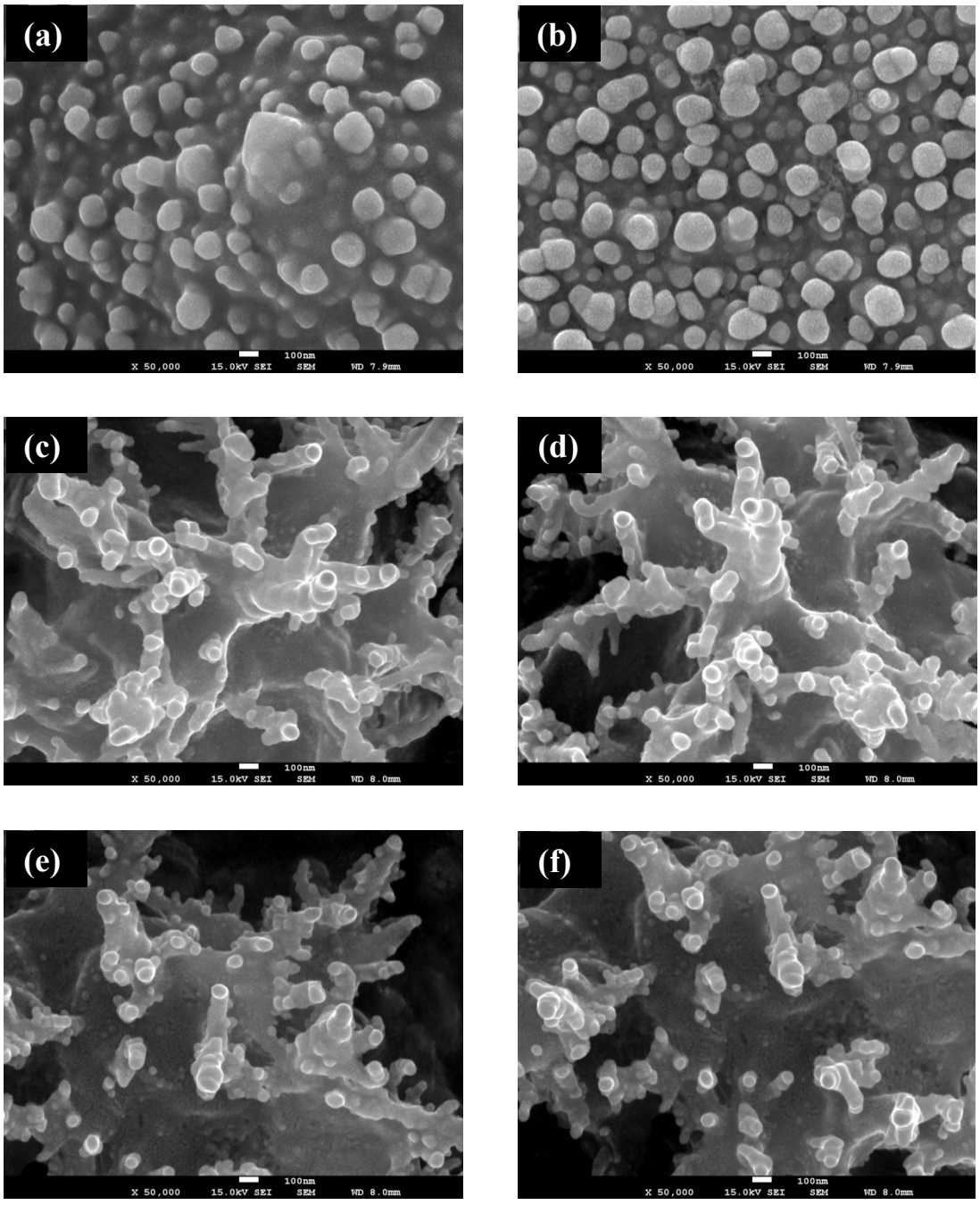

Figure 4.27 FE-SEM images of polyanilines synthesized in H_2SO_4 solution using (a) 5 (b) 10 (c) 15 (d) 20 (e) 25 (f) 30 of oxygen plasma generated from PICP device

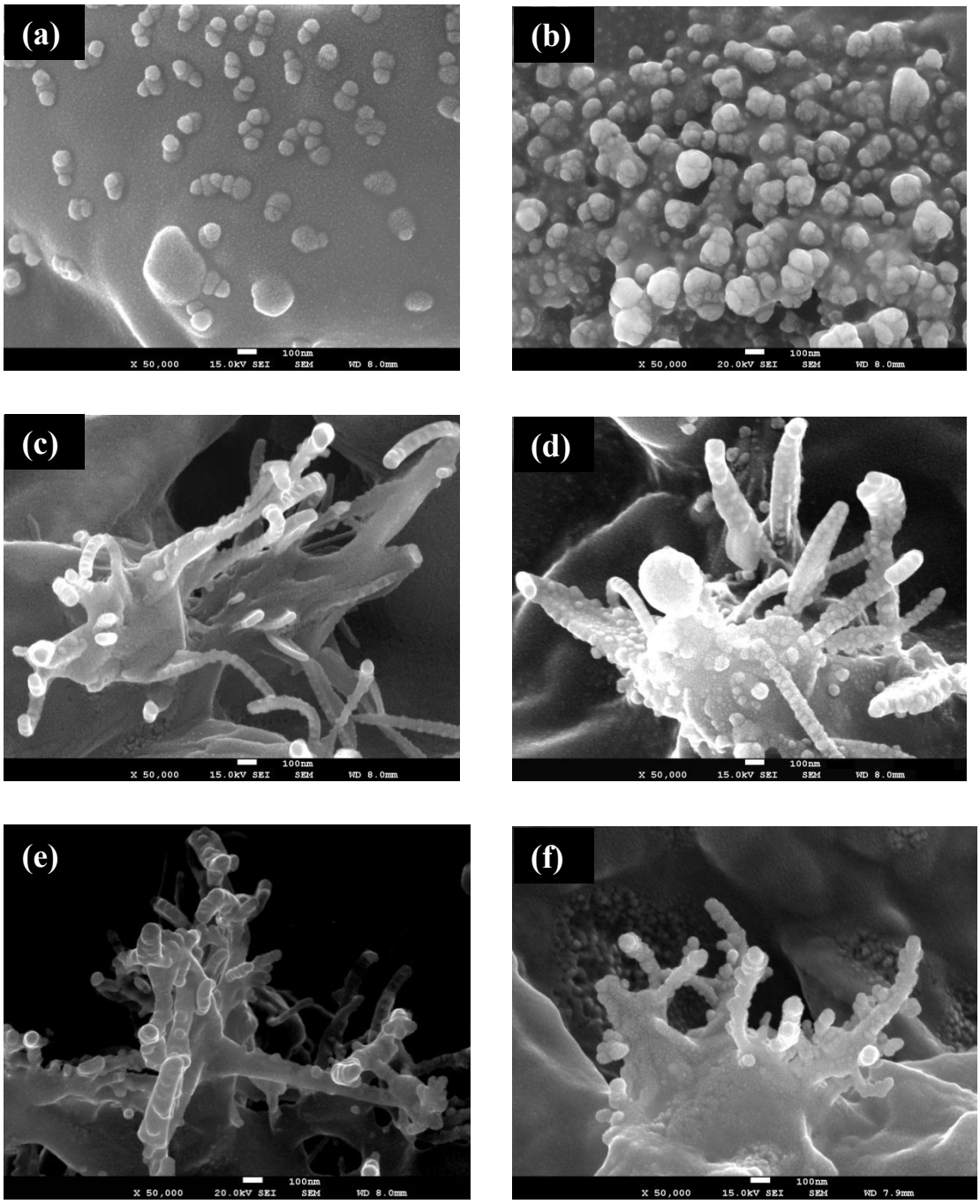

Figure 4.28 FE-SEM images of polyanilines synthesized in H_2SO_4 solution using (a) 5 (b) 10 (c) 15 (d) 20 (e) 25 (f) 30 of nitrogen plasma generated from PICP device

All the results suggest that the structures of polyaniline synthesized in H_2SO_4 solution using argon plasma consist of the mixtures of the emeraldine salt and emeraldine base as shown below depending on the number of the plasma shots. On the other hand, those synthesized using oxygen and nitrogen plasma exhibit mainly the undoped structure of emeraldine base as also confirmed by FTIR and UV-VIS spectra and conductivity measurement.

Emeraldine salt:
(green color)

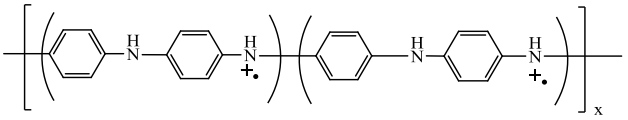

Emeraldine base:
(brown color)

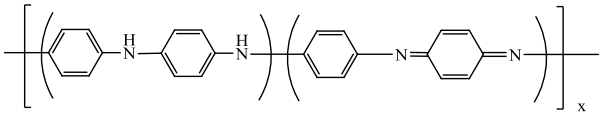

4.2.2 Polyanilines synthesized in hydrochloric solution

4.2.2.1 Chemical structure

FTIR spectra of polyanilines synthesized in HCl solution using various shots of argon plasma generated from PICP device are displayed in Figure 4.29 and their peaks are interpreted and given in Table 4.12. FTIR spectra show broad absorption peak at 3421 cm^{-1} corresponding to N-H stretching of aromatic amine at all the number of plasma shots. The main peak at 1612 cm^{-1} is assigned to quinoid ring stretching deformation. The peaks at 1378 cm^{-1} assigned to C-N stretching in the neighbourhood of a quinoid ring of undoped polyaniline or polyaniline emeridine base [87-90] are found when the plasma shots higher than 10 shots were applied. Moreover, a decrease in the absorption peaks at 1048 cm^{-1} corresponding to the characteristic skeletal vibrations of halogen substituted aromatic rings are also observed [87]. This may be due to too high energy of plasma exposure resulting in increasing plasma etching. In addition, the absorption peaks at 740 and 680 cm^{-1}

corresponding to 1,4-disubstitution of benzene ring were not found in these conditions.

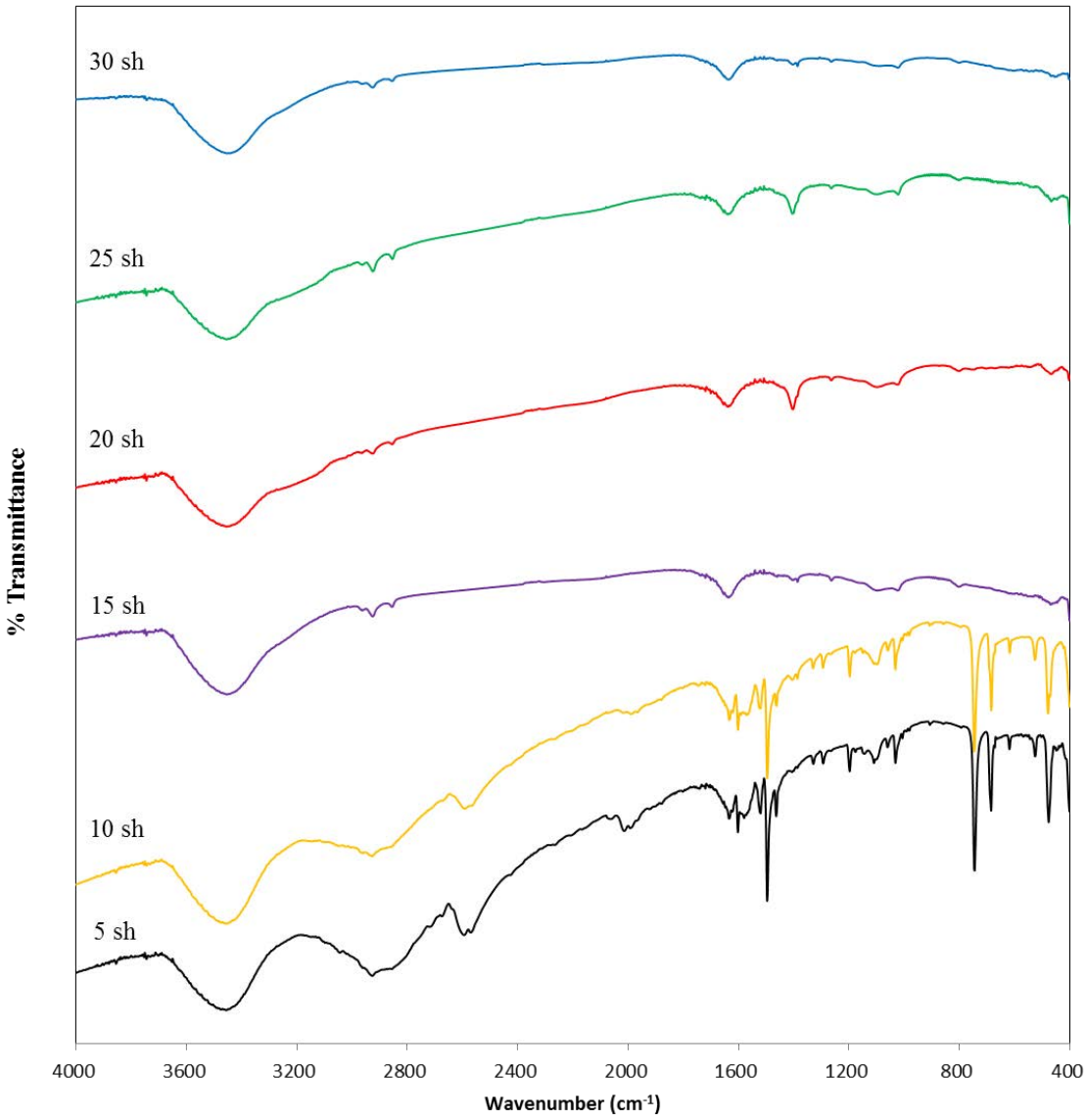

Figure 4.29 FTIR spectra of polyanilines synthesized in HCl solution using various shots of argon plasma generated from PICP device

Table 4.12 Interpretation of FTIR spectra of polyanilines synthesized in HCl solution using various shots of argon plasma generated from PICP device

Assignments	Wavenumber (cm^{-1})					
	5	**10**	**15**	**20**	**25**	**30**
1. N-H stretching of aromatic amine	3421	3421	3421	3421	3421	3421
2. O-H stretching	-	-	3206	3206	3206	3206
3. C-H stretching of aliphatic	2908	2908	-	-	-	-
4. C=C stretching of quinoid ring	1612	1612	1612	1612	1612	1612
5. C=C stretching of benzene ring	1490	1490	-	-	-	-
6. C-N stretching in the neighbourhood of quiniod ring	-	-	1378	1378	1378	1378
7. Halogen substituted aromatic rings	1048	1048	1048	1048	1048	1048
8. C-H out of plane blending	740	740	-	-	-	-
(1,4-disubstitution in benzene ring)	680	680	-	-	-	-

FTIR spectra of polyanilines synthesized in HCl solution using various shots of oxygen plasma generated from PICP device are displayed in Figure 4.30 and their peaks are interpreted and given in Table 4.13. The similar characteristic peaks as in the spectra of those synthesized using argon plasma are observed. However, the peaks at 1378 cm^{-1} assigned to C-N stretching in the neighbourhood of a quinoid ring of undoped polyaniline or polyaniline emeridine base are found and a decrease in the absorption peaks at 1048 cm^{-1} corresponding to the characteristic skeletal vibrations

of halogen substituted aromatic rings are also observed when the plasma shots higher than 15 shots were applied.

FTIR spectra of polyanilines synthesized in HCl solution using various shots of nitrogen plasma generated from PICP device are displayed in Figure 4.31 and their peaks are interpreted and given in Table 4.14. The similar characteristic peaks as in the spectra of those synthesized using argon plasma are observed. On the other hand, the peaks at 1378 cm^{-1} assigned to C-N stretching in the neighbourhood of a quinoid ring of undoped polyaniline or polyaniline emeridine base are found and a decrease in the absorption peaks at 1048 cm^{-1} corresponding to the characteristic skeletal vibrations of halogen substituted aromatic rings are also observed when the plasma shots higher than 5 shots were applied. In addition, the peaks at 3078 cm^{-1} assigned to C-H stretching of aromatic occur only at 15 and 20 shots of the plasma were applied resulting from the presence of the aromatic ring due to longest conjugated chain of polyaniline.

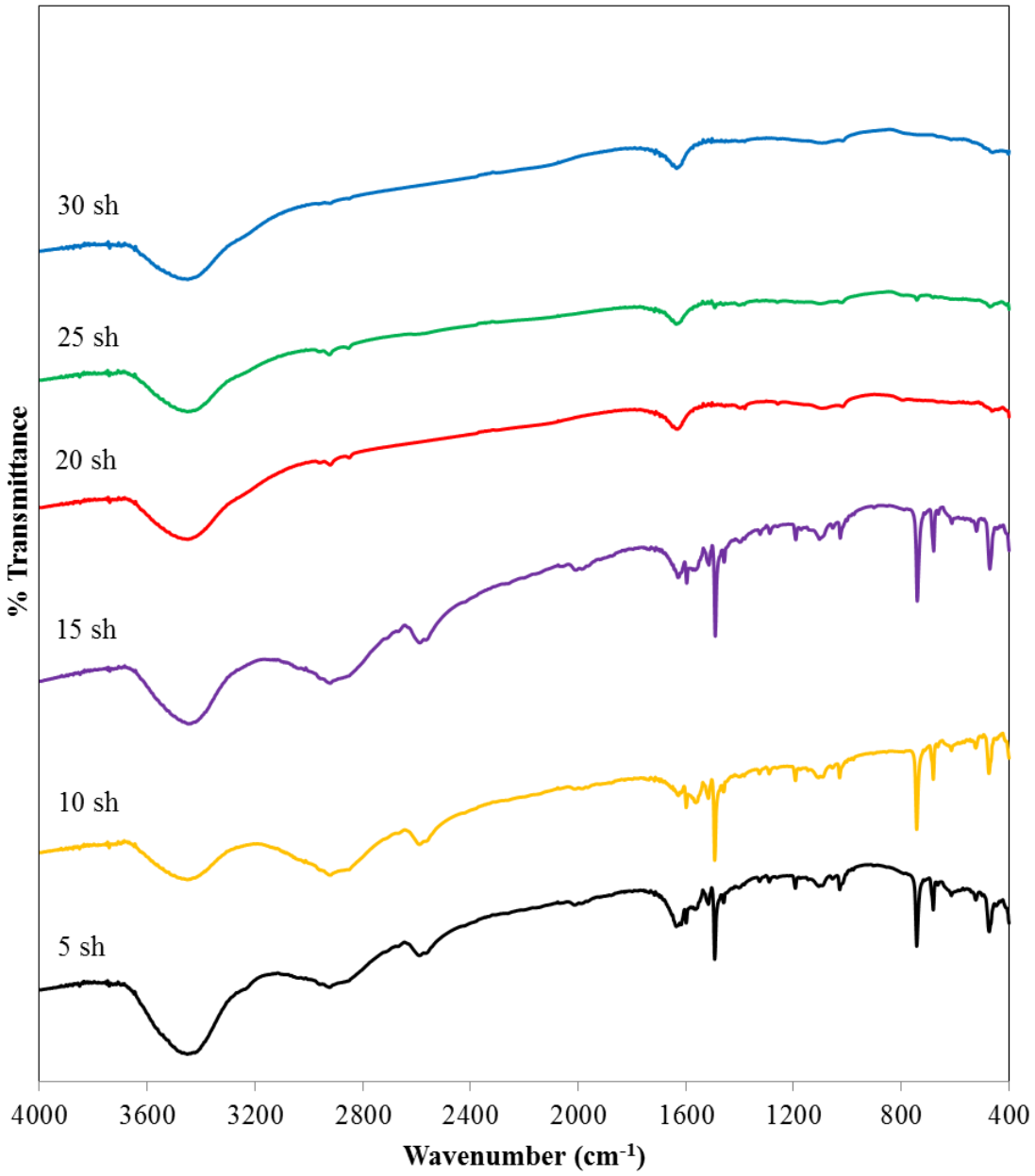

Figure 4.30 FTIR spectra of polyanilines synthesized in HCl solution using various shots of oxygen plasma generated from PICP device

Table 4.13 Interpretation of FTIR spectra of polyanilines synthesized in HCl solution using various shots of oxygen plasma generated from PICP device

Assignments	Wavenumber (cm^{-1})					
	5	**10**	**15**	**20**	**25**	**30**
1. N-H stretching of aromatic amine	3421	3421	3421	3421	3421	3421
2. O-H stretching	-	-	-	3210	3210	3210
3. C-H stretching of aliphatic	2908	2908	2908	-	-	-
4. C=C stretching of quinoid ring	1612	1612	1612	1612	1612	1612
5. C=C stretching of benzene ring	1490	1490	1490	-	-	-
6. C-N stretching in the neighbourhood of quiniod ring	-	-	-	1378	1378	1378
7. Halogen substituted aromatic rings	1048	1048	1048	1048	1048	1048
8. C-H out of plane blending	740	740	740	-	-	-
(1,4-disubstitution in benzene ring)	680	680	681	-	-	-

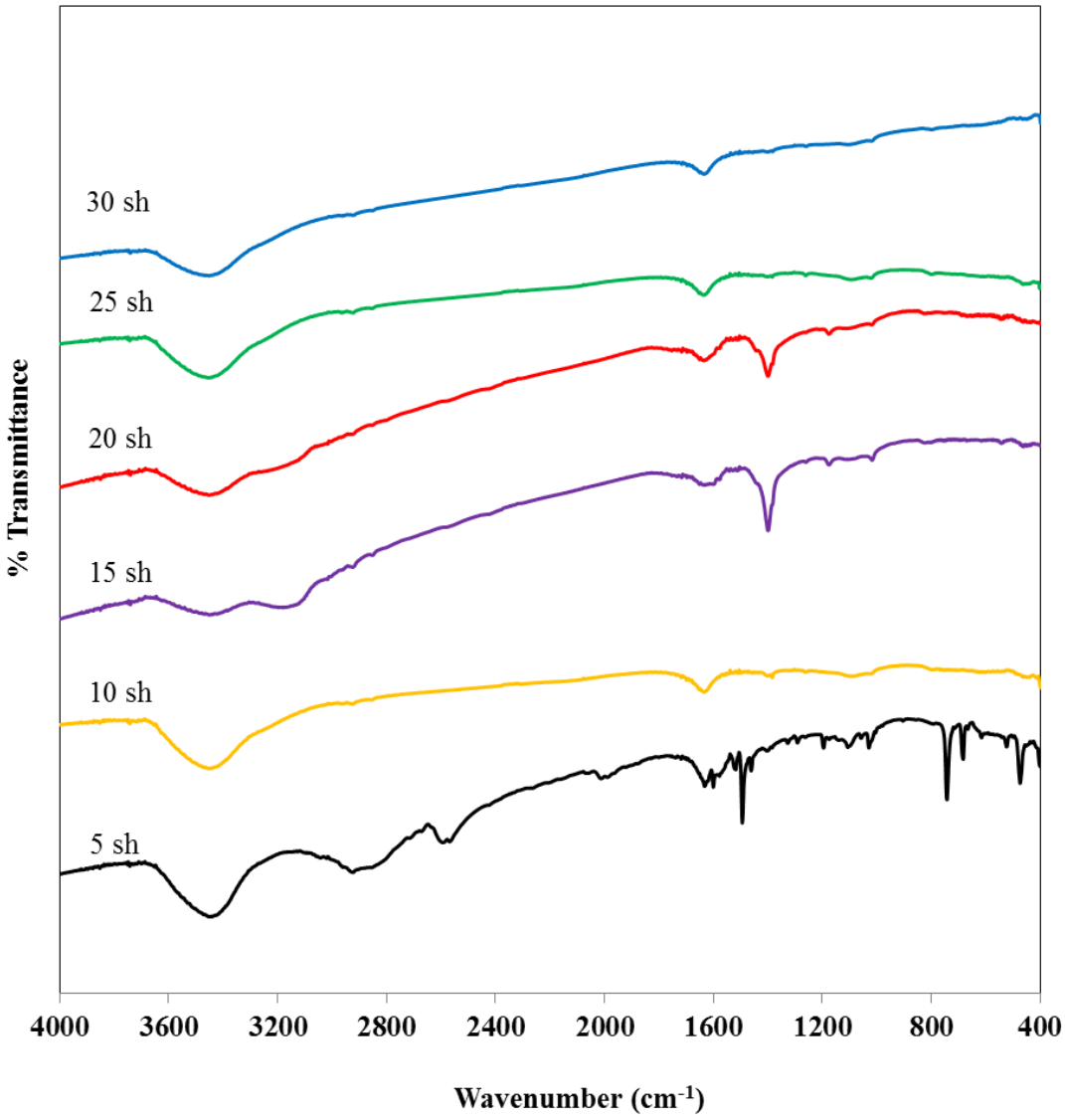

Figure 4.31 FTIR spectra of polyanilines synthesized in HCl solution using various shots of nitrogen plasma generated from PICP device

Table 4.14 Interpretation of FTIR spectra of polyanilines synthesized in HCl solution using various shots of nitrogen plasma generated from PICP device

Assignments	Wavenumber (cm^{-1})					
	5	**10**	**15**	**20**	**25**	**30**
1. N-H stretching of aromatic amine	3421	3421	3421	3421	3421	3421
2. O-H stretching	-	-	3181	3176	3214	3206
3. C-H stretching of aliphatic	2908	-	-	-	-	-
4. C-H stretching of aromatic	-	-	3078	3078	-	-
5. C=C stretching of quinoid ring	1612	1612	1612	1612	1612	1612
6. C=C stretching of benzene ring	1490	-	-	-	-	-
7. C-N stretching in the neighbourhood of quiniod ring	-	1378	1378	1378	1378	1378
8. Halogen substituted aromatic rings	1048	1048	1048	1048	1048	1048
9. C-H out of plane blending	740	-	-	-	-	-
(1,4-disubstitution in benzene ring)	680	-	-	-	-	-

4.2.2.2 Optical characteristics

As shown in Figure 4.32, polyanilines synthesized using 5 and 10 shots of argon plasma exhibit three absorption bands at about 260, 290 and 345 nm which are attributes to π-π* transition, the π-polaron transition in benzene rings and the polarons of polyaniline emeridine base, respectively. The number of plasma shots at 15 ,20 and 25 shots exhibit two peaks at 260 and 290 nm assigned to π-π* transition and π-polaron transition, respectively. In addition, high plasma exposure at 30 shots was too high to break down on conjugated chain of polyaniline resulting in the presence of one absorption peak at 260 nm.

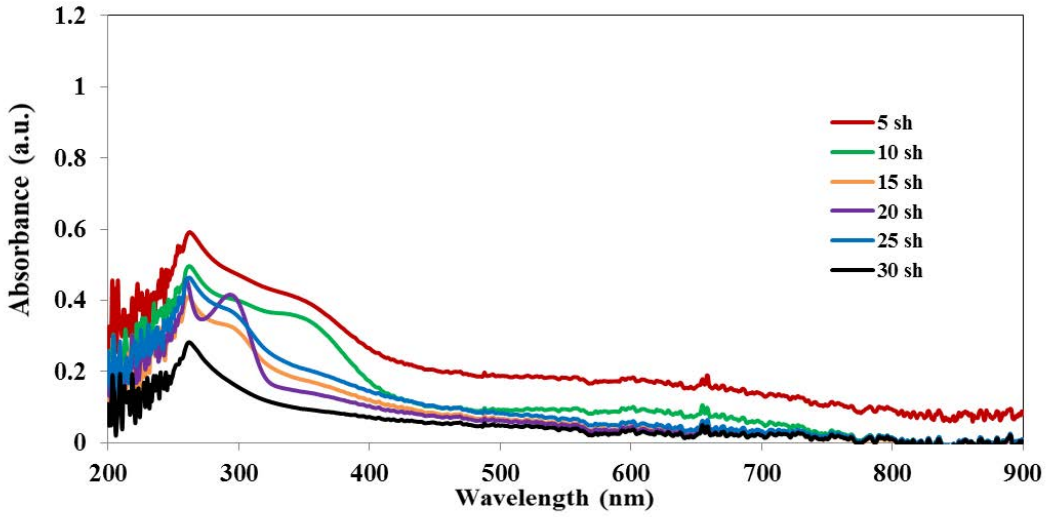

Figure 4.32 UV-Vis spectra of polyanilines synthesized in HCl solution using various shots of argon plasma generated from PICP device

UV-VIS spectra of polyanilines synthesized in HCl solution using various shots of oxygen are shown in Figures 4.33. It can be seen that polyaniline synthesized at 5 shots was exhibited three absorption bands at about 260, 290 and 345 nm assigned to π-π* transition, the π-polaron transition in benzene rings and the polarons of polyaniline emeridine base, respectively. The number of plasma shots at 10 and 15 shots exhibit two peaks at 260 and 290 nm assigned to π-π* transition and

π-polaron transition, respectively. In addition, high plasma exposure at 20, 25 and 30 shots were too high to break down on conjugated chain of polyaniline resulting in the presence of one absorption peak at 260 nm.

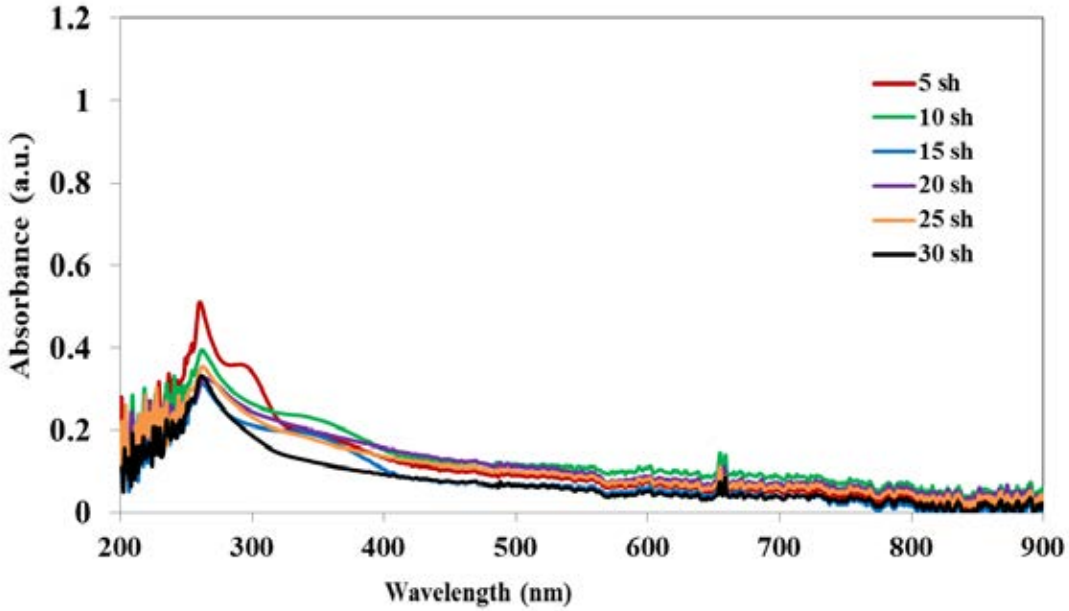

Figure 4.33 UV-Vis spectra of polyanilines synthesized in HCl solution using various shots of oxygen plasma generated from PICP device

UV-VIS spectra of polyanilines synthesized in HCl solution using various shots of nitrogen are shown in Figures 4.34. It can be seen that polyaniline synthesized at 5, 10 and 15 shots was exhibited three absorption bands at about 260, 290 and 345 nm assigned to π-π* transition, the π-polaron transition in benzene rings and the polarons of polyaniline emeridine base, respectively. The number of plasma shots at 20, 25 and 30 shots exhibit two peaks at 260 and 290 nm assigned to π-π* transition and π-polaron transition, respectively.

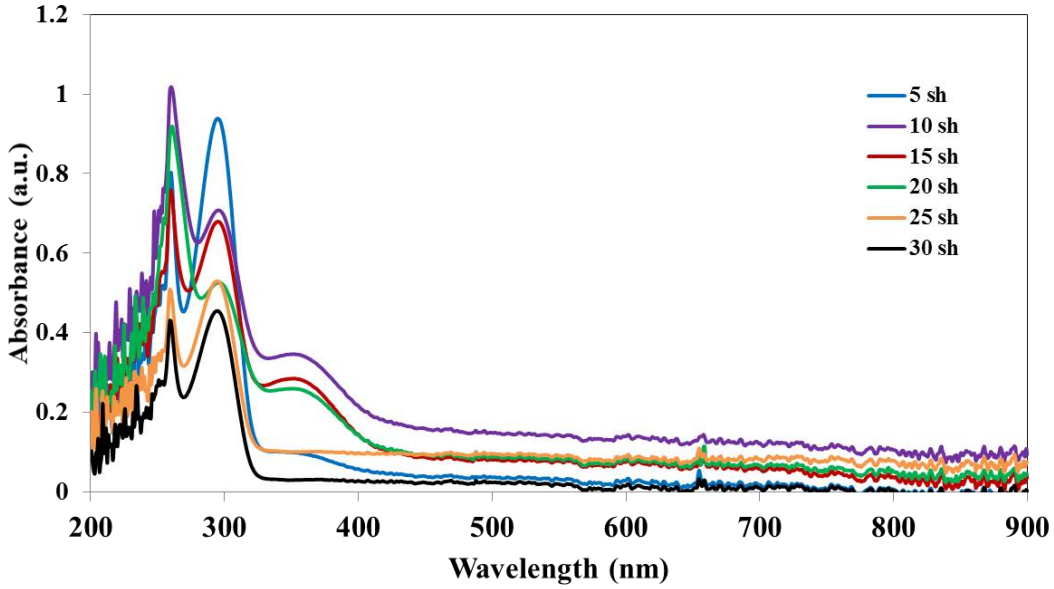

Figure 4.34 UV-Vis spectra of polyanilines synthesized in HCl solution using various shots of nitrogen plasma generated from PICP device

4.2.2.3 Solubility

Generally, polyaniline is difficult to dissolve in common solvents but it is easily dissolved in *N*-methyl-2-pyrrolidone as same as aniline monomer as shown in Table 4.15-4.17. However, its water solubility is completely different from that of aniline as also present in Table 4.18. While aniline is water-soluble in both neutral and alkaline conditions, polyaniline is insoluble in neutral water but partially soluble in water having alkaline condition. This suggests the formation of some acidic functional groups on polyaniline chain and the amounts of these functional groups depend on the type of the gas and the number of the plasma shots. When 5 and 10 shots of argon were applied, polyanilines synthesized at these two conditions exhibit higher solubility than the others as shown in Table 4.20. On the other hand, in the case of oxygen plasma, higher solubility of the polymer was obtained when 5, 10 and 15 shots were used. While higher solubility of the polyaniline synthesized was obtained to 5 shots of nitrogen plasma.

Table 4.15 Solubility of aniline and polyanilines synthesized in HCl solution using various shots of argon plasma generated from PICP device

Solvent	Aniline	Polyanilines synthesized at various numbers of plasma shots					
		5	10	15	20	25	30
water (neutral condition)	+++	-	-	-	-	-	-
water (alkaline condition)	+++	++	++	+	+	+	-
N-Methyl-2-pyrrolidone	+++	+++	+++	+++	+++	+++	+++

(-) insoluble (+, ++) partially soluble (+++) fully soluble

Table 4.16 Solubility of aniline and polyanilines synthesized in HCl solution using various shots of oxygen plasma generated from PICP device

Solvent	Aniline	Polyanilines synthesized at various numbers of plasma shots					
		5	10	15	20	25	30
water (neutral condition)	+++	-	-	-	-	-	-
water (alkaline condition)	+++	++	++	++	+	+	-
N-Methyl-2-pyrrolidone	+++	+++	+++	+++	+++	+++	+++

(-) insoluble (+, ++) partially soluble (+++) fully soluble

Table 4.17 Solubility of aniline and polyanilines synthesized in HCl solution using various shots of nitrogen plasma generated from PICP device

Solvent	Aniline	Polyanilines synthesized at various numbers of plasma shots					
		5	10	15	20	25	30
water (neutral condition)	+++	-	-	-	-	-	-
water (alkaline condition)	+++	++	+	+	+	+	-
N-Methyl-2-pyrrolidone	+++	+++	+++	+++	+++	+++	+++

(-) insoluble (+, ++) partially soluble (+++) fully soluble

4.2.2.4 Electrical conductivity

Electrical conductivity values of polyanilines synthesized using PICP device are summarized in Table 4.9. Their values are higher than those of polyaniline synthesized by chemical and electrical polymerization without doping in the range of 10^{-10}-10^{-12} S.cm^{-1}. It is clearly seen from Figure 4.35 that using argon plasma yielded polyanilines with highest conductivity at every plasma shots due to structural difference as confirmed by FTIR and UV-VIS spectra. Moreover, as corresponding to the highest intensities of UV-VIS absorption peaks, polyanilines which have highest conductivity for each type of plasma are those synthesized with 5 shots of argon, oxygen and nitrogen plasma.

Table 4.18 Electrical conductivities of polyanilines synthesized in HCl solution using PICP device

The number of plasma shots	Conductivity ($S.cm^{-1}$)		
	Ar	**O_2**	**N_2**
5	$(4.64\pm0.35)\times10^{-8}$	$(2.96\pm0.12)\times10^{-8}$	$(1.94\pm0.23)\times10^{-8}$
10	$(4.05\pm0.07)\times10^{-8}$	$(2.52\pm0.10)\times10^{-8}$	$(1.57\pm0.13)\times10^{-8}$
15	$(3.52\pm0.15)\times10^{-8}$	$(2.47\pm0.04)\times10^{-8}$	$(1.16\pm0.14)\times10^{-8}$
20	$(2.68\pm0.48)\times10^{-8}$	$(1.88\pm 0.08)\times10^{-8}$	$(8.57\pm0.03)\times10^{-9}$
25	$(1.59\pm0.08)\times10^{-8}$	$(1.38\pm0.16)\times10^{-8}$	$(7.24\pm0.61)\times10^{-9}$
30	$(1.56\pm0.11)\times10^{-8}$	$(1.19\pm0.11)\times10^{-8}$	$(6.12\pm0.14)\times10^{-9}$

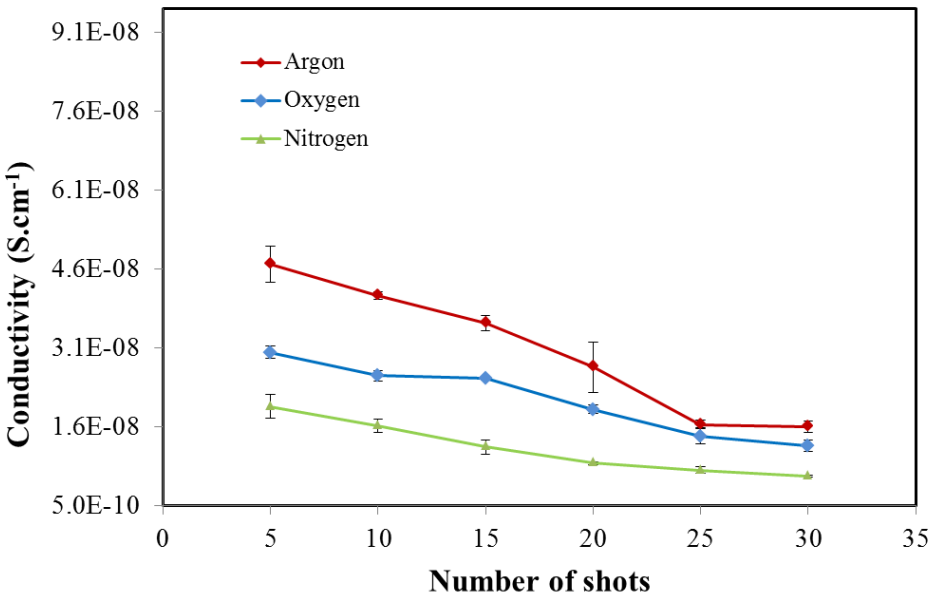

Figure 4.35 The effect of the type of gas on the conductivity of polyanilines synthesized in HCl solution using PICP device

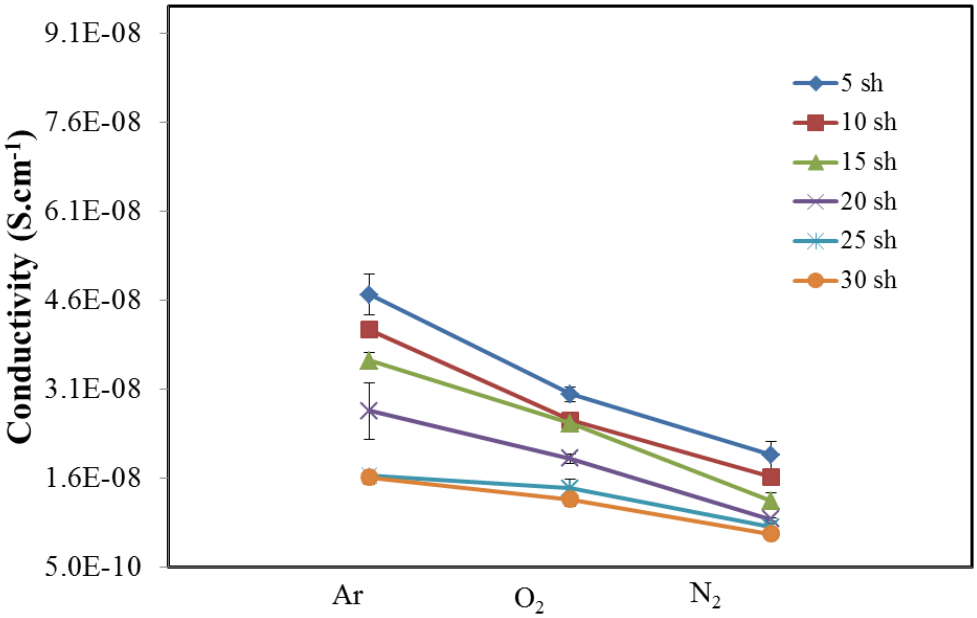

Figure 4.36 The effect of the number of the plasma shots on the conductivity of polyanilines synthesized in HCl solution using PICP device

4.2.2.5 Crystal structure

X-ray diffraction patterns of polyanilines synthesized in HCl solution using various shots of argon, oxygen and nitrogen plasma are shown in Figures 4.37-4.39, respectively. Most of polyanilines exhibit the amorphous structure with broad peak at $2\Theta = 25.98^{o}$. For argon plasma, polyanilines synthesized at 5 and 10 shots show small crystalline peak at $2\Theta = 31.84^{o}$ which can be assigned to the (212) reflections of polyaniline [81]. This peak appears when the number of the plasma shots of 5 to 25 shots for oxygen and 5 and 10 shots for nitrogen were applied. This peak was not found at high plasma shots. In addition, the diffraction peak at $2\Theta = 25.98^{o}$ of these polyanilines are most relatively intense due to increase of effective delocalization in polymer chain. This crystalline peak of polyaniline synthesized indicated that it is semi-crystalline structure. The integrated intensity of the peaks can be used to indicate the crystallinity in polyaniline as shown in Table 4.19. The

synthesized polyaniline using 5 shots of oxygen plasma is selected for integrated amorphous intensity for calculation of all degree of crystallinity values because this condition shows lower integrated amorphous structure than others.

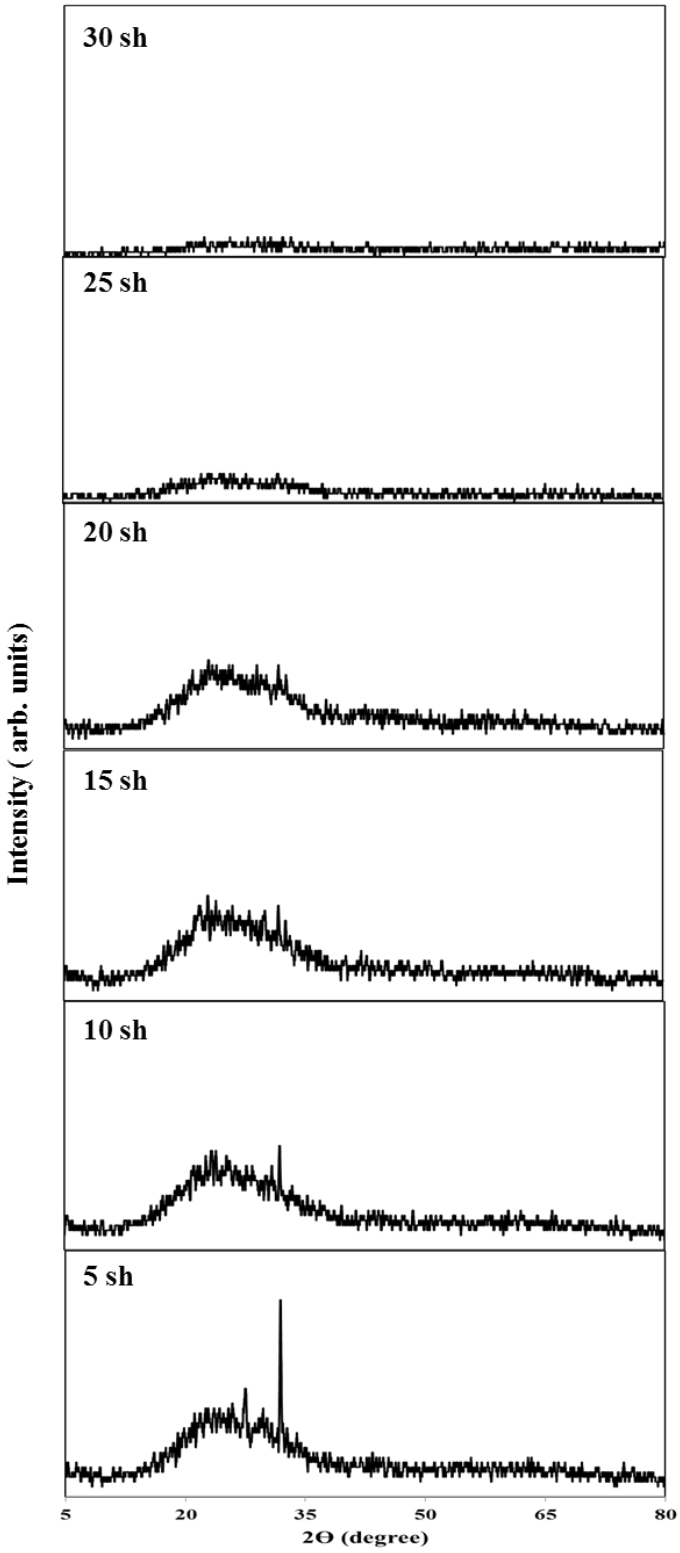

Figure 4.37 XRD patterns of polyanilines synthesized in HCl solution using various shots of argon plasma generated from PICP device

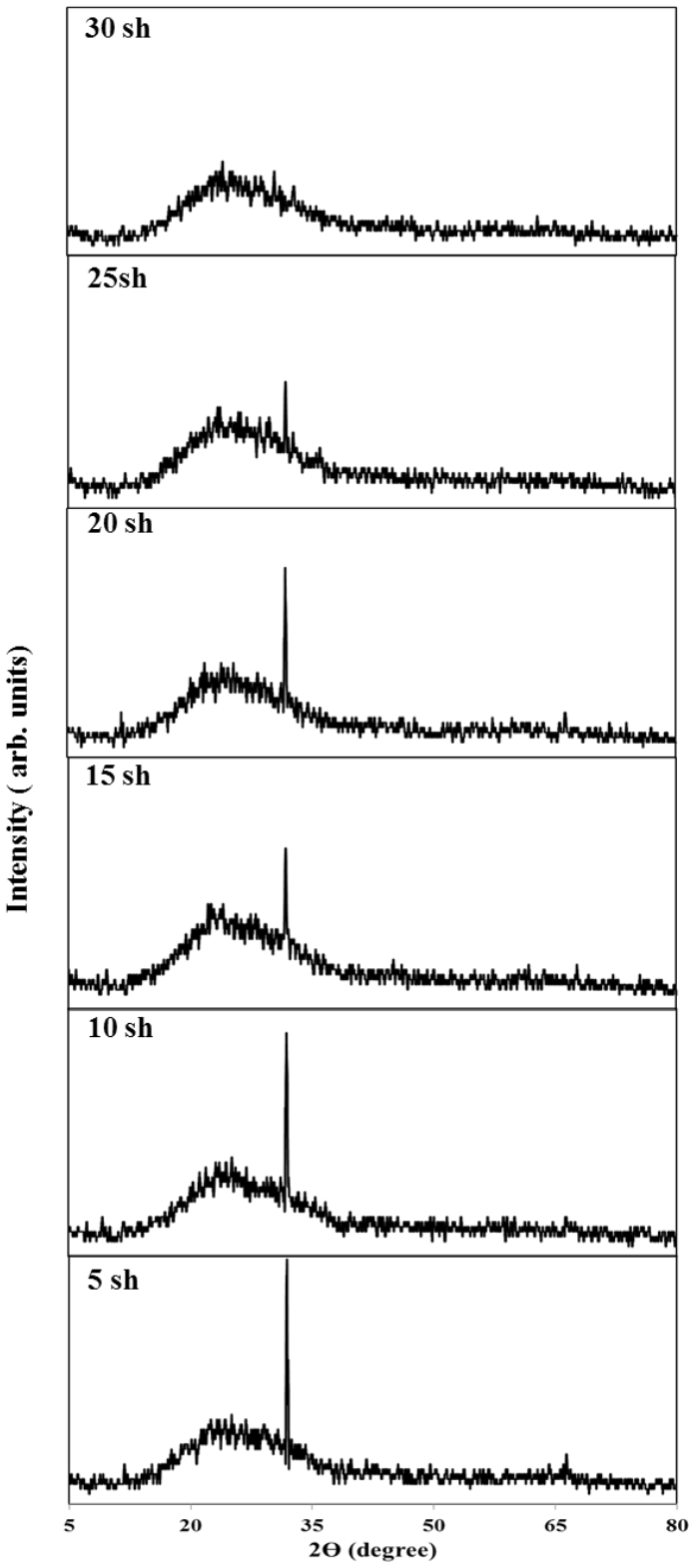

Figure 4.38 XRD patterns of polyanilines synthesized in HCl solution using various shots of oxygen plasma generated from PICP device

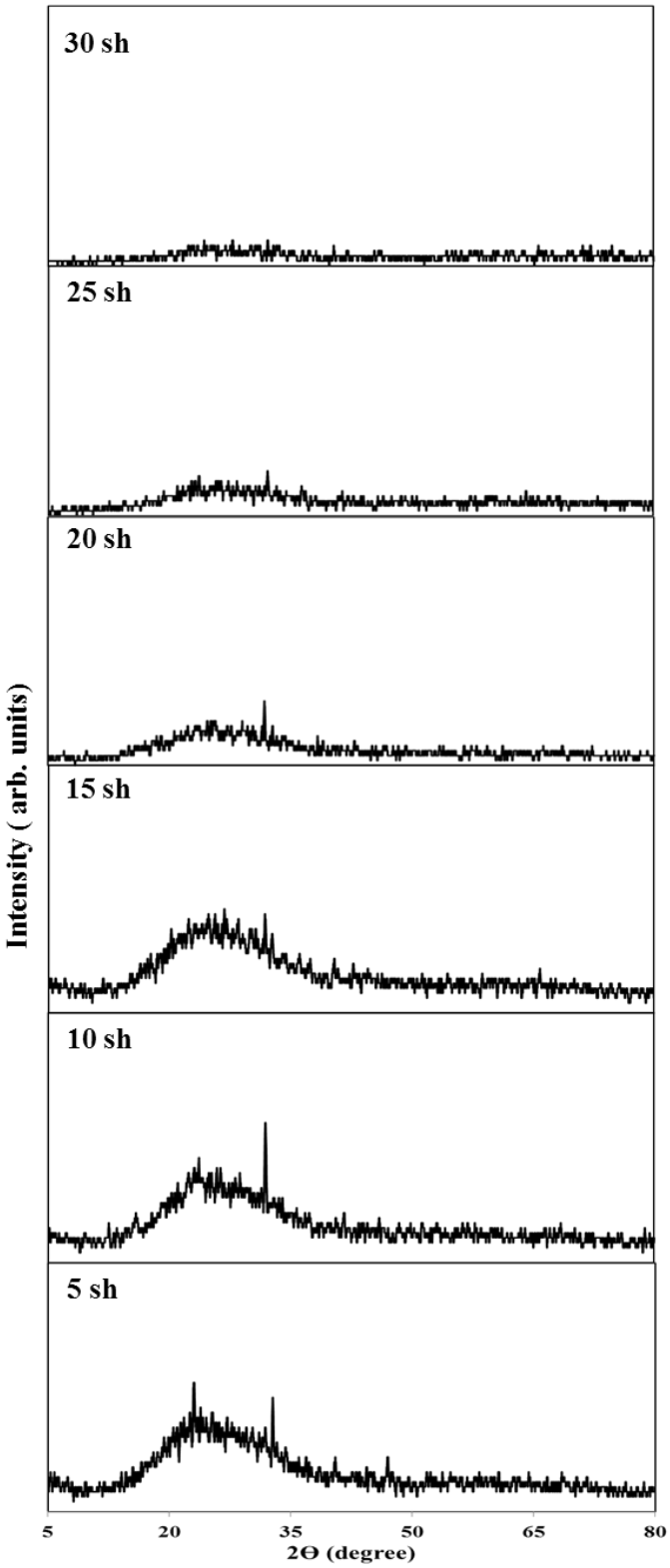

Figure 4.39 XRD patterns of polyanilines synthesized in HCl solution using various shots of nitrogen plasma generated from PICP device

Table 4.19 The degree of crystallinity (%) of polyanilines synthesized in HCl solution using PICP device

The degree of crystallinity (%)						
Gas Type	**The number of plasma shots**					
	5	**10**	**15**	**20**	**25**	**30**
Argon	8.38	8.78	-	-	-	-
Oxygen	5.38	11.37	20.15	6.78	10.37	-
Nitrogen	16.16	15.36	-	-	-	-

4.2.2.6 Thermal properties

The decomposition temperatures of polyanilines synthesized in HCl solution using PICP device are summarized in Table 4.20 and TGA thermograms are shown in Figures 4.40-4.42. Similar trend as observed in the case of polyanilines synthesized using sulfuric acid was found. However, the decomposition temperatures of those synthesized using sulfuric acid are higher. This may be because of the difference in the structures of the obtained polyanilines.

Table 4.20 Decomposition temperatures of polyanilines synthesized in HCl solution using PICP device

Gas Type	The number of plasma shots	Decomposition Temperature (^oC)
Ar	5	176.04
	10	175.33
	15	173.65
	20	169.33
	25	172.13
	30	174.66
O_2	5	159.22
	10	159.28
	15	166.25
	20	166.54
	25	162.51
	30	169.37
N_2	5	175.82
	10	158.15
	15	158.81
	20	158.77
	25	158.72
	30	177.65

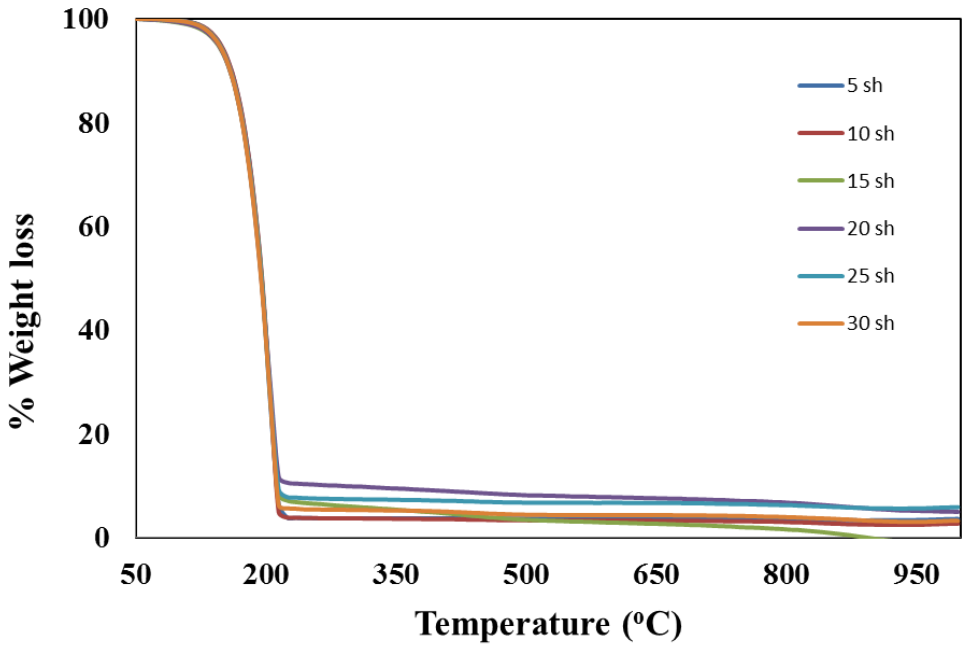

Figure 4.40 TGA Thermograms of polyanilines synthesized in HCl solution using various shots of argon plasma generated from PICP device

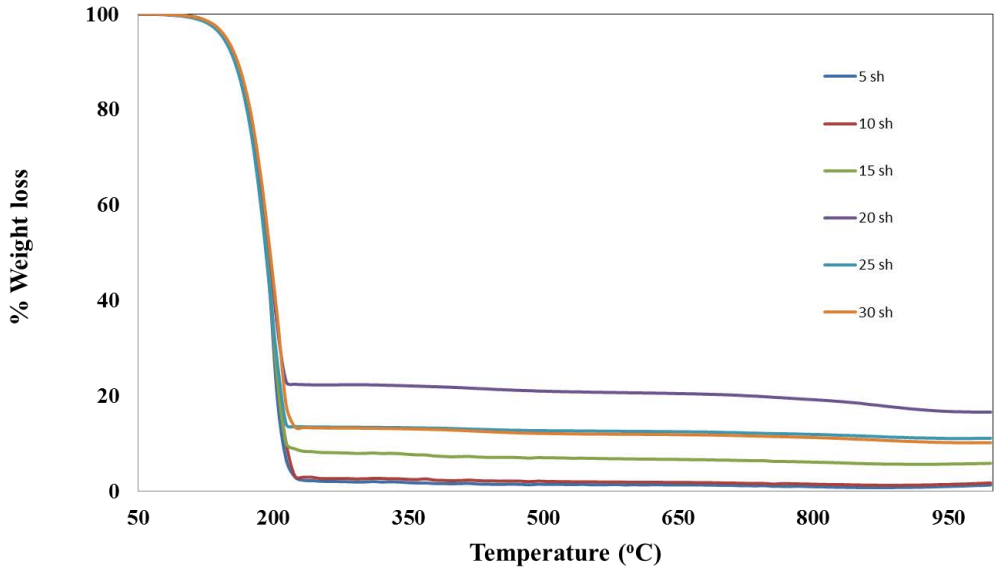

Figure 4.41 TGA Thermograms of polyanilines synthesized in HCl solution using various shots of oxygen plasma generated from PICP device

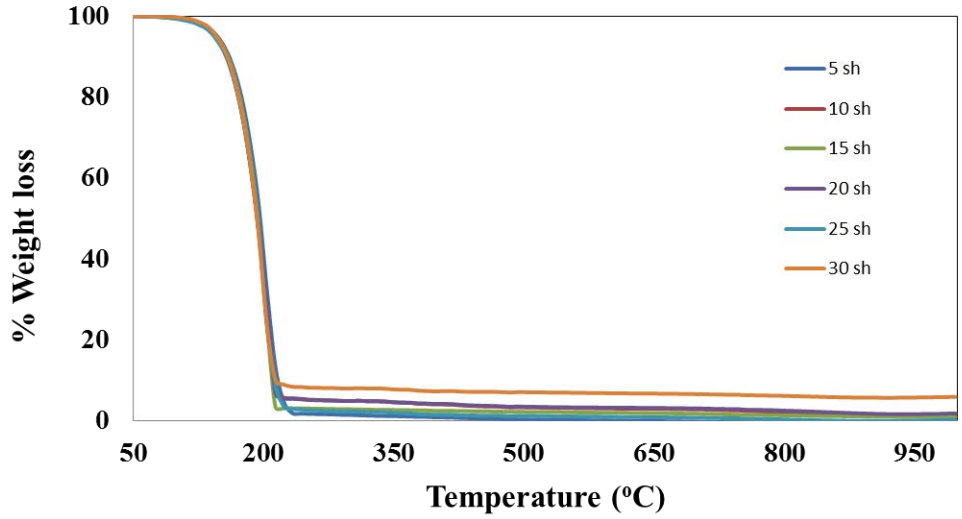

Figure 4.42 TGA Thermograms of polyanilines synthesized in HCl solution using various shots of nitrogen plasma generated from PICP device

4.2.2.7 Morphology

Polyanilines synthesized using HCl solution exhibit rod-like and granular structures depending on the type of gas and the number of plasma shots as shown in Figures 4.43-4.45. In case of argon, all polyanilines show granular and rod-like structure as seen in Figures 4.43 (a-f). An increase in the number of the plasma shots leads to lower amounts of rod-like structure. However, the granules still occur and they agglomerate at 30 shots of plasma (Figure 4.43f). In case of oxygen (Figure 4.44) and nitrogen (Figure 4.45), small clusters of the bulk-like structure were observed in all synthesized polyanilines. The number of plasma shots affects the size of these clusters and their dispersion. It was found that for polyanilines synthesized at low plasma shots, the clusters were much dense than those synthesized at high plasma shots.

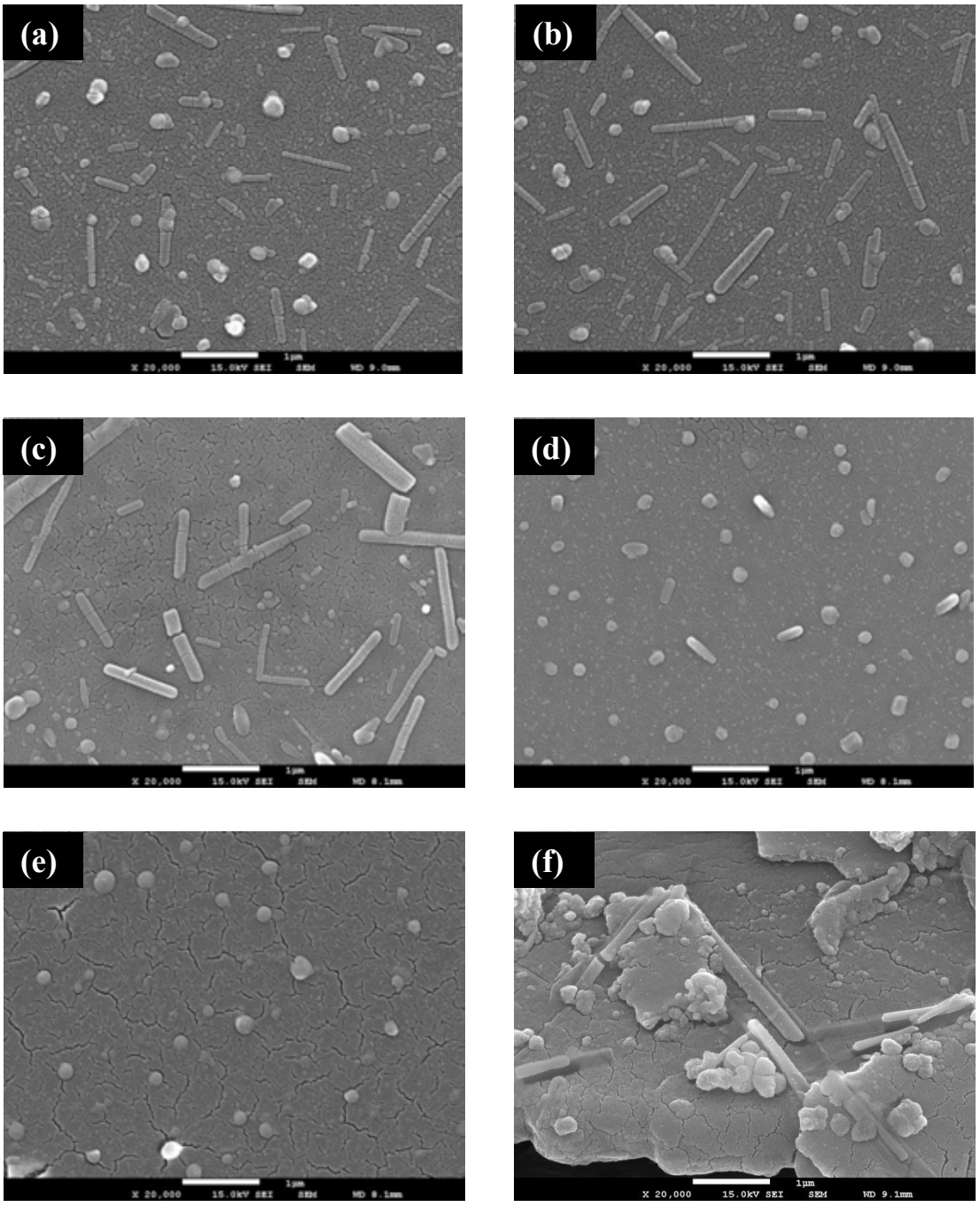

Figure 4.43 FE-SEM images of polyanilines synthesized in HCl solution using (a) 5 (b) 10 (c) 15 (d) 20 (e) 25 (f) 30 of argon plasma generated from PICP device

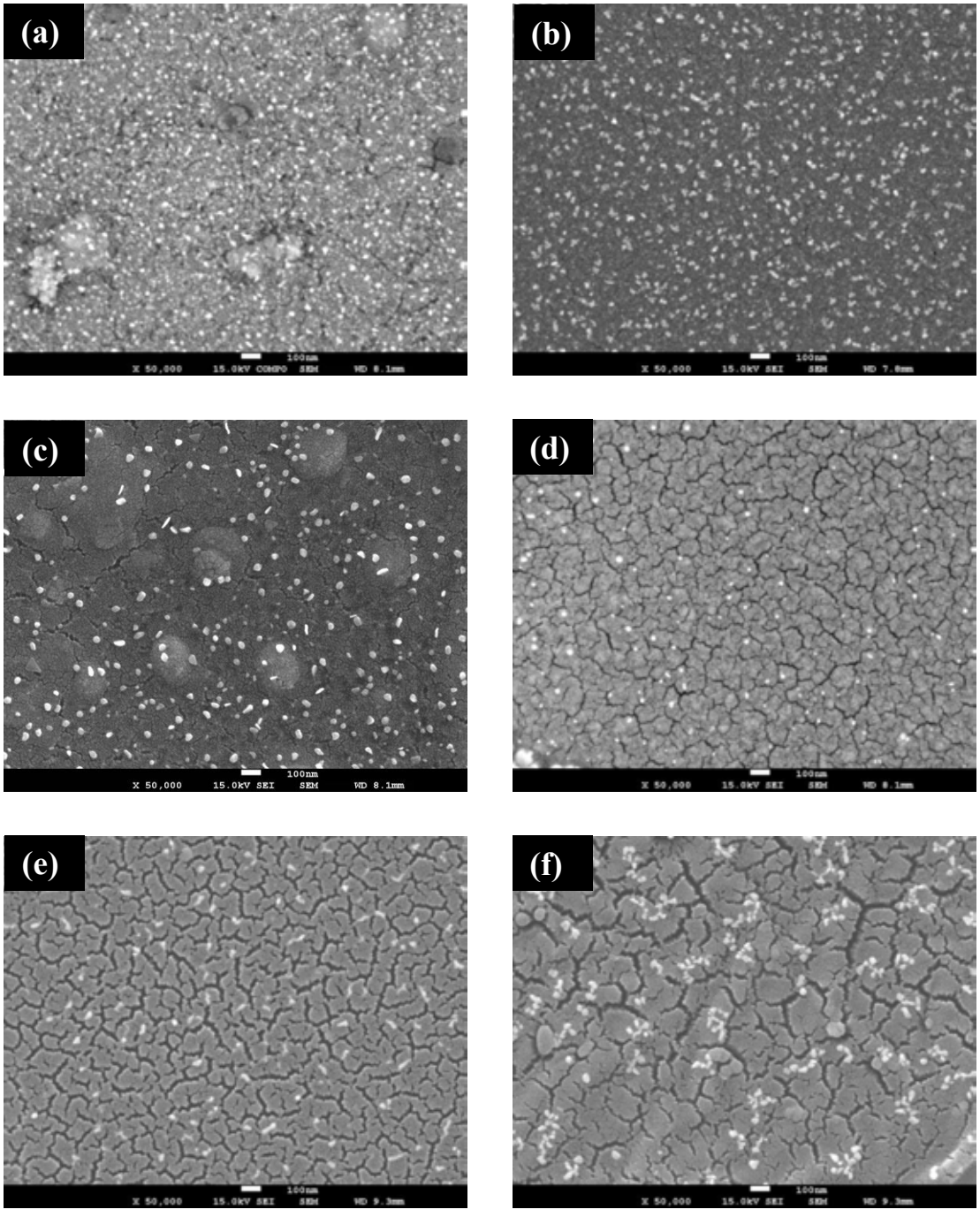

Figure 4.44 FE-SEM images of polyanilines synthesized in HCl solution using (a) 5 (b) 10 (c) 15 (d) 20 (e) 25 (f) 30 of oxygen plasma generated from PICP device

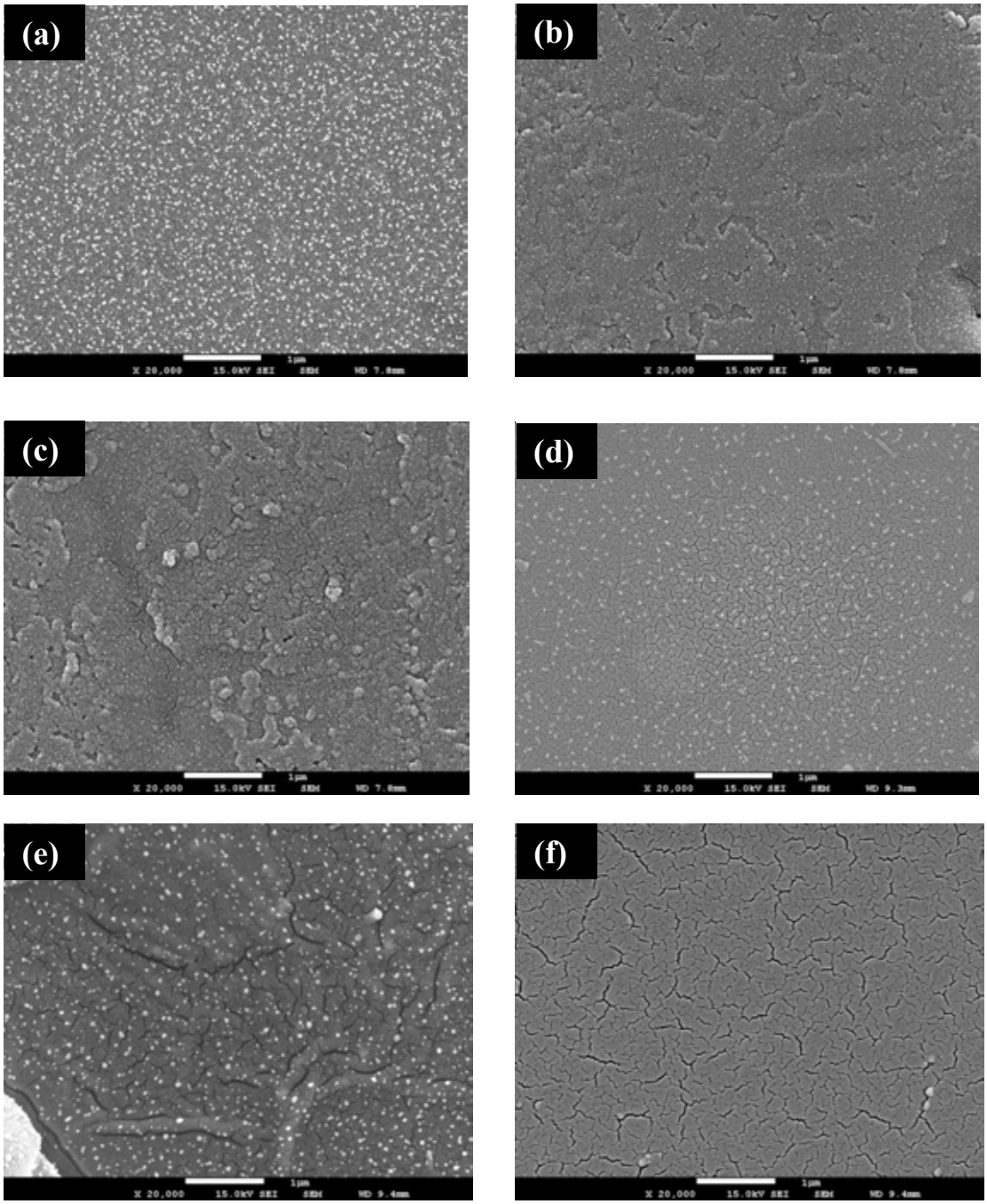

Figure 4.45 FE-SEM images of polyanilines synthesized in HCl solution using (a) 5 (b) 10 (c) 15 (d) 20 (e) 25 (f) 30 of nitrogen plasma generated from PICP device

All the results suggest that all polyaniline synthesized in HCl solution using argon, oxygen and nitrogen plasma exhibit the emeraldine base structure in conjunction with lower amount of the emeraldine salt as shown below depending on the number of the plasma shots as confirmed by UV-VIS spectra and FTIR spectra and the conductivity measurement.

Emeraldine salt:
(green color)

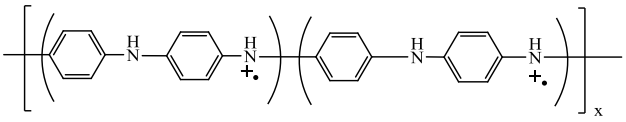

Emeraldine base:
(brown color)

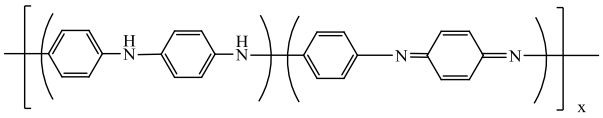

When compared all polyanilines synthesized in H_2SO_4 and HCl solutions using PICP device, the results indicate that polyaniline synthesized in H_2SO_4 solution using 20 shots of argon plasma exhibit highest electrical conductivity. Therefore, this polyaniline was selected for investigating the potential for film formation on other substrates such as silicon instead of the glass substrate. Figure 4.46 shows that this polyaniline can be synthesized and form the film on silicon substrate.

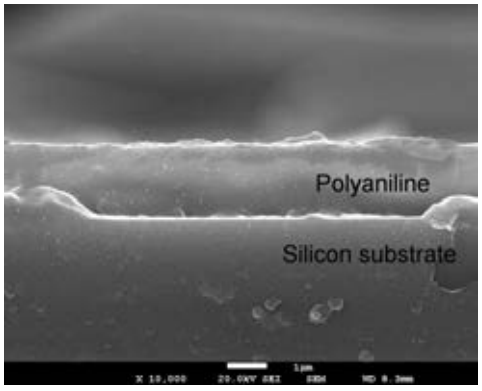

Figure 4.46 FE-SEM image of polyaniline film on silicon substrate

4.3 Characteristics and properties of polyanilines filled with silver particles

In this part of the experiment, PICP device was selected for the synthesis instead of theta-pinch device because it operates at lower voltage and polyaniline obtained from this device has higher conductivity. Nitric acid was also used instead of sulfuric acid because using the later may result in the precipitation of silver salt [22]. The number of the plasma shots used for each gas was selected from the conditions that yielded polyanilines with highest conductivity which were 20 shots for argon and oxygen and 15 shots for nitrogen.

4.3.1 Chemical Structure

FTIR spectra of polyanilines filled with silver particles synthesized using argon, oxygen and nitrogen plasma at different concentrations of silver nitrate solution are shown in Figures 4.47-4.49 and their peaks are interpreted and given in Table 4.21-4.23., respectively. Their spectra are quite comparable. The positions of quinonoid and bezenoid stretching vibrations are observed at 1630 and 1493 cm^{-1}. The absorption peak at 1300 cm^{-1} can be assigned to C-N vibrations. The sharp peak at 1383 cm^{-1} corresponds to nitrate counter-ions in the protonated form of polyaniline [21,91] as shown in Scheme 2.4. However, the peak at 1376 cm^{-1} assigned to characteristic of polyaniline base is not found. The peak at 1144 cm^{-1} is contributed to the vibration mode of $–NH^{+}=$ structure of conducting polyaniline [87]. However, a slight shift of this peak to 1156 cm^{-1} occurs when the concentrations of silver nitrate of 1.5 and 2.0 M were applied. The peaks at 820 and 688 cm^{-1} are assigned to C-C and C-H stretching of benzenoid unit and out of plane C-H vibration of polyaniline, respectively [18].

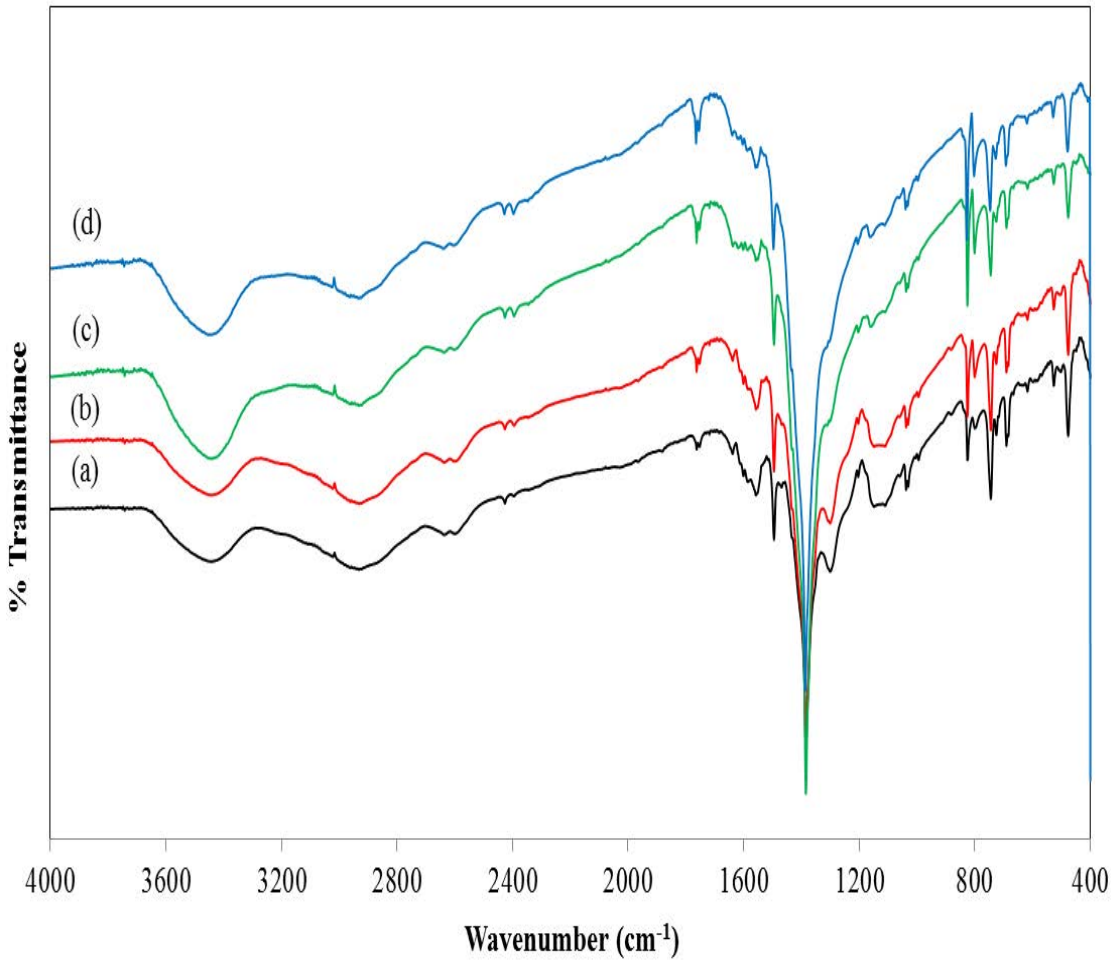

Figure 4.47 FTIR spectra of silver-filled polyanilines synthesized using argon plasma at (a) 0.5 (b) 1.0 (c) 1.5 (d) 2.0 mol/l of silver nitrate solution

Table 4.21 Interpretation of FTIR spectra of silver-filled polyanilines synthesized using argon plasma at (a) 0.5 (b) 1.0 (c) 1.5 (d) 2.0 mol/l of silver nitrate solution

Assignments	Wavenumber (cm^{-1})			
	0.5	**1.0**	**1.5**	**2.0**
1. N-H stretching of aromatic amine	3434	3437	3437	3437
2. C-H stretching of aliphatic	2934	2931	2925	2925
3. C=C stretching of quinoid ring	1556	1556	1556	1556
4. C=C stretching of benzenoid group	1495	1495	1495	1495
5. Nitrate counter-ions	1383	1383	1383	1383
6. C-N stretching of vibrations	1300	1300	1297	1294
7. NH^{+}= vibration mode	1144	1144	1156	1156
8. C-H out of plane blending	823	823	823	823
9. C-H vibration of polyaniline	691	691	688	688

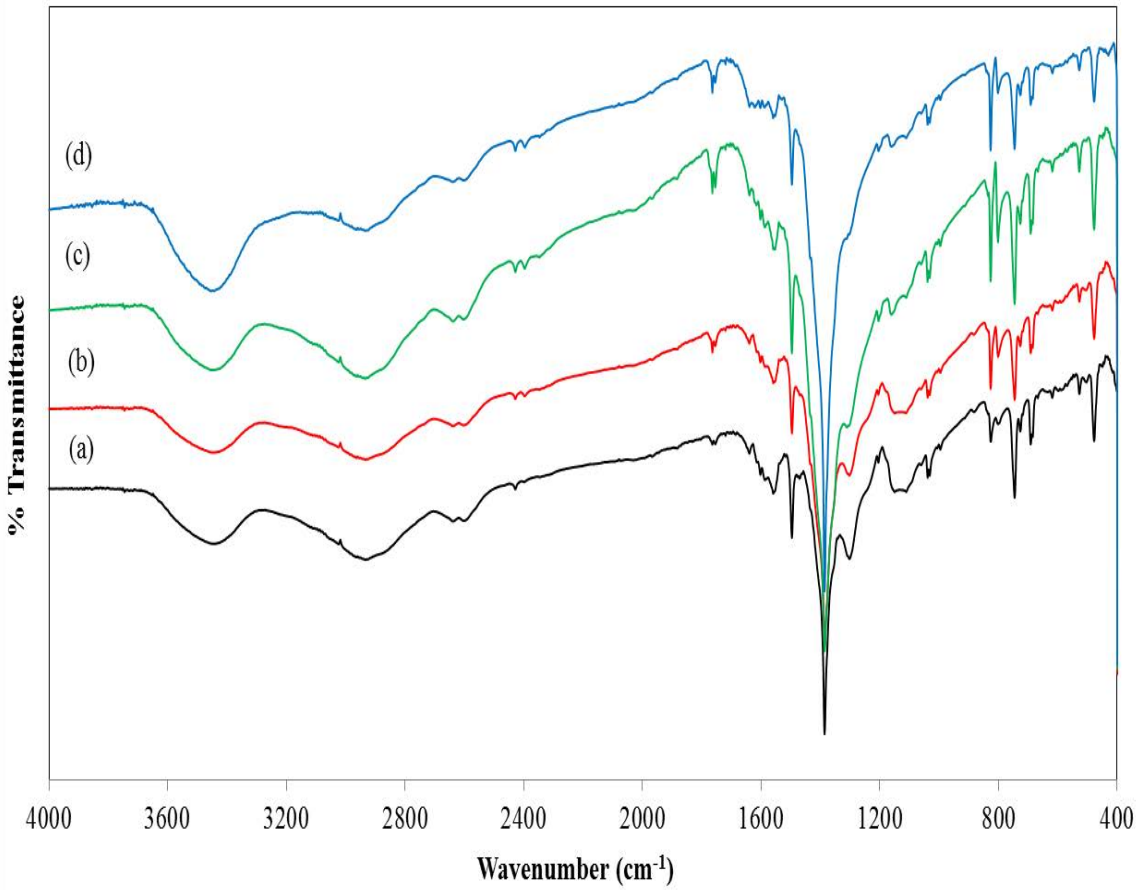

Figure 4.48 FTIR spectra of silver-filled polyanilines synthesized using oxygen plasma at (a) 0.5 (b) 1.0 (c) 1.5 (d) 2.0 mol/l of silver nitrate solution

Table 4.22 Interpretation of FTIR spectra of silver-filled polyanilines synthesized using oxygen plasma at (a) 0.5 (b) 1.0 (c) 1.5 (d) 2.0 mol/l of silver nitrate solution

Assignments	Wavenumber (cm^{-1})			
	0.5	**1.0**	**1.5**	**2.0**
1. N-H stretching of aromatic amine	3437	3437	3440	3440
2. C-H stretching of aliphatic	2919	2925	2931	2931
3. C=C stretching of quinoid ring	1556	1556	1556	1556
4. C=C stretching of benzenoid group	1495	1495	1495	1495
5. Nitrate counter-ions	1383	1383	1383	1383
6. C-N stretching of vibrations	1300	1300	1300	1291
7. NH^{+}= vibration mode	1144	1144	1156	1156
8. C-H out of plane blending	823	823	823	823
9. C-H vibration of polyaniline	691	688	685	685

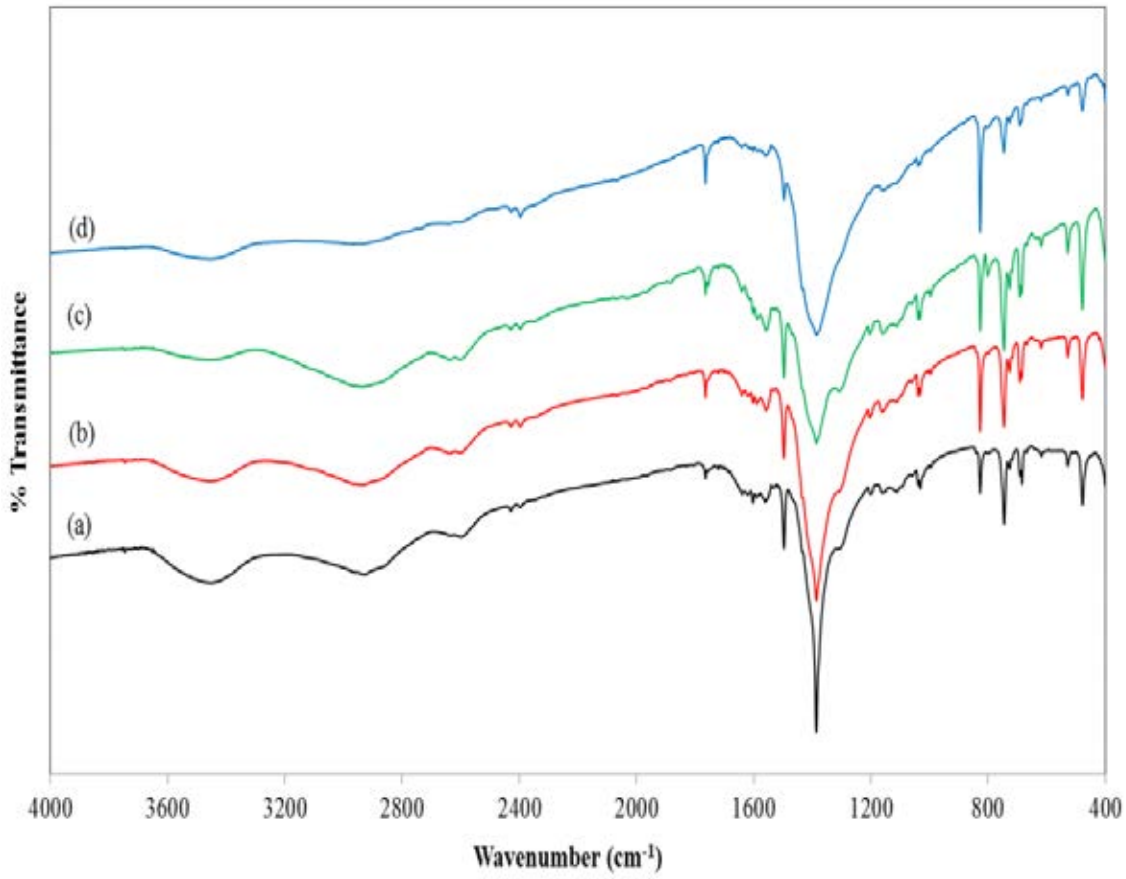

Figure 4.49 FTIR spectra of silver-filled polyanilines synthesized using nitrogen plasma at (a) 0.5 (b) 1.0 (c) 1.5 (d) 2.0 mol/l of silver nitrate solution

Table 4.23 Interpretation of FTIR spectra of silver-filled polyanilines synthesized using nitrogen plasma at (a) 0.5 (b) 1.0 (c) 1.5 (d) 2.0 mol/l of silver nitrate solution

Assignments	Wavenumber (cm^{-1})			
	0.5	**1.0**	**1.5**	**2.0**
1. N-H stretching of aromatic amine	3443	3443	3443	3440
2. C-H stretching of aliphatic	2925	2928	2934	2937
3. C=C stretching of quinoid ring	1556	1556	1553	1553
4. C=C stretching of benzenoid group	1495	1495	1492	1492
5. Nitrate counter-ions	1383	1383	1383	1383
6. C-N stretching of vibrations	1303	1300	1300	-
7. NH^+= vibration mode	1156	1156	1156	1156
8. C-H out of plane blending	823	823	823	823
9. C-H vibration of polyaniline	688	688	688	688

4.3.2 Optical characteristics

As seen from Figure 4.50, UV-VIS spectra of silver-filled polyanilines synthesized using argon plasma at all concentrations of silver nitrate exhibit 4 absorption peaks. From Table 4.24, the peaks attributed to π-π* transition and π-polaron transition of polyaniline filled with silver particles occur at 260 and 294 nm, respectively. Other characteristic peaks of polyaniline filled with silver particles corresponding to π-π* transition in benzenoid ring and the excitation in quinoid rings also occur at 320-326 and 590-620 nm, respectively [18,21,23]. However, the surface plasmon absorption peaks of silver particles normally found in wavelength range of

400 to 520 nm depending on the particle size does not occur in these spectra. This may be overlapped by the strong absorption maximum of polyaniline, and may cause the shift of emeraldine salt polyaniline to lower wavelengths [22].

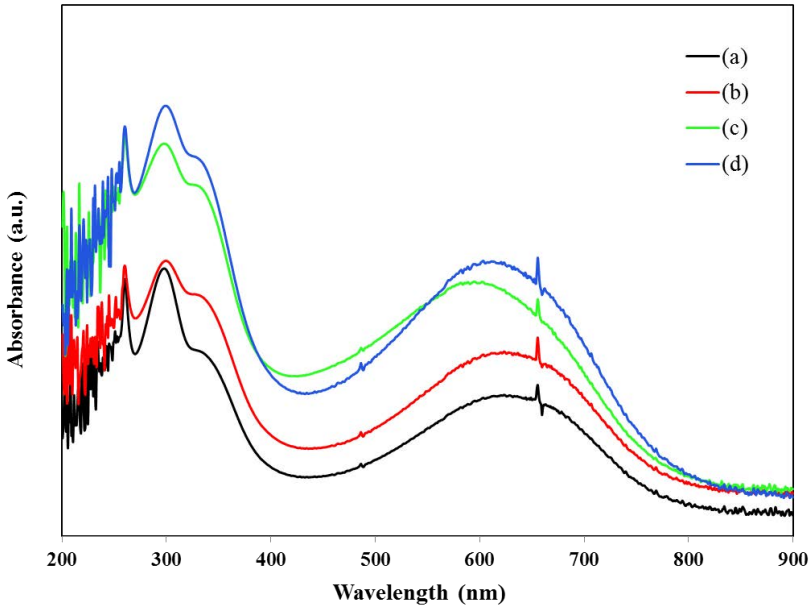

Figure 4.50 UV-VIS spectra of silver-filled polyanilines synthesized using argon plasma at (a) 0.5 (b) 1.0 (c) 1.5 (d) 2.0 mol/l of silver nitrate solution

Table 4.24 UV-VIS absorption peaks of silver-filled polyanilines synthesized using argon plasma

Conc. of silver nitrate solution (mol/l)	**λ_{max} (nm)**			
	1	**2**	**3**	**4**
0.5	260	294	326	620
1.0	260	294	326	617
1.5	260	294	320	600
2.0	260	294	320	590

As seen from Figure 4.51 and Table 4.25, silver-filled polyanilines synthesized using oxygen plasma exhibit UV-VIS absorption phenomena similar to those synthesized using argon plasma. On the other hand, those synthesized using nitrogen plasma show slightly different spectra as shown in Figure 4.52 and Table 4.26 due to different functional groups present.

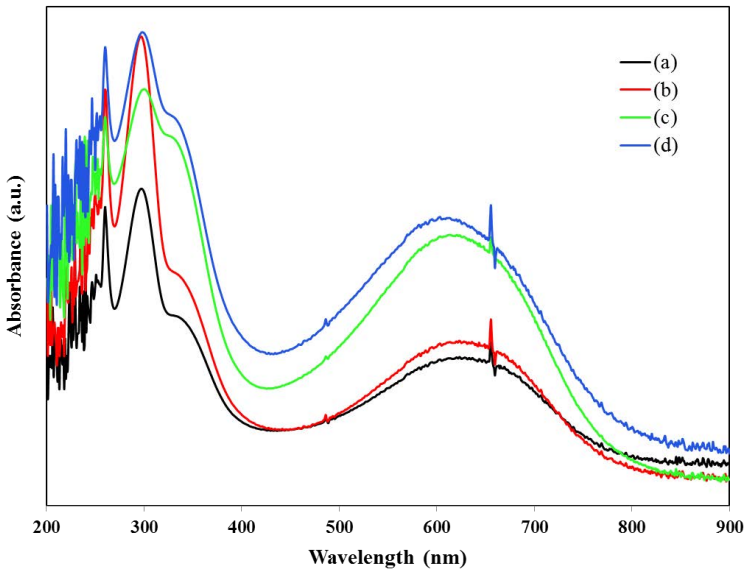

Figure 4.51 UV-VIS spectra of silver-filled polyanilines synthesized using oxygen plasma at (a) 0.5 (b) 1.0 (c) 1.5 (d) 2.0 mol/l of silver nitrate solution

Table 4.25 UV-VIS absorption peaks of silver-filled polyanilines synthesized using oxygen plasma

The concentration of silver nitrate	**λ_{max} (nm)**			
	1	**2**	**3**	**4**
0.5	260	294	330	623
1.0	260	294	330	620
1.5	260	294	320	610
2.0	260	294	320	600

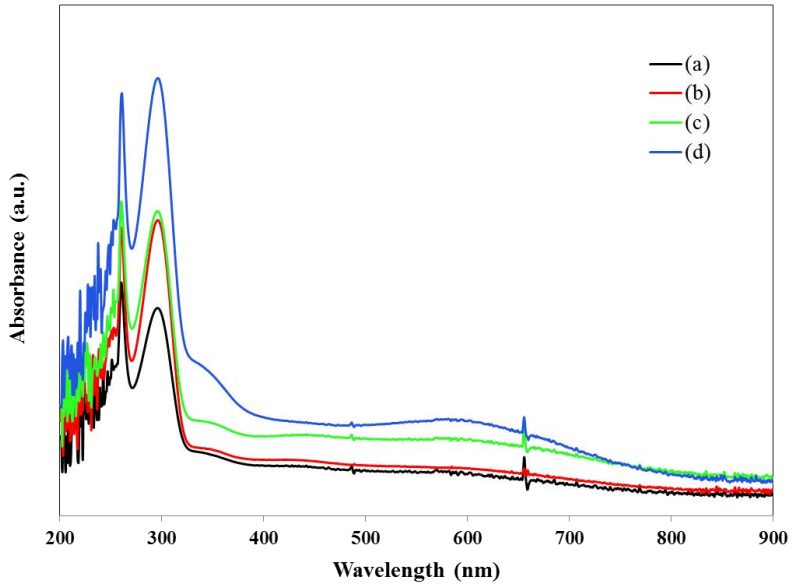

Figure 4.52 UV-VIS spectra of silver-filled polyanilines synthesized using nitrogen plasma at (a) 0.5 (b) 1.0 (c) 1.5 (d) 2.0 mol/l of silver nitrate solution

Table 4.26 UV-VIS absorption peaks of silver-filled polyanilines synthesized using argon plasma

The concentration of silver nitrate	**λ_{max} (nm)**			
	1	**2**	**3**	**4**
0.5	260	290	330	-
1.0	260	290	330	-
1.5	260	290	330	595
2.0	260	290	330	595

4.3.3 Electrical Conductivity

Electrical conductivity values of polyaniline filled with silver particles are given in Table 4.27. These values are higher than that of unfilled polyanilines as shown in previous sections. Generally, the electrical conductivity of silver is $6.3x10^5$ $S.cm^{-1}$ at 20^oC [92] but the electrical conductivity of silver-filled polyanilines exhibits just 10^{-4} $S.cm^{-1}$. This result may be caused by the interfaces between polyaniline and silver particles. This interface may produce barriers to the charge-carries and restrict the participation of silver in conduction [23]. The conductivity may depend on other results such as the morphology of both polyaniline and silver particles [35]. Such the nanofibers structure of polyaniline show higher well-oganized than the microfibers, brushes and spheres [93-94]. The highest conductivities for the synthese using argon, oxygen and nitrogen plasma are 3.31 $x10^{-4}$, 2.31 $x10^{-4}$, 1.32 $x10^{-4}$ $S.cm^{-1}$, respectively at 1.0 M of silver nitrate solution. These conditions show that nanofibers have longer and thinner shape than the others as confirmed by FE-SEM images.

Table 4.27 Electrical Conductivity of polyanilines filled with silver particles

The concentration of silver nitrate (mol/L)	**Conductivity ($S.cm^{-1}$)**		
	Ar	**O_2**	**N_2**
0.5	$(2.84\pm0.08)x10^{-4}$	$(2.14\pm 0.09)x10^{-4}$	$(1.26\pm 0.04)x10^{-4}$
1.0	$(3.31\pm0.23)x10^{-4}$	$(2.31\pm 0.13)x10^{-4}$	$(1.32\pm 0.02)x10^{-4}$
1.5	$(2.55\pm0.03)x10^{-4}$	$(1.82\pm 0.09)x10^{-4}$	$(1.12\pm 0.02)x10^{-4}$
2.0	$(1.92\pm0.05)x10^{-4}$	$(1.30\pm0.04)x10^{-4}$	$(1.08\pm 0.04)x10^{-4}$

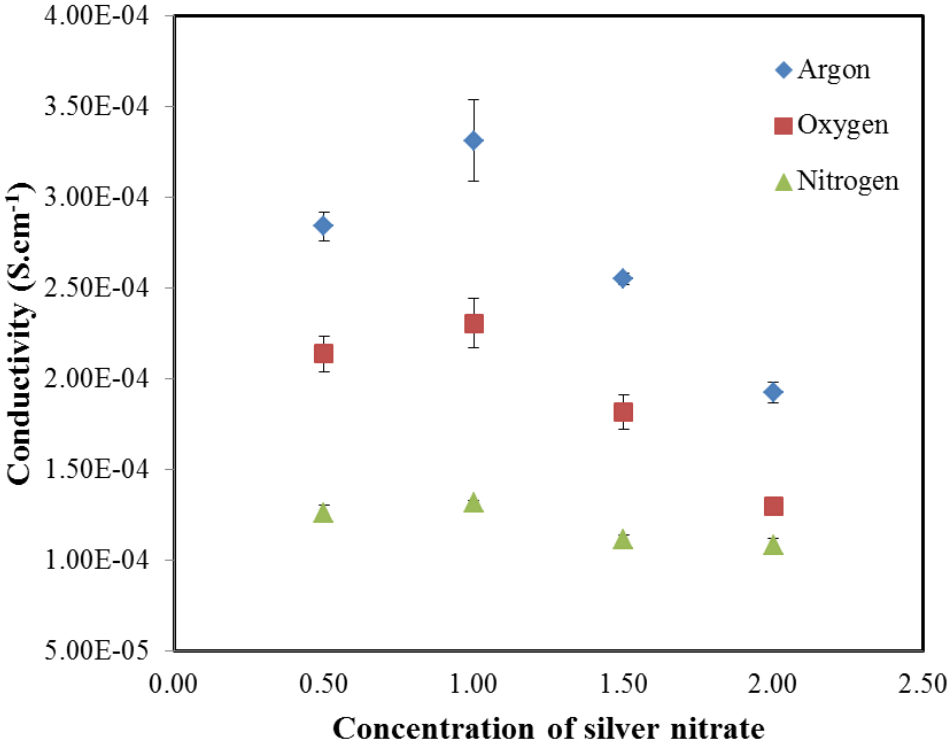

Figure 4.53 The effect of the gas type on the conductivity of polyanilines filled with silver particles

4.3.4 Crystal Structure

X-ray diffraction patterns of polyanilines filled with silver particles synthesized using argon, oxygen and nitrogen palsma are shown in Figures 4.54-4.56, respectively. The presences of silver particles and polyaniline are observed. The broad peak at $2\theta = 25^{o}$ assigned to characteristic of polyaniline is present. Moreover, it also exhibits the sharp peaks at 11 and 22^{o} [95]. The sharp peaks centered at $2\theta = 38$, 44, 64 and 77^{o} corresponding to (111), (200), (220) and (311) plane of face-centered cubic phase of silver particles (JCPDS standard no. 40-0783) [95-96] are present. The crystallite sizes of silver particles can be calculated from Scherrer's equation [97] as follows:

$$D=k\lambda/(\beta\cos\theta)$$

Where λ is the X-ray wavelength (0.1540 nm), k = is the shape factor (0.89), D is the average diameter of the crystals (in Armstrong units), θ is the Bragg angle (in degree), β is full width at half maximum (FWHM) of the peak intensity (in 2θ units). The value at 2θ=38^{o} is used to determine in Scherrer's equation due to highest intensity than those peaks of silvers particles. From calculation obtained 50 nm of diameter of silver particles. In addition, an increasing in the peak intensity corresponds to an increase in the particle size. Moreover, the crystalline peak at about 36^{o} was observed with increasing the concentration of silver nitrate because silver azide is presented (JCPDS standard no. 00-003-0906) [98].

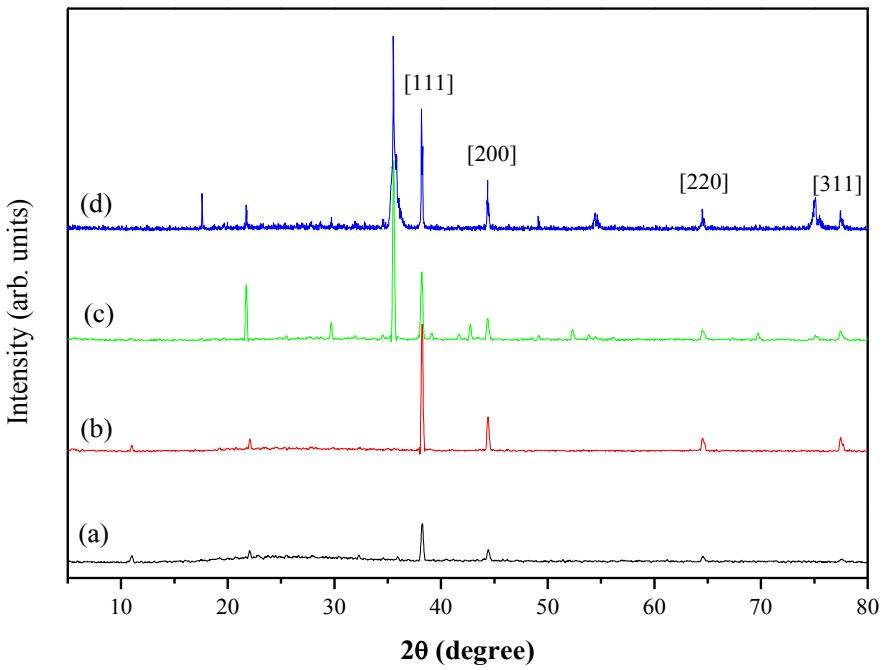

Figure 4.54 XRD patterns of silver-filled polyanilines synthesized using argon plasma at (a) 0.5 (b) 1.0 (c) 1.5 (d) 2.0 mol/l of silver nitrate solution

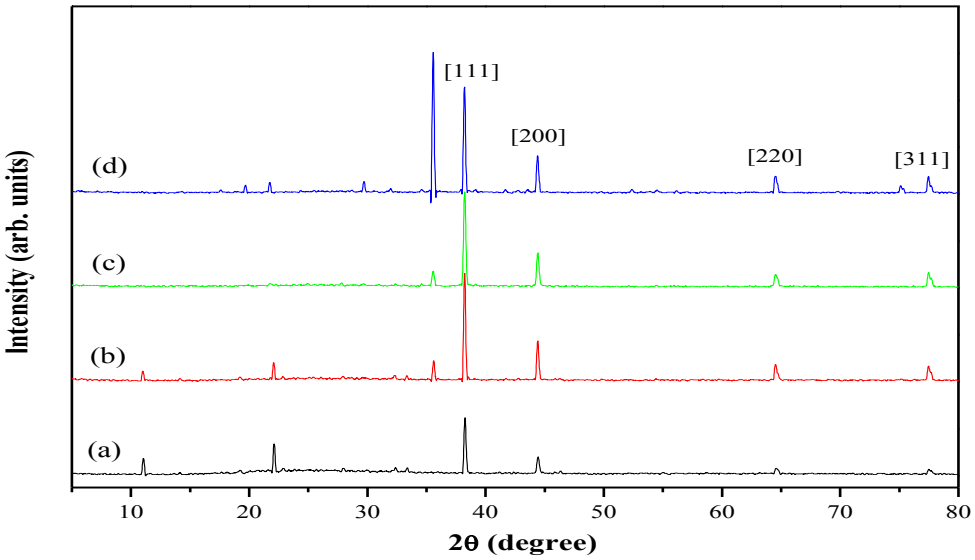

Figure 4.55 XRD patterns of silver-filled polyanilines synthesized using oxygen plasma at (a) 0.5 (b) 1.0 (c) 1.5 (d) 2.0 mol/l of silver nitrate solution

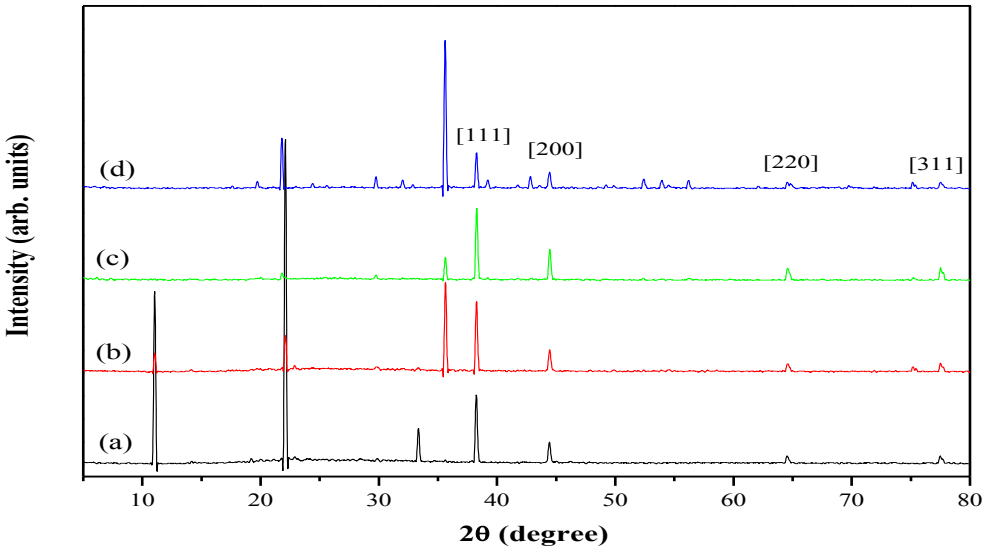

Figure 4.56 XRD patterns of silver-filled polyanilines synthesized using nitrogen plasma at (a) 0.5 (b) 1.0 (c) 1.5 (d) 2.0 mol/l of silver nitrate solution

4.3.5 Thermal Properties

The decomposition temperatures of silver-filled polyanilines synthesized using PICP device are summarized in Table 4.20 and TGA thermograms are shown in Figures 4.57-4.59. The decomposition tempearatures of these polyanilines are in the range of 187-243 ^{o}C which are better than those of pure polyaniline suggesting that silver particles can improve thermal properties of polyaniline. The decomposition temperature of silver-filled polyanilines started with the degradation of low molecular weight fragments of the polymer. Consequently, at low concentration of silver nitrate, polyanilines synthesized using all types of plasma show higher decomposition temperatures due to longer fibrils corresponding to results from the electrical conductivity and FE-SEM results.

Table 4.28 Decomposition temperature of silver-filled polyanilines synthesized using PICP device

Gas Type	The concentration of silver nitrate (mol/L)	Decomposition Temperature (^{o}C)
Ar	0.5	209.47
	1.0	243.53
	1.5	189.50
	2.0	200.01
O_2	0.5	211.05
	1.0	210.06
	1.5	194.93
	2.0	193.58
N_2	0.5	204.30
	1.0	201.60
	1.5	198.99
	2.0	187.93

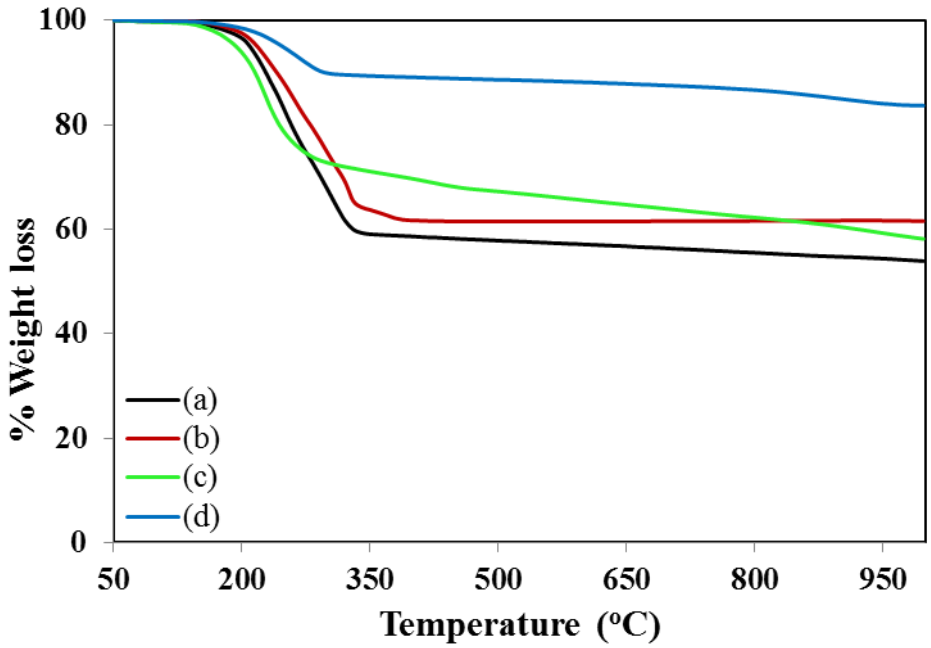

Figure 4.57 TGA thermograms of silver-filled polyanilines synthesized using argon plasma at (a) 0.5 (b) 1.0 (c) 1.5 (d) 2.0 mol/l of silver nitrate solution

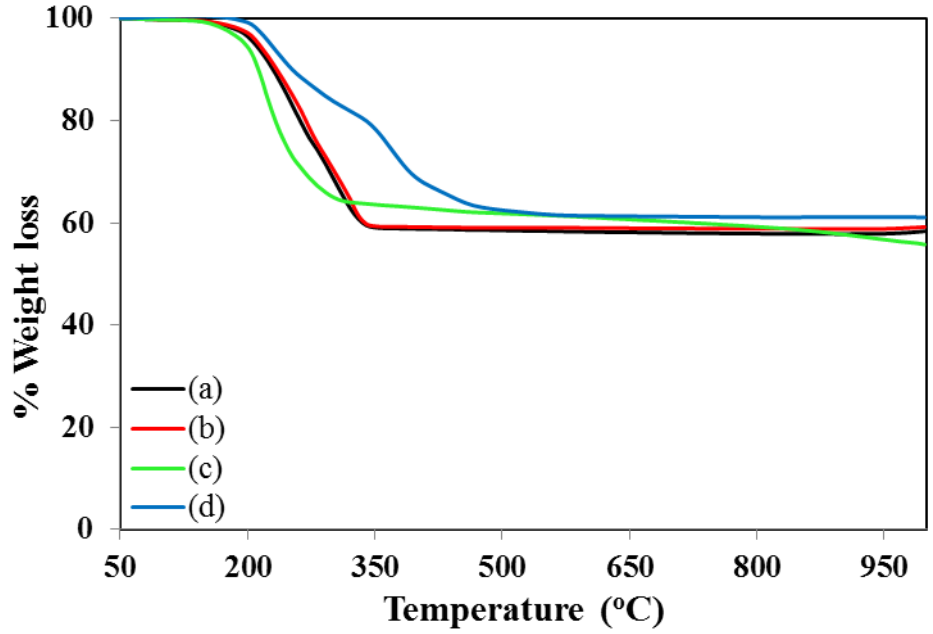

Figure 4.58 TGA thermograms of silver-filled polyanilines synthesized using oxygen plasma at (a) 0.5 (b) 1.0 (c) 1.5 (d) 2.0 mol/l of silver nitrate solution

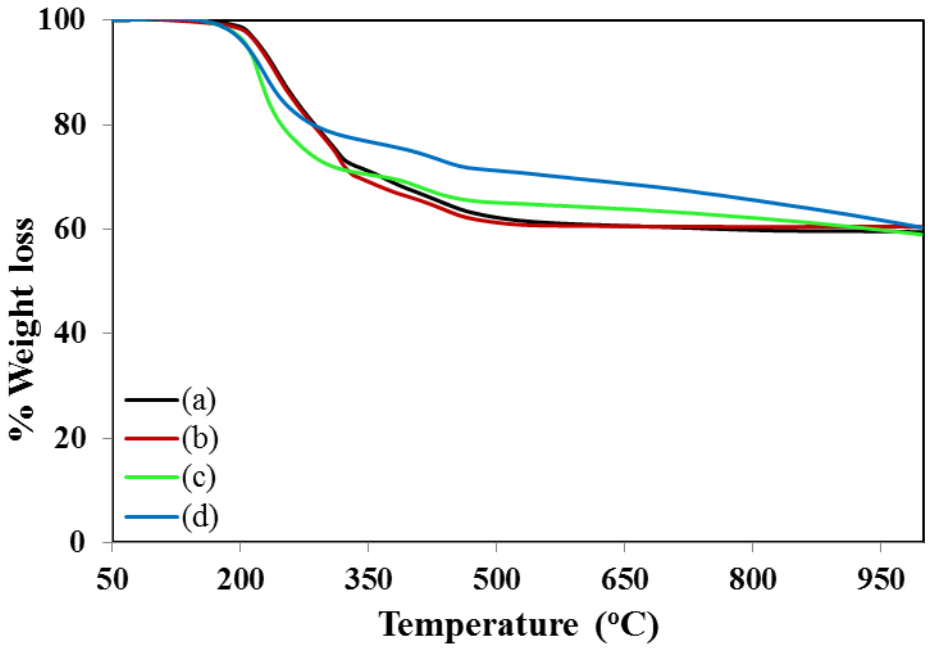

Figure 4.59 TGA thermograms of silver-filled polyanilines synthesized using nitrogen plasma at (a) 0.5 (b) 1.0 (c) 1.5 (d) 2.0 mol/l of silver nitrate solution

4.3.6 Morphology

Figures 4.60-4.62 reveal that all synthesized polyanilines filled with silver particles exhibit the fibril structure of polyaniline with average diameter of 50-100 nm and the spherical structure of silver particles with diameter about 50-80 nm. The amounts of silver particles increase with increasing the concentration of silver nitrate solution.

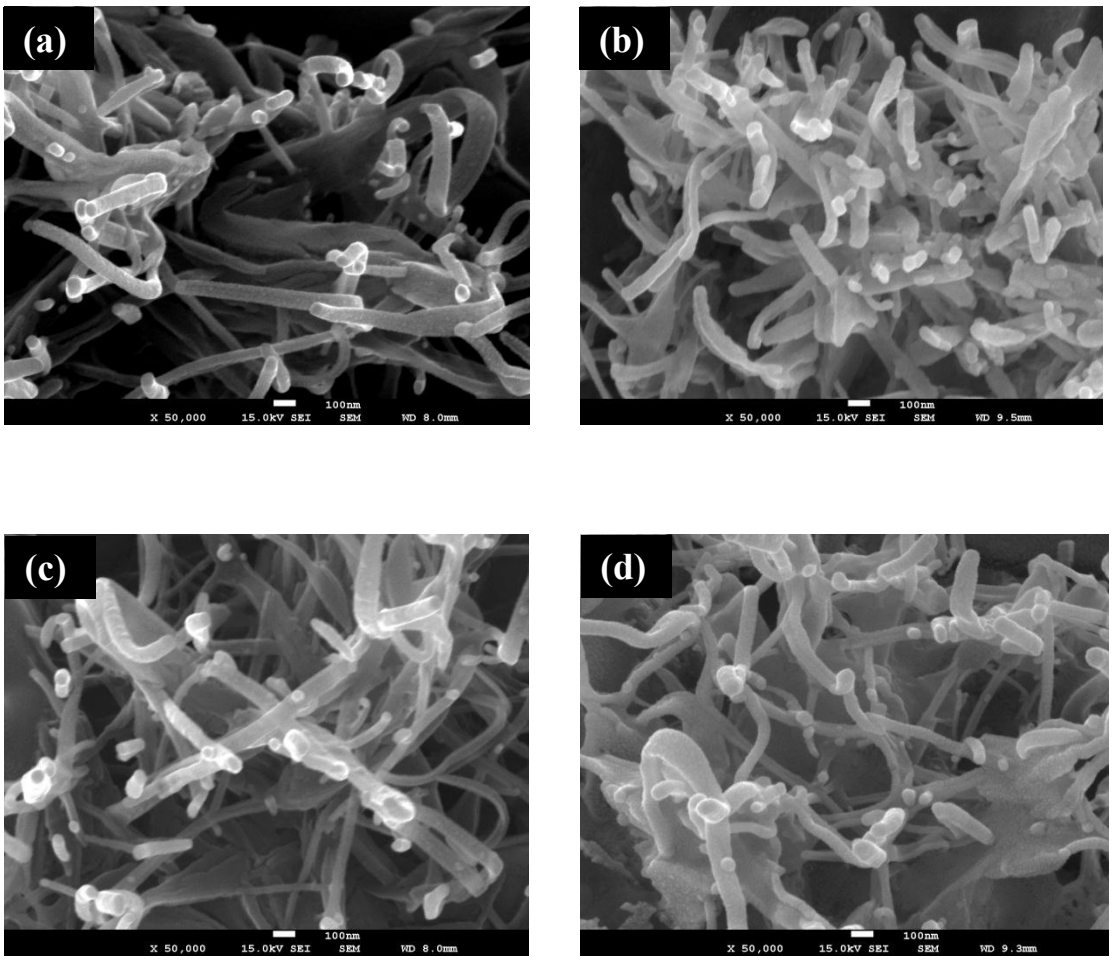

Figure 4.60 FE-SEM images of silver-filled polyanilines synthesized using argon plasma at (a) 0.5 (b) 1.0 (c) 1.5 (d) 2.0 mol/l of silver nitrate solution

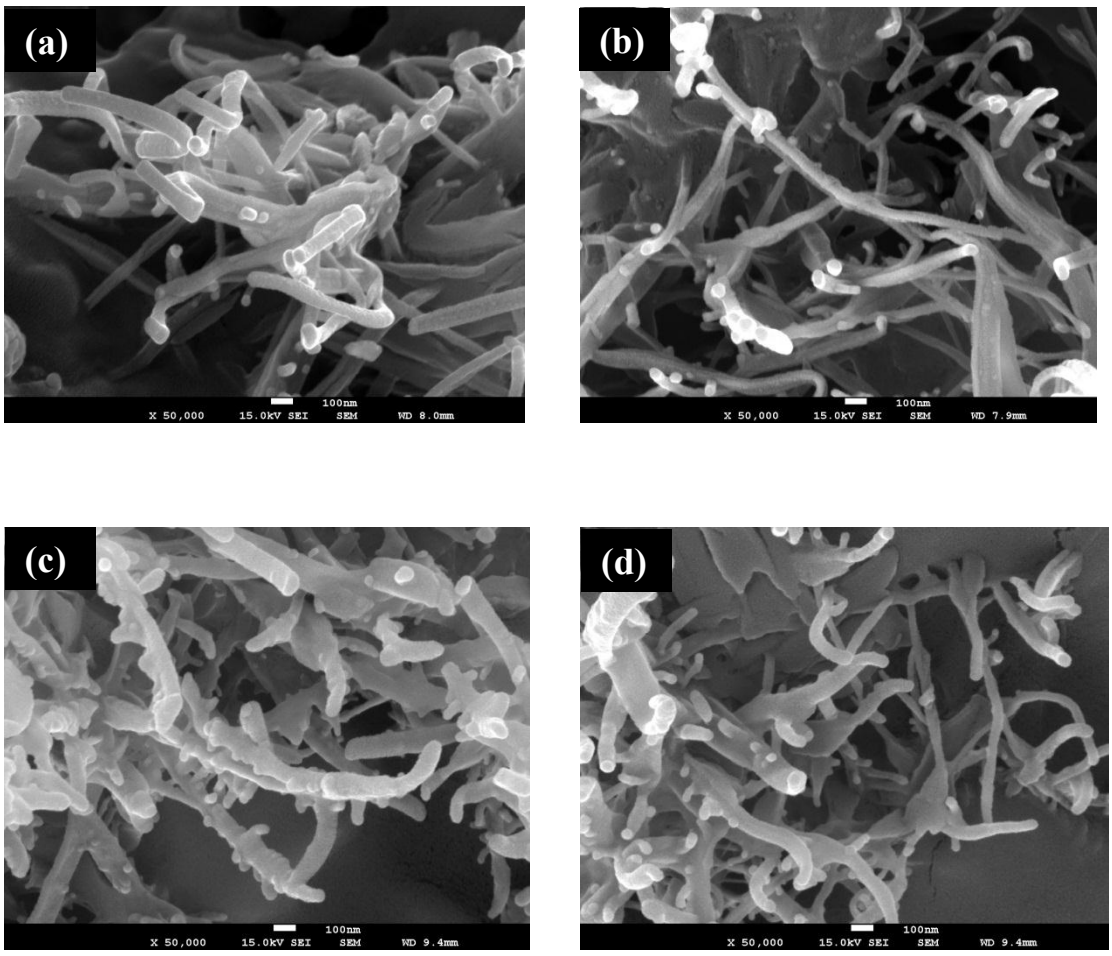

Figure 4.61 FE-SEM images of silver-filled polyanilines synthesized using oxygen plasma at (a) 0.5 (b) 1.0 (c) 1.5 (d) 2.0 mol/l of silver nitrate solution

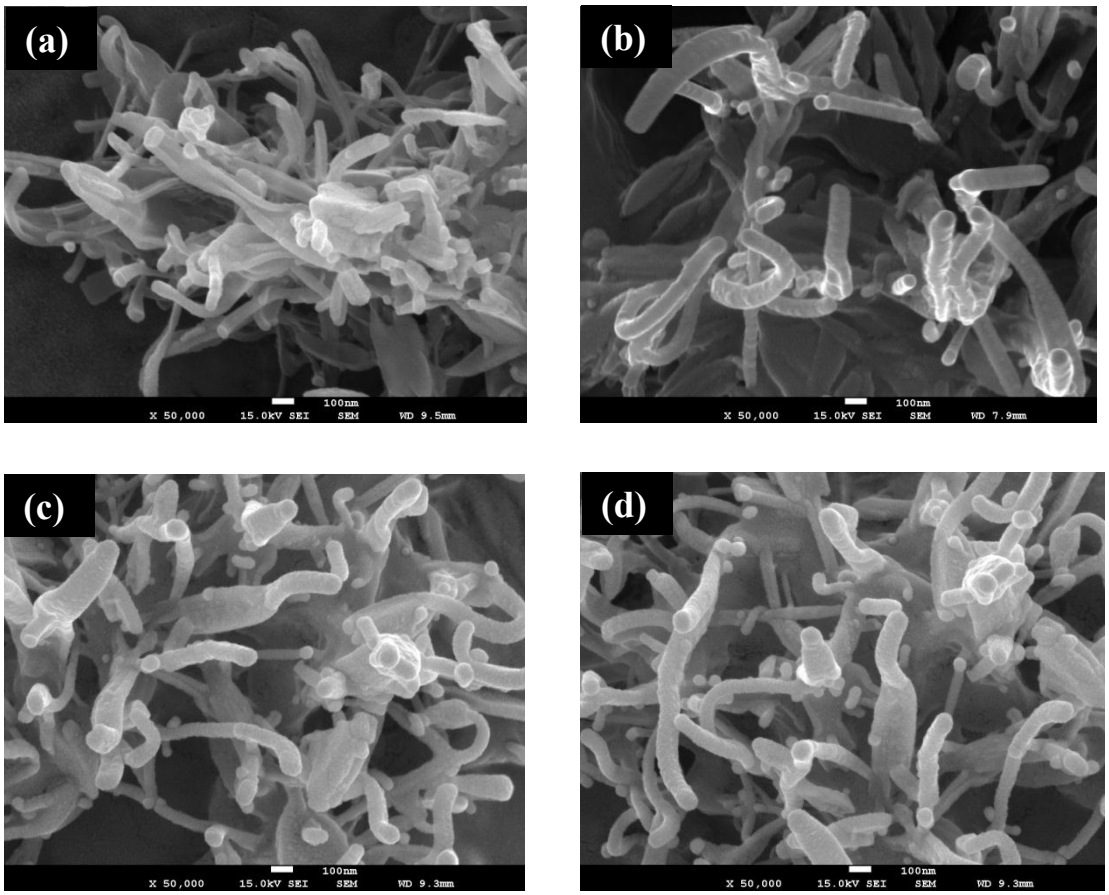

Figure 4.62 FE-SEM images of silver-filled polyanilines synthesized using nitrogen plasma at (a) 0.5 (b) 1.0 (c) 1.5 (d) 2.0 mol/l of silver nitrate solution

All the results suggest that silver-filled polyanilines synthesized using argon, oxygen and nitrogen plasma exhibit the following emeraldine salt structure as confirmed by FTIR and UV-VIS spectra and the conductivity measurement.

Emeraldine salt: 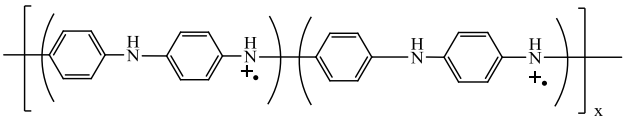

(green color)

CHAPTER V

CONCLUSIONS AND RECOMMENDATIONS

5.1 Conclusions

In this research, polyanilines and polyanilines filled with silver particles were successfully synthesized by plasma polymerization using pulsed plasma generators. In the case of polyanilines, they were synthesized using AAAPT theta-pinch device and pulsed inductively coupled plasma (PICP) device. The effects of the gas type and the number of the plasma shots on the characteristics and the properties of the obtained polyanilines were studied. It was found that plasma polymerization of aniline into polyaniline and acid doping can be done in one step. The results can be concluded as follows:

1. Polyanilines obtained from the syntheses in H_2SO_4 solution using AAAPT theta-pinch device exhibited the characteristic peaks of polyaniline including quinoid and benzenoid rings at 1630 and 1403 cm^{-1} in FTIR spectra, respectively. The structures of emeraldine salt and emeraldine base were formed depending on the gas type and the number of the plasma shots. UV-VIS spectra showed the absorption peaks of doped polyaniline with highest intensity when 20 shots of argon and oxygen plasma and 15 shots of nitrogen plasma were applied. Using 20 shots of argon plasma yielded a semi-crystalline polyaniline with highest conductivity and decomposition temperature at 262 ^{o}C.

2. Polyanilines obtained from the syntheses in H_2SO_4 solution using PICP device exhibited the characteristic peaks of polyaniline including quinoid and benzenoid rings around 1612 and 1400 cm^{-1} in FTIR spectra, respectively. The structures of polyaniline synthesized using argon plasma consisted of the mixtures of the emeraldine salt and emeraldine base depending on the number of the plasma shots. On the other hand, those synthesized using oxygen and nitrogen plasma exhibited mainly the undoped structure of emeraldine base. Consequently, the former exhibited

highest conductivity at every plasma shots. The obtained semi-crystalline polyanilines were easily dissolved in *N*-methyl-2-pyrrolidone, insoluble in neutral water but partially soluble in water having alkaline condition. Their decomposition temperatures were in the range of 182-188^{o}C depending on the gas type and the number of the plasma shots. Fibril structures with diameter of 100±7.4 nm were observed in all polyanilines except for those synthesized with 5 and 10 shots of oxygen and nitrogen plasma. The latters had the granular structure with grain size about 150±10.7 nm. An increase in the number of the plasma shots leads to higher amounts of fibrils but shorter length due to plasma etching at high plasma exposure.

3. Polyanilines obtained from the syntheses in HCl solution using PICP device exhibited the characteristic peaks of polyaniline including quinoid and benzenoid rings around 1612 and 1378 cm^{-1} in FTIR spectra, respectively. All polyanilines synthesized in HCl solution using argon, oxygen and nitrogen plasma exhibited the emeraldine base structure in conjunction with lower amount of the emeraldine salt depending on the number of the plasma shots. Using 5 shots of these plasma yielded polyanilines with highest conducitivity. The obtained semi-crystalline polyanilines were easily dissolved in *N*-methyl-2-pyrrolidone, insoluble in neutral water but partially soluble in water having alkaline condition. Their decomposition temperatures were in the range of 158-178^{o}C depending on the gas type and the number of the plasma shots due to structural difference. Polyanilines synthesized using argon plasma exhibited granular and rod structures. On the other hand, those synthesized using oxygen and nitrogen plasma exhibited small clusters as the bulk-like structure.

4. The above results indicated that PICP device was more suitable than theta-pinch device for the synthesis of polyaniline with acid doping in one step since it yielded polyanilines with higher conductivity. Therefore, this device was selected for the synthesis of polyanilines filled with silver particles in later section of the experiment.

5. The above results also indicated that using sulfuric acid resulted in polyanilines with higher conductivity and higher decomposition temperatures than using hydrochloric acid.

In the case of polyanilines filled with silver particles, they were synthesized in nitric acid solution using PICP device. The effects of the gas type and the concentration of silver nitrate on the characteristics and the properties of the obtained polyanilines were studied. It was found that the obtained polyanilines exhibited the characteristic peaks of polyaniline including quinoid and benzenoid rings around 1556 and 1495 cm^{-1} in FTIR spectra, respectively. All polyanilines synthesized using argon, oxygen and nitrogen plasma had the emeraldine salt structure as confirmed by FTIR and UV-VIS spectra. Their conductivities and decomposition temperatures were higher than pure polyaniline. They exhibited the fibril structure of polyaniline with average diameter of 50-100 nm and the spherical structure of silver particles with diameter about 50-80 nm. The amounts of silver particles increase with increasing the concentration of silver nitrate solution. These results indicated that plasma polymerization of aniline into polyaniline and the synthesis of silver particles can be done in one step.

5.2 Recommendations

1. The effect of other operating conditions of the plasma generator such as pressure should be studied.

2. The effect of other types of metal particles such as copper and gold should be studied.

3. The applications of the obtained polyanilines and polyanilines filled with silver particles such as for sensors should be studied.

REFERENCES

[1] Ameen, S., Ansari, S.G., Song, M., Kim, Y.S., and Shin, H-S. Fabrication of polyaniline/TiO_2 heterojunction structure using plasma enhanced polymerization technique. Superlattices and Microstructures 46 (2009): 745-751.

[2] Syed, A.A., and Dinesan, M.K. Review: Polyaniline-A novel polymeric material. Talanta 38 (1991): 815-837.

[3] Malinauskas, A. Chemical deposition of conducting polymer. Polymer 42 (2001): 3957-3972.

[4] Kim, J-S., Sohn, S-O., and Huh, J-S. Fabrication and sensing behavior of PVF2 coated-polyaniline sensor for volatile organic compounds. Sensors and Actuators B 108 (2005): 409-413.

[5] Reemts, T., Parisi, J., and Schlettwein, D. Electrochemical growth of gas-sensitive polyaniline thin films across an insulating gap. Thin Solid Films 466 (2004): 320-325.

[6] Agbor, N.E., and Petty, M.C., and Monkman, A.P. Polyaniline thin fillm for gas sensing. Sensors and Actuators B 28 (1995): 173-179.

[7] Zhang, D., and Wang, Y. Synthesis and applications of one-dimensional nano-structured polyaniline: An overview. Materials Science and Engineering B 134 (2006): 9-19.

[8] Zhang, H., Wang, J., Wang, Z., Zhang, F., and Wang, S. Electrodeposition of polyaniline nanostructures: A lamellar structure. Synthetic metals 159 (2009): 277-281.

[9] Paterno, L.G., Manolache, S., and Denes, F. Synthetic of polyaniline-type thin layer structures under low-pressure RF-plasma condition. Synthetic Metals 130 (2002): 85-97.

[10] Wang, J., Neoh, K.G., Zhao, L., and Kang, E.T. Plasma polymerization of aniline on different surface functionalized substrates. Journal of Colloid and Interface Science 251 (2002): 214-224.

[11] Airoudj, A., Debarnot, D., Beche, B., and Poncin-Epaillard, F. New sensitive layer based on pulsed plasma-polymerized aniline for integrated optical ammonia sensor. Analytica Chima Acta 626 (2008): 44-52.

[12] Merian, T., Debarnot, D., Rouessac, V., and Poncin-Epaillard, F. Ammonia absorption study of pulsed-plasma polyaniline by quartz crystal microgravimetry and UV/vis spectrometry. Talanta 81 (2010): 602-608.

[13] Ngamaroonchote, A., Mongkolnavin, R., and Pimpan, V. Pulsed plasma treatment of poly(ethylene terephthalate) films. Polymeric Materials: Science & Engineering 102 (2010): 507-508.

[14] Prasertsung, I., Mongkolnavin, R. Kanokpanont, S., and Damrongsakkul, S. The effect of pulsed inductively coupled plasma (PICP) on physical properties and biocompatibility of crosslinked gelatin films. International Journal of Biological Macromolecules 46 (2010): 72-78.

[15] Chuenchon, S. Kamsing, P. Mongkolnavin, R., Pimpan, V., and Wong, C.S. Surface modification of rayon fiber using pulsed plasma generated from theta pinch device. Journal of Science and Technology for the Tropics 1 (2007): 21-26.

[16] Pimpan, V., Khaymapunya, P., Kamsing, P., and Mongkolnavin, R. Abstracts to The 232nd ACS National Meeting, 10-14 September 2006, San Francisco, California, U.S.A.

[17] Pimpan, V., Chuenchon, S., Kamsing, P., and Mongkolnavin, R. Properties and Morphology of Surface-modified Polypropylene Fibers using Theta-pinch Device. Jurnal Fizik Malaysia 27 (2006): 59-62.

[18] Gupta, K., Jana, P.C., and Meikap, A.K. Optical and electrical transport properties of polyaniline-silver nanocomposite. Synthetic Metals 160 (2010):1566-1573.

[19] Rajesh, Ahuja, T., and Kumar, D. Review: Recent progress in the development of nano-structured conducting polymers/nanocomposites for sensor applications. Sensors and Actuators B 136 (2009): 275-286.

[20] Tamboli, M.S., Kulkarni, M.V., Patil, R.H., Gade, W.N., and Navale, S.C. Nanowires of silver-polyaniline nanocomposite synthesized via in situ polymerization and its novel functionally as an antibacterial agent. Colloids and surfaces B: Biointerfaces 92 (2012): 35-41.

[21] Blinova, N.V., Stejskal, J., Trchova, M., Sapurina, I., and Citric-Marjanovic, G. The oxidation of aniline with silver nitrate to polyaniline-silver composites. Polymer 50 (2009): 50-56.

[22] Bober, P., Trchova, M., Prokes, Jan., Varga, M., and Stejskal, J. Polyaniline-silver composites prepared by the oxidation of aniline with silver nitrate in solutions of sulfonic acid. Electrochimica Acta 56 (2011): 3580-3585.

[23] Khanna, P.K., Singh, N., Charan, S., and Viswanath, A.K. Synthesis of Ag/polyaniline nanocomposite via an in situ photo-redox mechanism. Materials Chemistry and Physics 92 (2005): 214-219.

[24] Chaisombat, S., Design and construction of 1.4 kJ pulsed incuctively coupled plasma device. Master' Thesis, Department of Physics, Faculty of Science, Chulalongkorn University, 2010.

[25] Pron, A., Kucharski, Z., Budrowski, C., Zagorska, M., Krichene, S., Suwalski, J., and Dehe, G., and Lefrant, S. Mossbauer spectroscopy studies of selected conducting polypyrroles. Journal of Chemical Physics 83 (1985): 5923-5927.

[26] Freund, M.S., and Deore, B.A. Self-doped conducting polymers. England: John Wiley & Sons Ltd, 2007.

[27] Bhadra, S., Khastgir, D., Singha, N.K., and Lee, J.H. Progress in preparation, processing and applications of polyaniline. Progress in Polymer Science 34 (2009): 783-810.

[28] Thanpitcha, T. Synthesis and characterization of polyaniline nanoparticles using template technique. Doctoral' Thesis, The Petroleum and Petrochemical College, Chulalongkorn University, 2009.

[29] Jang, J. Conducting polymer nanocomposites and their applications. Advances in Polymer Science 199 (2006): 189-259.

[30] Lange, U., Roznyatovskaya, N.V., and Mirsky, V.M. Review article: Conducting polymers in chemical sensors and arrays. Analytica Chimica Acta 614 (2008): 1-26.

[31] Patil, A.O., Heeger, A.J., and Wudl, F. Optical-properties of conducting polymer. Chemical Reviews 88 (1988): 183-200.

[32] Nalwa, H.S. Encyclopedia of Nanoscience and Nanotechnology, vol. 2, Los Angeles: American Scientific Publishers, 2004: 153-169.

[33] MacDiarmid, A.G. "Synthetic Metals": A Novel Role for Organic Polymers (Nobel Lecture). Angew Chem Int Ed Engl 40 (2001): 2581-2590.

[34] Chiang, J.C., and MacDiarmid, A.G. 'Polyaniline': Protonic acid doping of the emeraldine form to the metallic regime. Synthetic Metals 13 (1986): 193–205.

[35] Stejskal, J., Sapurina, I., and Trchova, M. Polyaniline nanostructures and the role of aniline oligomers in their formation. Progress in Polymer Science 35 (2012): 1420-1481.

[36] Stejskal, J., and Sapurina I. Polyaniline: thin films and colloidal dispersions. Pure and Applied Chemistry 77 (2005): 815–826.

[37] Shedd, B., Baker, C.O., Heller, M.J., Kaner, R.B., and Hahn, H.T. Fabrication of monolithic microstructures from polyaniline nanofibres. Materials Science and Engineering: B 162 (2009): 111–115.

[38] Huang, Y.F., Lin, C.W. Introduction of methanol in the formation of polyaniline nanotubes in acid-free aqueous solution through a selfcurling process. Polymer 50 (2009): 775–782.

[39] Stejskal, J. Colloidal dispersions of conducting polymers. Journal of polymer materials 18 (2001): 225-258.

[40] Stejskal, J., Sapurina, I., Trchova, M., Konyushenko, E.N., and Holler, P. The genesis of polyaniline nanotubes. Polymer 47 (2006): 8253–8262.

[41] Yano, J., Sanada, K., Patil, R., Ooyama, Y., Komaguchi, K., and Harima, Y. Poly(N-methylaniline) microsphere formation and control of the average diameter by simple chemical polymerization. Materials Chemistry and Physics 106 (2007) :279–285.

[42] Li, X., Wang, Y., Yang, X., Chen, J., Fu, H., and Cheng, T. Conducting polymers in environmental analysis. Trends in Analytical Chemistry 39 (2012): 163-179.

[43] Prokes, J., and Stejskal, J. Polyaniline prepared in the presence of various acids 2. Thermal stability of conductivity. Polymer Degradation and Stability 86 (2004): 187-195.

[44] Jin, X., Xiao, C., Wang, W. Electrical and mechanical properties of novel polyaniline coated polycaprolactam fibers. Synthetic Metals 160 (2010): 368-372.

[45] Mu, S., and Kan, J. Energy density and IR spectra of polyaniline synthesized electrochemically in the solutions of strong acids. Synthetic Metals 98 (1998): 51- 55.

[46] Kuramoto, N., and Tomita, A. Chemical oxidative polymerization of dodecylbenzenesulfonic acid aniline salt in chloroform. Synthetic Metals 88 (1997):147-151.

[47] Huang, J., Virji, S., Weiller, B.H., and Kaner, R.B. Polyaniline Nanofibers: Facile Synthesis and Chemical Sensors. Journal of the American Chemical Society 125 (2003): 314–315.

[48] Chen, J., Chao, D., Lu, X., Zhang, W. Novel interfacial polymerization for radially oriented polyaniline nanofibers. Materials Letters 61 (2007): 1419-1423.

[49] Zhang, X., and Manohar, S.K. Bulk synthesis of polypyrrole nanofibers by a seeding approach. Journal of the American Chemical Society 126 (2004): 12714- 12715.

[50] Jing, X.L., Wang, Y.Y., Wu, D., She, L., and Guo, Y. Polyaniline nanofibers prepared with ultrasonic irradiation. Journal of Polymer Science Part A: Polymer Chemistry 44 (2006): 1014-1019.

[51] Yang, C.H., Huang, L.R., Chih, Y.K., Lin, W.C., Liu, F.J., and Wang, T.L. Molecular assembled self-doped polyaniline copolymer ultra-thin films. Polymer 48 (2007): 3237-3247.

[52] Kim, J.Y., Lee, J.H., and Kwon, S.J. The manufacture and properties of polyaniline nano-films prepared through vapor-phase polymerization. Synthetic Metals 157 (2007): 336-342.

[53] Langer, J.J., and Czajkowski, I. Polyaniline Microrods. Advanced Materials for Optics and Electronics 7 (1997): 149–156.

[54] Stejskal, J., Trchova, M., Kovarova, J., Brozava, L., and Prokes, J. The reducing of silver nitrate with various polyaniline salts to polyaniline-silver composites. Reactive&Functional Polymers 69 (2009): 86-90.

[55] De Barros, R.A., and De Azevedo, W.M. Polyaniline/silver nanocomposite preparation under extreame or non-classical conditions. Synthetic Metals 158 (2008): 922-926.

[56] Chan, C.M. Polymer surface modification and characterization. New York: Hanser/Garder Publication, 1994.

[57 Yoon, J.H. Characterization of atmospheric pressure plasma interactions with textile/polymer substrates. Doctoral' Thesis, Department of fiber and Polymer Science, North Carolina State University, 2003..

[58] Shi, F.F. Review: Recent advances in polymer thin films prepared by plasma polymerization; Synthesis, structural characterization, properties and applications. Surface and Coatings Technology 82 (1996): 1-15.

[59] Shen, M., and Bell, A.T. A review of recent advances in plasma polymerization. ACS Synposium Series; American Chemical Society: Washington, DC, 1979;1-33.

[60] Chu, P.K., Chen, J.Y., Wang, L.P., and Huang, N. Plasma-surface modification of biomaterials. Materials Science and Engineering R 36 (2002): 143-206.

[61] Friedrich, J. Mechanisms of Plasma Polymerization – Reviewed from a Chemical Point of View. Plasma Processes and Polymers 8 (2011): 783–802.

[62] Kobayashi, H., Bell, A.T., and Shen, M. Formation of an amorphous powder during the polymerization of ethylene in a radio-frequency discharge. Journal of Applied Polymer Science 17 (1973): 885–892.

[63] Merche, D., Vandencasteele, N., and Reniers, F. Atmospheric plasmas for thin film deposition: A critical review. Thin Solid Films 520 (2012):4219-4236.

[64] Lakshmi, G.B.V.S., Dhillon, A., Siddiqui, A.M., Zulfequar, M., and Avasthi, D.K. RF-plasma polymerization and characterization of polyaniline. European Polymer Journal 45 (2009):2873-2877.

[65] Cruz, G.J., Morales, J., Castillo-Ortega, M.M., and Olayo, R. Synthesis of polyaniline films by plasma polymerization. Synthetic Metals 88 (1997): 213-218.

[66] Shepsis, L.V., Pedrow, P.D., Mahalingam, R., and Osman, M.A. Modeling and experimental comparison of pulsed plasma deposition of aniline. Thin Solid Films 385 (2001): 11-21.

[67] Li, Y.A., Ye, M.F., and Xu, F.Z. Introduction to Theta-pinch Discharge. Institute of Physics, 2002.

[68] Meeks, W.C., and Rovey, J.L. On the delayed gas breakdrown in a ringing theta-pinch with bias magnetic field. Physics of Plasmas 19 (2012): 052505(1)-052505(7).

[69] Chuenchon, S. Properties and morphology of surface modified man-made fibers using theta-pinch device. Master' Thesis, Department of Materials Science, Faculty of Science, Chulalongkorn University, 2004.

[70] Khaymapanya, P. Surface modification of synthetic and natural-fiber fabrics using a theta-pinch device. Master' Thesis, Department of Materials Science, Faculty of Science, Chulalongkorn University, 2005.

[71] Ngamaroonchote, A. Preparation of adhesive free laminated poly(ethylene terephthalate) films by plasma modification. Master' Thesis, Department of Materials Science, Faculty of Science, Chulalongkorn University, 2005.

[72] Ivanov, V.D., Zhuzhel'skii, D.V., and Malev, V.V. Comparison ofproperties of aniline and o-aminophenol polymers obtained using hydrogen peroxide. Russian Journal of Electrochemistry 44 (2008): 1204-1211.

[73] Barkade, S.S., Naik, J.B., and Sonawane, S.H. Ultrasound assisted miniemulsion synthesis of polyaniline/Ag nanocomposite and its application for ethanol vapor sensing. Colloids and Surface A: Physicochemical and Engineering Aspects 378 (2011): 94-98.

[74] Wang, X., and Grundmeier, G. Surface analytical studies of Ar-plasma etching of thin heptadecafluoro-1-decene plasma polymer films. Applied Surface Science 252 (2006): 8331-8336.

[75] Airoudj, A., Debarnot, D., Beche, B., and Poncin-Epaillar, F. Development of an optical ammonia sensor based on polyaniline/epoxy resin (SU-8) composite Talanta 77 (2009): 1590-1596.

[76] Koul, S., Dhawan, S.K., and Chandra, R. Compensated sulphonated polyaniline - correlation of processibility and crystalline structure. Synthetic Metals 124 (2001): 295-299.

[77] Nastase, C., Nastase, F., Vaseashta, A., and Stamatin, I. Nanocomposites based on functionalized nanotubes in polyaniline matrix by plasma polymerization. Progress in Solid State Chemistry 34 (2006): 181-189.

[78] Malmonge, J.A., and Mattoso, L.H.C. Doping of polyaniline and derivatives induced by X-ray radiation. Synthetic Metals 84 (1997): 779-780.

[79] Xiuqin, Z., Guolun, Y., Hanming, D., and Yongkui, S. Fabrication and photovoltaic properties of self-assembled sulfonated polyaniline/TiO2 nanocomposite ultrathin films. Materials Chemistry and Physics 102 (2007): 249-254.

[80] Srivastava, R., Dwivedi, R., and Srivastava, S.K. Effect of oxygen and hydrogen plasma treatment on the room temperature sensitivity of SnO_2 gas sensors. Microelectronics Journal 29 (1998):833-838.

[81] Mani, A., Athinarayanasamy, K., and Kamaraj, P. Crystalline order in polyaniline. Journal of Materials Science Letters 14 (1995): 1594-1596.

[82] Yang, J., Wang, X., Wang, X., Jia, R., and Huang, J. Preparation of highly conductive CNTs/polyaniline composites through plasma pretreating and in-situ polymerization. Journal of Physics and Chemistry of Solids 71 (2010): 448-452.

[83] Adhikari, S., and Banerji, P. Enhanced conductivity in iodine doped polyaniline thin film formed by thermal evaporation. Thin Solid Films 518 (2010): 5421–5425.

[84] Goel, S., Gupta, A., Singh, K.P., Mehrotra, R., and Kandpal, H.C. Optical studies of polyaniline nanostructures. Material Science and Engineering A 443 (2007): 71-76.

[85] Zengin, H., and others. Carbon Nanotube Doped Polyaniline. Advanced Materials 14 (2002): 1480–1483.

[86] Dey, A., De, S., De, A., and De, S.K. Characterization and dielectric properties of polyaniline–TiO_2 nanocomposites. Nanotechnology 15 (2004): 1277-1283.

[87] Sedenkova, I., Prokes, J., Trchova, M., and Stejskal, J. Conformational transition in polyaniline films – Spectroscopic and conductivity studies of ageing. Polymer Degradation and Stability 93 (2008): 428-435.

[88] Molina, J., Esteves, M.F., Fernandez, J., Bonastre, J., and Cases, F. Polyaniline coated conducting fabrics. Chemical and electrochemical characterization. European Polymer Journal 47 (2011): 2002-2015.

[89] Oxana, L. and others. Chemical synthesis of polyanilne in the presence of poly(amidosulfonic acids) with different rigidity of the polymer chain. Polymer 52 (2011): 2474-2484.

[90] Wang, Y., and Jing, X. Effect of solution concentration on the UV-vis spectroscopy measured oxidation state of polyaniline base. Polymer Testing 24 (2004): 153-156.

[91] Trchova, M., and Stejskal, J. The reduction of silver nitrate to metallic silver inside polyaniline nanotubes and on oligoaniline microsperes. Synthetic Metals 160 (2010): 1479-1486.

[92] Lide, D.R. and Frederikse, H.P.R. CRC handbook of chemistry and physics. 76th ed. Boca Raton: CRC press, 1995.

[93] Zhang, Z., Deng, J., Yu, L., and Wan, M. Chrysanthemum flower-like constructed polyaniline nanofibers synthesized by adding inorganic salts as additives. Synthetic Metals 158 (2008): 712-716.

[94] Han, J., Song, G., and Guo, R. Nanostructure-based leaf-ike polyaniline in the presence of an amphiphilic triblock copolymer. Advanced Materials 19 (2007): 2993-2999.

[95] Fuke, M.V., Kanitkar, P., Kulkarni, M., Kale, B.B., and Aiyer, R.C. Effect of particle size variation of Ag nanoparticles in polyaniline composite on humidity sensing. Talanta 81(2010): 320-326.

[96] Yang, C.H., Chih, Y-K., Tsai, M-S., and Chen, C-H. Self-doped polyaniline nanostructures for casting metal nanorods. Electrochemical and Solid-State Letters 9 (2006): G49-G52.

[97] Drury, A., and others. Fabrication and Characterization of silver/polyaniline composite nanowires in porous anodic alumina. Chemistry of Materials 19 (2007): 4252-4258.

[98] Sari, A.H., Akhavan, A., and Salem, M.K. Microstructure and surface properties of silver after high dose nitrogen ion implantation. Journal of Fusion Energy 30 (2011): 126-129.

Appendices

Appendix A

Determination of Ohmic Linear Regime

Linear regime or ohmic regime is the regime that applied voltage depends directly on the apply current according to ohmic law in equation A1. Linear regime was determined by plotting applied voltage (V) versus current (I). The range that gives the straight line is acceptable for using in conductivity measurement.

$$V = IR \tag{A1}$$

where V = applied voltage (V)

I = current (A)

R = resistance (Ω)

In this study, resistivity is determined from a resistance (R) of material using a two-point probe technique. Two voltage probes are at a fixed spacing distance. Current is sent through one probe and exist through the second probe. The voltage between the two probes is measured be a voltmeter. Two point probe test set up is shown in Figure A1. Most surface resistivity measurements are made on thin films on a small surface area substrate. The specific conductivity was calculated from equation A2

$$\sigma = \frac{1}{\rho} = \frac{I}{2\pi SV} \tag{A2}$$

Where σ is the specific conductivity (S/cm), ρ is the specific resistivity (Ω.cm), V is applied voltage to tips, I is the measured current, and S is the distance between the voltage measurement and the current probe.

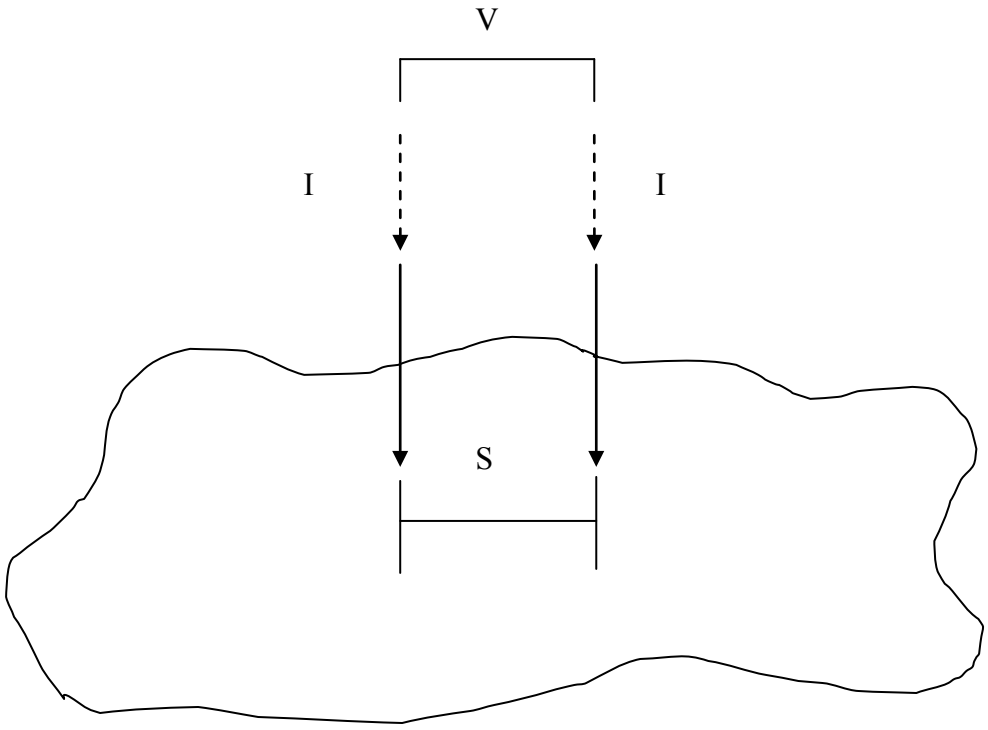

Figure A1 Two point probe test set up

Appendix B

Electrical conductivity of Sample

Table B1 Electrical conductivity of plasma synthesized PAni/H_2SO_4 with argon gas using AAAPT Theta-pinch device

The number of plasma shots	Resistivity (Ω.cm)			Conductivity (S/cm)			
	1	2	3	1	2	3	Average
5 sh	3.88×10^{7}	5.59×10^{7}	3.39×10^{7}	2.58×10^{-8}	1.79×10^{-8}	2.95×10^{-8}	2.44×10^{-8}
10 sh	1.74×10^{7}	1.88×10^{7}	1.55×10^{7}	5.76×10^{-8}	5.33×10^{-8}	6.46×10^{-8}	5.85×10^{-8}
15 sh	1.38×10^{7}	1.25×10^{7}	1.37×10^{7}	7.25×10^{-8}	7.98×10^{-8}	7.32×10^{-8}	7.52×10^{-8}
20 sh	9.35×10^{5}	1.17×10^{6}	1.34×10^{6}	1.07×10^{-6}	8.52×10^{-7}	7.44×10^{-7}	8.89×10^{-7}
25 sh	1.41×10^{6}	2.26×10^{6}	1.65×10^{6}	7.08×10^{-7}	4.43×10^{-7}	6.05×10^{-7}	5.85×10^{-7}
30 sh	1.23×10^{7}	5.41×10^{6}	7.87×10^{6}	8.14×10^{-8}	1.85×10^{-7}	1.27×10^{-7}	1.31×10^{-7}

Table B2 Electrical conductivity of plasma synthesized PAni/H_2SO_4 with oxygen gas using AAAPT Theta-pinch device

The number of plasma shots	Resistivity (Ω.cm)			Conductivity (S/cm)			
	1	2	3	1	2	3	Average
5 sh	-	-	-	-	-	-	-
10 sh	8.40×10^{9}	8.40×10^{9}	8.55×10^{9}	1.19×10^{-10}	1.19×10^{-10}	1.17×10^{-10}	1.18×10^{-10}
15 sh	8.06×10^{9}	6.67×10^{9}	7.69×10^{9}	1.24×10^{-10}	1.50×10^{-10}	1.30×10^{-10}	1.35×10^{-10}
20 sh	2.53×10^{9}	3.82×10^{9}	1.06×10^{8}	3.96×10^{-10}	2.62×10^{-10}	9.40×10^{-9}	3.35×10^{-9}
25 sh	1.53×10^{9}	2.46×10^{9}	2.53×10^{9}	6.53×10^{-10}	4.06×10^{-10}	3.96×10^{-10}	4.85×10^{-10}
30 sh	5.15×10^{9}	6.49×10^{9}	5.78×10^{9}	1.94×10^{-10}	1.54×10^{-10}	1.73×10^{-10}	1.74×10^{-10}

Table B3 Electrical conductivity of plasma synthesized PAni/H_2SO_4 with argon gas using PICP device

The number of plasma shots	Resistivity (Ω.cm)			Conductivity (S/cm)			
	1	2	3	1	2	3	Average
5 sh	8.62×10^{6}	8.85×10^{6}	1.00×10^{7}	1.16×10^{-7}	1.13×10^{-7}	1.00×10^{-7}	1.10×10^{-7}
10 sh	7.04×10^{6}	7.19×10^{6}	7.19×10^{6}	1.42×10^{-7}	1.39×10^{-7}	1.39×10^{-7}	1.40×10^{-7}
15 sh	6.29×10^{6}	6.29×10^{6}	6.71×10^{6}	1.59×10^{-7}	1.59×10^{-7}	1.59×10^{-7}	1.56×10^{-7}
20 sh	1.33×10^{6}	3.23×10^{6}	3.61×10^{6}	7.51×10^{-7}	3.10×10^{-7}	2.77×10^{-7}	4.46×10^{-7}
25 sh	4.78×10^{6}	4.78×10^{6}	3.86×10^{6}	2.09×10^{-7}	2.09×10^{-7}	2.59×10^{-7}	2.26×10^{-7}
30 sh	5.75×10^{6}	4.85×10^{6}	5.59×10^{6}	1.74×10^{-7}	2.06×10^{-7}	1.79×10^{-7}	1.86×10^{-7}

Table B4 Electrical conductivity of plasma synthesized PAni/H_2SO_4 with oxygen gas using PICP device

The number of plasma shots	Resistivity (Ω.cm)			Conductivity (S/cm)			
	1	2	3	1	2	3	Average
5 sh	5.68×10^{7}	5.68×10^{7}	7.09×10^{7}	1.73×10^{-8}	1.76×10^{-8}	1.41×10^{-8}	1.64×10^{-8}
10 sh	4.22×10^{7}	4.85×10^{7}	4.85×10^{7}	2.37×10^{-8}	2.06×10^{-8}	2.06×10^{-8}	2.16×10^{-8}
15 sh	3.36×10^{7}	3.47×10^{7}	4.52×10^{7}	2.98×10^{-8}	2.88×10^{-8}	2.21×10^{-8}	2.69×10^{-8}
20 sh	7.58×10^{6}	1.24×10^{7}	9.71×10^{6}	1.32×10^{-7}	8.05×10^{-8}	1.03×10^{-7}	1.05×10^{-7}
25 sh	1.80×10^{7}	1.62×10^{7}	1.62×10^{7}	5.57×10^{-8}	6.16×10^{-8}	6.19×10^{-8}	5.97×10^{-8}
30 sh	1.57×10^{7}	3.39×10^{7}	2.28×10^{7}	6.38×10^{-8}	2.95×10^{-8}	4.39×10^{-8}	4.57×10^{-8}

Table B5 Electrical conductivity of plasma synthesized PAni/H_2SO_4 with nitrogen gas using PICP device

The number of plasma shots	Resistivity (Ω.cm)			Conductivity (S/cm)			
	1	2	3	1	2	3	Average
5 sh	1.08×10^{9}	1.83×10^{9}	1.04×10^{9}	9.28×10^{-10}	5.47×10^{-10}	9.58×10^{-10}	8.11×10^{-10}
10 sh	1.01×10^{8}	2.05×10^{8}	1.35×10^{8}	9.94×10^{-9}	4.87×10^{-9}	7.40×10^{-9}	7.40×10^{-9}
15 sh	3.45×10^{8}	8.00×10^{8}	3.92×10^{8}	2.90×10^{-9}	1.25×10^{-9}	2.55×10^{-9}	2.23×10^{-9}
20 sh	2.67×10^{7}	7.41×10^{7}	8.47×10^{7}	3.74×10^{-8}	1.35×10^{-8}	1.18×10^{-8}	2.09×10^{-8}
25 sh	5.03×10^{8}	7.30×10^{8}	5.56×10^{8}	1.99×10^{-9}	1.37×10^{-9}	1.80×10^{-9}	1.72×10^{-9}
30 sh	5.38×10^{8}	2.26×10^{8}	6.90×10^{8}	1.86×10^{-9}	4.42×10^{-9}	1.45×10^{-9}	2.58×10^{-9}

Table B6 Electrical conductivity of plasma synthesized PAni/HCl with argon gas using PICP device

The number of plasma shots	Resistivity (Ω.cm)			Conductivity (S/cm)			
	1	2	3	1	2	3	Average
5 sh	2.06×10^{7}	2.36×10^{7}	2.07×10^{7}	4.85×10^{-8}	4.24×10^{-8}	4.83×10^{-8}	4.64×10^{-8}
10 sh	2.52×10^{7}	2.43×10^{7}	2.46×10^{7}	3.97×10^{-8}	4.11×10^{-8}	4.07×10^{-8}	4.05×10^{-8}
15 sh	2.90×10^{7}	2.92×10^{7}	2.71×10^{7}	3.45×10^{-8}	3.43×10^{-8}	3.69×10^{-8}	3.52×10^{-8}
20 sh	4.13×10^{7}	3.10×10^{7}	4.18×10^{7}	2.42×10^{-8}	3.23×10^{-8}	2.39×10^{-8}	2.68×10^{-8}
25 sh	5.99×10^{7}	6.29×10^{7}	6.58×10^{7}	1.67×10^{-8}	1.59×10^{-8}	1.52×10^{-8}	1.59×10^{-8}
30 sh	6.62×10^{7}	5.95×10^{7}	6.76×10^{7}	1.51×10^{-8}	1.68×10^{-8}	1.48×10^{-8}	1.56×10^{-8}

Table B7 Electrical conductivity of plasma synthesized PAni/HCl with oxygen gas using PICP device

The number of plasma shots	Resistivity (Ω.cm)			Conductivity (S/cm)			
	1	2	3	1	2	3	Average
5 sh	3.51×10^{7}	3.39×10^{7}	3.24×10^{7}	2.85×10^{-8}	2.95×10^{-8}	3.09×10^{-8}	2.96×10^{-8}
10 sh	3.98×10^{7}	3.82×10^{7}	4.12×10^{7}	2.51×10^{-8}	2.62×10^{-8}	2.43×10^{-8}	2.52×10^{-8}
15 sh	3.98×10^{7}	4.10×10^{7}	4.07×10^{7}	2.51×10^{-8}	2.44×10^{-8}	2.46×10^{-8}	2.47×10^{-8}
20 sh	5.10×10^{7}	5.56×10^{7}	5.32×10^{7}	1.96×10^{-8}	1.80×10^{-8}	1.88×10^{-8}	1.88×10^{-8}
25 sh	6.94×10^{7}	6.71×10^{7}	8.33×10^{7}	1.44×10^{-8}	1.49×10^{-8}	1.20×10^{-8}	1.38×10^{-8}
30 sh	7.69×10^{7}	8.33×10^{7}	9.35×10^{7}	1.30×10^{-8}	1.20×10^{-8}	1.07×10^{-8}	1.19×10^{-8}

Table B8 Electrical conductivity of plasma synthesized PAni/HCl with nitrogen gas using PICP device

The number of plasma shots	Resistivity (Ω.cm)			Conductivity (S/cm)			
	1	2	3	1	2	3	Average
5 sh	5.95×10^{7}	4.93×10^{7}	4.76×10^{7}	1.68×10^{-8}	2.03×10^{-8}	2.10×10^{-8}	1.94×10^{-8}
10 sh	6.21×10^{7}	6.99×10^{7}	5.95×10^{7}	1.61×10^{-8}	1.43×10^{-8}	1.68×10^{-8}	1.57×10^{-8}
15 sh	9.09×10^{7}	9.35×10^{7}	7.58×10^{7}	1.10×10^{-8}	1.07×10^{-8}	1.32×10^{-8}	1.16×10^{-8}
20 sh	1.21×10^{8}	1.13×10^{8}	1.16×10^{8}	8.28×10^{-9}	8.83×10^{-9}	8.59×10^{-9}	8.57×10^{-9}
25 sh	1.47×10^{8}	1.26×10^{8}	1.43×10^{8}	6.81×10^{-9}	7.94×10^{-9}	6.98×10^{-9}	7.24×10^{-9}
30 sh	1.66×10^{8}	1.59×10^{8}	1.65×10^{8}	6.02×10^{-9}	6.28×10^{-9}	6.05×10^{-9}	6.12×10^{-9}

Table B9 Electrical conductivity of plasma synthesized polyaniline filled with silver particles at different the concentration of silver nitrate with argon gas using PICP device.

The concentration of Silver nitrate	Resistivity (Ω.cm)			Conductivity (S/cm)			
	1	2	3	1	2	3	Average
0.50	3.52×10^{3}	3.42×10^{3}	3.62×10^{3}	2.84×10^{-4}	2.92×10^{-4}	2.76×10^{-4}	2.84×10^{-4}
1.00	2.99×10^{3}	2.84×10^{3}	3.26×10^{3}	3.35×10^{-4}	3.52×10^{-4}	3.07×10^{-4}	3.31×10^{-4}
1.50	3.92×10^{3}	3.97×10^{3}	3.88×10^{3}	2.55×10^{-4}	2.52×10^{-4}	2.58×10^{-4}	2.55×10^{-4}
2.00	5.05×10^{3}	5.21×10^{3}	5.35×10^{3}	1.98×10^{-4}	1.92×10^{-4}	1.87×10^{-4}	1.92×10^{-4}

Table B10 Electrical conductivity of plasma synthesized polyaniline filled with silver particles at different the concentration of silver nitrate with oxygen gas using PICP device.

The concentration of Siler nitrate	Resistivity (Ω.cm)			Conductivity (S/cm)			
	1	2	3	1	2	3	Average
0.50	4.46×10^{3}	4.72×10^{3}	4.88×10^{3}	2.24×10^{-4}	2.12×10^{-4}	2.05×10^{-4}	2.14×10^{-4}
1.00	4.07×10^{3}	4.52×10^{3}	4.44×10^{3}	2.46×10^{-4}	2.21×10^{-4}	2.25×10^{-4}	2.31×10^{-4}
1.50	5.85×10^{3}	5.32×10^{3}	5.38×10^{3}	1.71×10^{-4}	1.88×10^{-4}	1.86×10^{-4}	1.82×10^{-4}
2.00	7.52×10^{3}	7.94×10^{3}	7.69×10^{3}	1.33×10^{-4}	1.26×10^{-4}	1.30×10^{-4}	1.30×10^{-4}

Table B11 Electrical conductivity of plasma synthesized polyaniline filled with silver particles at different the concentration of silver nitrate with nitrogen gas using PICP device.

The concentration of Siler nitrate	Resistivity (Ω.cm)			Conductivity (S/cm)			
	1	2	3	1	2	3	Average
0.50	7.75×10^{3}	8.26×10^{3}	7.81×10^{3}	1.29×10^{-4}	1.21×10^{-4}	1.28×10^{-4}	1.26×10^{-4}
1.00	7.58×10^{3}	7.52×10^{3}	7.69×10^{3}	1.32×10^{-4}	1.33×10^{-4}	1.30×10^{-4}	1.32×10^{-4}
1.50	9.17×10^{3}	8.77×10^{3}	8.93×10^{3}	1.09×10^{-4}	1.14×10^{-4}	1.12×10^{-4}	1.12×10^{-4}
2.00	9.17×10^{3}	8.93×10^{3}	9.62×10^{3}	1.09×10^{-4}	1.12×10^{-4}	1.04×10^{-4}	1.08×10^{-4}

BIOGRAPHY

Miss Sasiakan Suwanprateep was born in Suphanburi, Thailand, on October 23th, 1981. She received the Bachelor Degree in Engineering with a major in Petrochemicals and Polymeric Materials, Faculty of Engineering and Industrial Technology from Silpakorn University, Nakornpathom, Thailand in 2003. She earned the Master Degree in Petrochemistry and Polymer Science, Faculty of Science from Chulalongkorn University, Bangkok, Thailand in 2006. She started as a Ph.D. student in 2008 in the field of Materials Science, Department of Materials Science, Chulalongkorn University and completed the program in 2013.